

Eco-Hydrological Simulation Environment (echse)

Documentation of model engines



Developer:

Author	David Kneis
Affiliation	Institute of Earth and Environmental Sciences Geo-Ecology Section, University of Potsdam, Germany
Contact	david.kneis@uni-potsdam.de
Project	PROGRESS
Sub-project	D2.2
Funding	German Ministry of Education and Research (BMBF)

Contributor(s):

Author	Tobias Pilz
Affiliation	Institute of Earth and Environmental Science University of Potsdam, Germany
Contact	tpilz@uni-potsdam.de
Funding	GeoSim (Helmholtz graduate school)
Contributions	Added Chap. 10 , re-formatted and extended Chap. 9

Last update March 18, 2016

Contents

1	Introduction	9
I	Hydrological model engines	11
2	Model engine hypsoRR	13
2.1	Basic facts	13
2.2	Classes	13
2.3	Selected applications	13
II	Classes	15
3	Classes for hydrological catchment modeling	17
3.1	Default sub-basin class	17
3.1.1	Simulated processes	17
3.1.2	Data members	17
3.2	Default reach class	21
3.2.1	Simulated processes	21
3.2.2	Data members	21
3.3	Minireach class	21
3.3.1	Simulated processes	21
3.3.2	Data members	21
3.4	Node classes	22
3.4.1	Simulated processes	22
3.4.2	Data members	22
3.5	Lake class	22
3.5.1	Simulated processes	22
3.5.2	Data members	22
3.6	Gage class	23
3.6.1	Simulated processes	23
3.6.2	Data members	23
3.7	Rain gage class	23
3.7.1	Simulated processes	23
3.7.2	Data members	24
3.8	External inflow class	24
3.8.1	Simulated processes	24
3.8.2	Data members	24

3.8.3	Reservoir class	24
3.8.4	Flood control storage basin class	24

III Mathematical description of hydrological processes 25

4 Dynamics of the snow cover 27

4.1	Energy balance method	27
4.1.1	Capabilities and limitations	27
4.1.2	Basics of the energy balance method	27
4.1.3	Simulation of the snow albedo	31
4.1.4	Energy flux rates	32
4.1.5	Mass flux rates	34
4.1.6	Test application	37
4.2	Degree-day method	37

5 Runoff generation 41

5.1	Introduction	41
5.2	Simple four components model	41
5.2.1	Processes and equations	41
5.2.2	Combination with other models	44
5.2.3	Mathematical solution	44
5.2.4	Implementation	44
5.2.5	Hints for application	44
5.3	Process-based approaches	45
5.3.1	Soil water movement	45
5.3.2	Runoff generation	53
5.4	Contributions and TODOs	55

6 Runoff concentration 57

6.1	Introduction	57
6.2	Parallel storage model	57
6.2.1	Processes and equations	57
6.2.2	Mathematical solution	58
6.2.3	Implementation	58
6.2.4	Hints for application	59

7 Channel flow 61

7.1	Introduction	61
7.2	Single reservoir approach	61
7.2.1	Processes and equations	61
7.2.2	Mathematical solution	63
7.2.3	Hints for application	63

8 Evaporation from Water Surfaces 65

8.1	Introduction	65
8.2	Makkink model	65

9	Evapotranspiration	67
9.1	Introduction	67
9.2	Models	73
9.2.1	Empirical equations	73
9.2.2	Process-based approaches	73
9.3	Actual vs. potential evapotranspiration	76
9.3.1	Reduction functions	76
9.3.2	Resistances	78
9.4	Contributions and TODOs	81
10	Meteorological quantities	83
10.1	Introduction	83
10.2	Important constants	83
10.3	Hydro-meteorological quantities	83
10.3.1	Atmospheric pressure – PA	83
10.3.2	Saturation vapor pressure – E	83
10.3.3	Vapor pressure – e	84
10.3.4	Vapor pressure deficit – D	85
10.3.5	Slope of the saturation vapor pressure curve – s	85
10.3.6	Dew point temperature – T_{dew}	85
10.3.7	Specific humidity – q	85
10.3.8	Latent heat of water evaporation – E_{wat}	85
10.3.9	Psychrometric constant – γ	85
10.3.10	Mole fraction of water vapor – x_v	85
10.3.11	Compressibility factor – Z	86
10.3.12	Density of moist air – ρ_{air}	86
10.4	Astronomical quantities	86
10.4.1	Solar declination – δ	86
10.4.2	Eccentricity correction factor – E_0	86
10.4.3	Daylight time factor – ω_s	87
10.4.4	Extraterrestrial radiation – R_{ex}	87
10.5	Energy budget	88
10.5.1	Incoming short-wave radiation – R_{inS}	88
10.5.2	Maximum (clear-sky) incoming short-wave radiation – $R_{inS,cs}$	88
10.5.3	Net emissivity – ε	89
10.5.4	Cloudiness correction factor – f	89
10.5.5	Incoming net long-wave radiation – R_{netL}	89
10.5.6	Incoming net radiation – R_{net}	90
10.5.7	Soil heat flux – G_{soil}	90
10.6	Turbulence	90
10.6.1	Displacement height of vegetation – d	90
10.6.2	Roughness length	90
11	Storage in lakes and reservoirs	91
11.1	Introduction	91
11.2	Storage in uncontrolled lakes	91
11.2.1	Processes and equations	91
11.2.2	Mathematical solution	92
11.2.3	Implementation	92
11.3	Notes on input data	92

11.3.1	Storage curve	92
11.3.2	Surface area curve	93
11.3.3	Rating curve (uncontrolled lakes)	93
List of figures		95
List of tables		97
Bibliography		98

Chapter 1

Introduction

This document is subdivided into three parts each of them addressing a different level of software hierarchy. The relation between the three parts is depicted by an example in Fig. 1.1.

Part I contains a brief description of hydrological model engines implemented with the **echse** modeling framework. It provides information on the model engine's purpose and lists the important classes (i. e. the types of objects that can be simulated) using references to the part II.

Part II holds a description of the classes, including information on state variables and external inputs, for example.

Part III addresses the mathematical representation of realworld hydrological processes, i. e. the mechanisms that cause the state variables to change their values over time. The concepts described in this part may be used by several of the classes portrayed in part II.

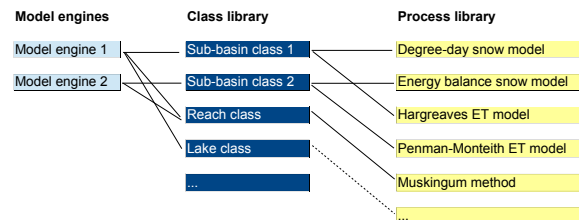


Figure 1.1: Classes and processes as the basic building blocks of hydrological model engines.

Part I

Hydrological model engines

Chapter 2

Model engine **hypsoRR**

2.1 Basic facts

The **hypsoRR** model engine was designed for the purpose of flood forecasting, and the verification of ensemble-based flood forecasts in particular.

- It is hydrologocal catchment model engine that simulates all major processes of the hydrological cycle.
- It is a rather simple, conceptual model engine to allow for fast computations. This is important in operational applications, especially when dealing with ensembles.
- The data requirements are adapted to the situation in Germany, where observation data for all major meteorological variables are typically available. However, the concept was also sucessfully applied to basins in Asia and Africa. The full set of variables is required only if snow accumulation/melt is relevant.
- Many concepts are copied from LARSIM ([Ludwig and Bremicker, 2006](#)) which is the hydrological model engine currently used for operational forecasting in SW Germany. **hypsoRR** can use most of LARSIM's input data, namely the information in tape12, tape35, etc.

2.2 Classes

The **hypsoRR** model engine currently comprises the classes listes in Table 2.1.

Table 2.1: Classes of the **hypsoRR** model engine.

Class	Details to be found at
Sub-basin	Sec. 3.1
Reach	Sec. 3.2
Minireach	Sec. 3.3
Node classes	Sec. 3.4
Lake	Sec. 3.5
Gage	Sec. 3.6
Rain gage	Sec. 3.7
External inflow	Sec. 3.8

2.3 Selected applications

As of March 2014, **hypsoRR** was set-up and calibrated for the river basins listes in Table 2.2.

Table 2.2: Applications of the **hypsoRR** model engine.

Basin/Gage	Country	km ²
Wilde Weißeritz / Ammeldorf	Germany	70
Rheraya	Morocco	220
Marikina	Philippines	570
Neckar / Kirchzellinsfurt	Germany	2317
Mahanadi / Mundali	India	135000

Part II

Classes

Chapter 3

Classes for hydrological catchment modeling

3.1 Default sub-basin class

3.1.1 Simulated processes

The class simulates the processes listed in Table 3.1.

The current version of the class does *not* allow for the representation of hydrological response units. Only three classes of land cover are currently distinguished: (1) water surfaces, (2) impervious surfaces, and (3) pervious surfaces, i. e. soil typically covered by vegetation.

3.1.2 Data members

A full list of the data members of the class is provided in Table 3.2. See Kneis (2012b) for an explanation of the abbreviations in the 'type' column.

Table 3.1: Considered processes in the default sub-basin class.

Process	Model concept
Runoff generation	Conceptual four components model (Sec. 5.2)
Runoff concentration	Parallel linear reservoirs (Sec. 6.2)
Evapotranspiration	Potential evapotranspiration after Makkink with crop factors and correction for soil water limitation (Sections 9.2.1.1, 9.3.1.1, and 9.3.1.2)
Snow storage and melt	Energy balance model (Sec. 4.1)

Table 3.2: Data members of the default sub-basin class.

Type	Name	Description	Unit
stateScal	wc	Soil water content (dimensionless, i.e. vol/vol or m/m)	dimensionless
stateScal	vol_surf	Storage volume of the linear reservoir controlling surface runoff retention	m3
stateScal	vol_pref	Storage volume of the linear reservoir controlling preferential flow retention	m3
stateScal	vol_inter	Storage volume of the linear reservoir controlling interflow retention	m3
stateScal	vol_base	Storage volume of the linear reservoir controlling baseflow retention	m3
stateScal	snow_swe	Snow water equivalent	m
stateScal	snow_sec	Energy content of the snow cover	kJ/m2
stateScal	snow_alb	Snow albedo	dimensionless
inputExt	precip_resid	Residuals of precipitation (time series)	mm / time step
inputExt	precip_slope	Slope of the linear model precip ~ elevation	mm / time step / meter
inputExt	precip_inter	Intercept of the linear model precip ~ elevation	mm / time step
inputExt	temper_resid	Residuals of air temperature (time series)	degree Celsius
inputExt	temper_slope	Slope of the linear model temperature ~ elevation	degree Celsius / meter
inputExt	temper_inter	Intercept of the linear model temperature ~ elevation	degree Celsius
inputExt	apress_resid	Residuals of air pressure (time series)	hPa
inputExt	apress_slope	Slope of the linear model pressure ~ elevation	hPa / meter
inputExt	apress_inter	Intercept of the linear model pressure ~ elevation	hPa
inputExt	windsp	Wind speed (time series)	m/s
inputExt	glorad	Short-wave radiation (time series)	W/m2
inputExt	rhumid	Relative humidity (time series)	%
inputExt	clness	Cloudiness (time series)	dimensionless (0...1)
inputExt	lai	Leaf area index	dimensionless
paramNum	area	Surface area of the catchment	m2
paramNum	elev	Representative elevation	m asl
paramNum	frac_noinf	Fraction of the catchment area with impervious surface	dimensionless (0...1)
paramNum	frac_water	Fraction of the catchment area covered by water surfaces	dimensionless (0...1)
paramNum	soildepth	Thickness of the modeled soil column	m
paramNum	wc_max	Maximum value soil water content (water content at saturation)	dimensionless
paramNum	exp_satfrac	Shape parameter, controls the fraction of saturated areas with increasing average saturation	dimensionless
paramNum	thr_surf	Threshold value. Direct runoff above this rate is considered as surface runoff	m/s
paramNum	relsat_inter	Relative filling of soil reservoir above which interflow is generated (threshold)	dimensionless (0...1)
paramNum	rate_inter	Rate of medium-fast runoff generation at soil saturation	m/s
paramNum	rate_base	Rate of ground-water recharge at soil saturation	m/s
paramNum	ct_index	Concentration time index (empirical Kirpich formula, for example)	s

Continued on next page

Table 3.2 – Continued from previous page

Type	Name	Description	Unit
paramNum	str_surf	Parameter to control retention of surface runoff	dimensionless
paramNum	str_pref	Parameter to control retention of preferential runoff	dimensionless
paramNum	str_inter	Parameter to control retention of medium-fast runoff	dimensionless
paramNum	str_base	Parameter to control retention in the ground-water reservoir	dimensionless
paramNum	relsat_etmin	Relative filling of soil reservoir below which evapotranspiration becomes zero	dimensionless (0...1)
paramNum	relsat_etmax	Relative filling of soil reservoir above which evapotranspiration is no longer moisture-limited	dimensionless (0...1)
paramNum	fac_precip	Precipitation correction factor (used for input updating, for example)	dimensionless
sharedParamNum	cropFac_slope	Constant "a" in "Makking crop factor = a * LAI + b"	dimensionless
sharedParamNum	cropFac_inter	Constant "b" in "Makking crop factor = a * LAI + b"	dimensionless
sharedParamNum	mult_surf	Factor applied to surface runoff before output (i¿ 1 for tests only)	dimensionless
sharedParamNum	mult_pref	Factor applied to preferentialrunoff before output (i¿ 1 for tests only)	dimensionless
sharedParamNum	mult_inter	Factor applied to medium-fast runoff before output (i¿ 1 for tests only)	dimensionless
sharedParamNum	mult_base	Factor applied to slow runoff (base flow) before output (i¿ 1 for tests only)	dimensionless
sharedParamNum	snow_a0	Constant describing the dependence of moisture and heat fluxes on wind speed (additive term in linear model)	m/s
sharedParamNum	snow_a1	Constant describing the dependence of moisture and heat fluxes on wind speed (factor in linear model)	dimensionless
sharedParamNum	snow_kSat	Saturated hydraulic conductivity of snow	m/s
sharedParamNum	snow_densDry	Density of dry snow	kg/m3
sharedParamNum	snow_specCapRet	Capillary retention volume as a fraction of the solid snow water equivalent	dimensionless
sharedParamNum	snow_emissivityMin	Minimum value of snow emissivity (for old snow surface)	dimensionless
sharedParamNum	snow_emissivityMax	Maximum value of snow emissivity (for old snow surface)	dimensionless
sharedParamNum	snow_tempAir_crit	Air temperature below which precipitation falls as snow	degree Celsius
sharedParamNum	snow_albedoMin	Minimum albedo of (old) snow	dimensionless
sharedParamNum	snow_albedoMax	Maximum albedo of (new) snow	dimensionless
sharedParamNum	snow_agingRate_tAirPos	Aging rate describing the decrease in snow albedo when air temperature is positive	1/s
sharedParamNum	snow_agingRate_tAirNeg	Aging rate describing the decrease in snow albedo when air temperature is negative	1/s
sharedParamNum	snow_soilDepth	Thickness of the soil column considered in computation of the snow energy balance	m
sharedParamNum	snow_soilDens	Density of the soil considered in computation of the snow energy balance	kg/m3
sharedParamNum	snow_soilSpecHeat	Specific heat capacity of the soil considered in computation of the snow energy balance	kJ/kg/K
sharedParamNum	snow_weightAirTemp	Weight used in the estimation of snow surface temperature from air temperature and mean snow temperature	dimensionless (0...1)
sharedParamNum	snow_fullShadowLAI	Reduces short-wave incoming radiation depeding on the LAI (rad'= rad * (1 - LAI/snow_fullShadowLAI))	m
sharedParamNum	heightZeroWind	Height above ground where wind speed approaches zero (used in precipitation correction)	m
output	qx_end	Outflow rate of the catchment at end of time step	m3/s
output	qx_avg	Outflow rate of the catchment, time step average	m3/s
output	swe	Snow water equivalent	m
output	etp	Rate of potential evapotranspiration	m/s

Continued on next page

Table 3.2 – *Continued from previous page*

Type	Name	Description	Unit
output	etr	Rate of actual evapotranspiration	m/s

3.2 Default reach class

3.2.1 Simulated processes

The reach class simulates the outflow from a river reach given information on the inflow and its storage characteristics. The concept is described in Sec. 7.2.

3.2.2 Data members

A list of the data members of the class is provided in Table 3.3. See Kneis (2012b) for an explanation of the abbreviations in the 'type' column.

Table 3.3: Data members of the default reach class.

Type	Name	Description	Unit
paramFun	v2k	Retention constant of the reach (s) as a function of storage (m3)	s
paramFun	q2k	Retention constant of the reach (s) as a function of flow rate (m3/s)	s
stateScal	vol	Storage volume of the reach	m3
inputSim	qi_end	Inflow rate at end of time step	m3/s
inputSim	qi_avg	Inflow rate, time step average	m3/s
output	qx_end	Outflow rate at end of time step	m3/s
output	qx_avg	Outflow rate, time step average	m3/s

3.3 Minireach class

3.3.1 Simulated processes

The minireach class simulates a reach (or pipe) of very short length so that the travel time is practically negligible. Thus, the outflow a minireach object is identical to the inflow.

3.3.2 Data members

A list of the data members of the class is provided in Table 3.4. See Kneis (2012b) for an explanation of the abbreviations in the 'type' column.

Table 3.4: Data members of the minireach class.

Type	Name	Description	Unit
inputSim	qi_end	Inflow rate at end of time step	m3/s
inputSim	qi_avg	Inflow rate, time step average	m3/s
output	qx_end	Outflow rate at end of time step	m3/s
output	qx_avg	Outflow rate, time step average	m3/s

3.4 Node classes

3.4.1 Simulated processes

The purpose of node objects is to merge flows from different sources. The typical case is a node with two inflows (e. g. a stream junction). Nodes with a higher number of inflows (or with just a single inflow) may be useful in some situations.

3.4.2 Data members

A list of the data members of the class is provided in Table 3.5 for the example of two inflows. See Kneis (2012b) for an explanation of the abbreviations in the 'type' column.

Table 3.5: Data members of the node class with two inflows.

Type	Name	Description	Unit
inputSim	qi_end_1	Inflow rate at end of time step (source 1)	m ³ /s
inputSim	qi_end_2	Inflow rate at end of time step (source 2)	m ³ /s
inputSim	qi_avg_1	Inflow rate, time step average (source 1)	m ³ /s
inputSim	qi_avg_2	Inflow rate, time step average (source 2)	m ³ /s
output	qx_end	Outflow rate at end of time step	m ³ /s
output	qx_avg	Outflow rate, time step average	m ³ /s

3.5 Lake class

3.5.1 Simulated processes

The class simulates the outflow from an uncontrolled lake/reservoir based on a rating curve and a storage curve. Precipitation and evaporation losses are taken into account. Details are described in Sec. 11.2.

3.5.2 Data members

A list of the data members of the class is provided in Table 3.6. See Kneis (2012b) for an explanation of the abbreviations in the 'type' column.

Table 3.6: Data members of the lake class.

Type	Name	Description	Unit
stateScal	v	Storage volume	m ³
stateScal	vp	Total precipitation input within a time step (temporary variable to compute the mass balance)	m ³
stateScal	ve	Total evaporation loss within a time step (temporary variable to compute the mass balance)	m ³
inputSim	qi_end	Inflow rate at end of time step	m ³ /s
inputSim	qi_avg	Inflow rate, time step average	m ³ /s
paramNum	area_max	Maximum water surface area (area collecting precipitation)	m ²
paramNum	fac_precip	Precipitation correction factor (used for input updating, for example)	dimensionless
paramFun	v2h	Storage curve (water level as a function of the storage volume)	m

Continued on next page

Table 3.6 – Continued from previous page

Type	Name	Description	Unit
paramFun	h2q	Rating curve at the lake's outflow (outflow rate as a function of the water level)	m ³ /s
paramFun	h2a	Function to compute the evaporating surface area from the water level	m ²
inputExt	precip	Precipitation (time series)	mm / time step
inputExt	glorad	Short-wave radiation (time series)	W/m ²
inputExt	tavg	Average air temperature (time series)	degree Celsius
output	qx_end	Outflow rate at end of time step	m ³ /s
output	qx_avg	Outflow rate, time step average	m ³ /s
output	h	Water level	m

3.6 Gage class

3.6.1 Simulated processes

In many situations it is sufficient to output the simulated flow rate of a river reach, making the explicit simulation of a gage object unnecessary. The advantage of instantiating an object of the gage class lies in the fact that the simulated flow may be optionally substituted by observed values. This is quite useful, for example, when a calibrating a model for the part of a river basins located downstream of a gage.

3.6.2 Data members

A list of the data members of the class is provided in Table 3.7. See Kneis (2012b) for an explanation of the abbreviations in the 'type' column.

Table 3.7: Data members of the gage class.

Type	Name	Description	Unit
inputSim	qi_end	Simulated inflow rate at end of time step	m ³ /s
inputSim	qi_avg	Simulated inflow rate, time step average	m ³ /s
inputExt	qobs_avg	Observed flow, time step average. May be used as an optional substitute for the simulated inflow.	m ³ /s
paramNum	obs_lbound	Threshold; The sim. flow (qi) is substituted by the obs. flow (qobs) only if qobs is greater/equal obs_lbound	m ³ /s
paramNum	obs_ubound	Threshold; The sim. flow (qi) is substituted by the obs. flow (qobs) only if qobs less/equal obs_ubound	m ³ /s
output	qx_avg	Outflow rate (observed or simulated, depending on qobs_avg and the thresholds), time step average	m ³ /s
output	qx_avg_sim	Copy of qi_avg (i.e. simulated flow)	m ³ /s
output	qx_end	Outflow rate at end of time step (observed or simulated, depending on qobs_avg and the thresholds)	m ³ /s
output	qx_end_sim	Copy of qi_end (i.e. simulated flow)	m ³ /s

3.7 Rain gage class

3.7.1 Simulated processes

Objects of this class can be used to query the precipitation at a point as computed from residual interpolation.

3.7.2 Data members

A list of the data members of the class is provided in Table 3.8. See Kneis (2012b) for an explanation of the abbreviations in the 'type' column.

Table 3.8: Data members of the rain gage class.

Type	Name	Description	Unit
inputExt	precip_resid	Residuals of precipitation (time series)	mm / time step
inputExt	precip_slope	Slope of the linear model $\text{precip} \sim \text{elevation}$	mm / time step / meter
inputExt	precip_inter	Intercept of the linear model $\text{precip} \sim \text{elevation}$	mm / time step
paramNum	elev	Elevation	m
output	precip	Precipitation	mm / time step

3.8 External inflow class

3.8.1 Simulated processes

This class provides a simple means to represent an external water source. The time-variable flow rates are pre-defined, i. e. read from a file. The class may also be helpful if a large-scale model is split into sub-models at the boundaries of major watersheds. In such a case, it may be desirable to save the runoff from an upstream area (sub-model A) to a file and re-read the data later when simulating the downstream part (sub-model B).

3.8.2 Data members

A list of the data members of the class is provided in Table 3.9. See Kneis (2012b) for an explanation of the abbreviations in the 'type' column.

Table 3.9: Data members of the external inflow class.

Type	Name	Description	Unit
inputExt	precip_resid	Residuals of precipitation (time series)	mm / time step
inputExt	precip_slope	Slope of the linear model $\text{precip} \sim \text{elevation}$	mm / time step / meter
inputExt	precip_inter	Intercept of the linear model $\text{precip} \sim \text{elevation}$	mm / time step
paramNum	elev	Elevation	m
output	precip	Precipitation	mm / time step

3.8.3 Reservoir class

This class is still experimental and not documented.

3.8.4 Flood control storage basin class

This class is still experimental and not documented.

Part III

Mathematical description of hydrological processes

Chapter 4

Dynamics of the snow cover

4.1 Energy balance method

4.1.1 Capabilities and limitations

In many catchments, snow storage and melting are important components of the water cycle. Snow melt, possibly accompanied (or caused) by rainfall is a major cause of flood generation in many catchments. However, the structure of a natural snow cover is very complex and the simulation of its dynamics is difficult. Therefore, any snow model is subject to a number of simplifying assumptions and limitations. The most important limitations of the snow model described in this section are:

- The snow pack is treated as homogeneous (well mixed) layer. Thus, possible stratification is neglected.
- Shortwave radiation is not corrected for slope and aspect, i. e. the model should be applied only to horizontal surfaces or larger areas where the effects of slope and aspect may be assumed to level out.
- The current model does not account for vegetation cover. In reality, vegetation may affect the snow dynamics in many ways (e. g. due to interception, sheltering, shadowing, long-wave emission, etc.).

4.1.2 Basics of the energy balance method

4.1.2.1 State variables

A physically-based simulation of the snow dynamics requires the water equivalent and the energy content of the snow pack to be considered as state variables (e. g. [Dyck and Peschke, 1995](#); [Tarboton and Luce, 1996](#)). In

the model described here, the snow albedo is introduced as an auxiliary state variable.

Snow water equivalent The snow water equivalent, SWE (m), represents the total volume of water (stored in solid and liquid form) contained in a snow pack covering an area of 1 m². SWE is defined by Eqn. 4.1

$$\Psi SWE = SH \cdot \frac{\rho_{snow}}{\rho_w} \quad (4.1)$$

where SH is the snow height (m) and ρ_{snow} and ρ_w represent the densities of snow and water (kg/m³). The unit of SWE or the snow height (meters) is equivalent to m³/m². To convert from units of m to units of kg/m², one has to multiply SWE with the density of water ρ_w in kg/m³ (even though a part or all of the stored water is in solid form).

Energy content The energy content, SEC (kJ/m²), represents the energy stored in the snow pack. SEC is defined relative to a reference energy content ($SEC = 0$ for ice at 0°C) as detailed below.

Snow albedo The snow albedo AS (–) represents the reflectivity of the snow surface for shortwave radiation. At each snowfall event, the snow surface is re-born and the albedo is reset to its maximum value associated with freshly fallen snow.

4.1.2.2 Processes

The dynamics of SWE is described by the mass balance and the dynamics of SEC is controlled by the energy balance. Both mass and energy balance are coupled as illustrated in Fig. 4.1. A simulation of the state variables therefore requires a simultaneous solution of

differential equations summarized in Table 4.1 using a matrix notation.

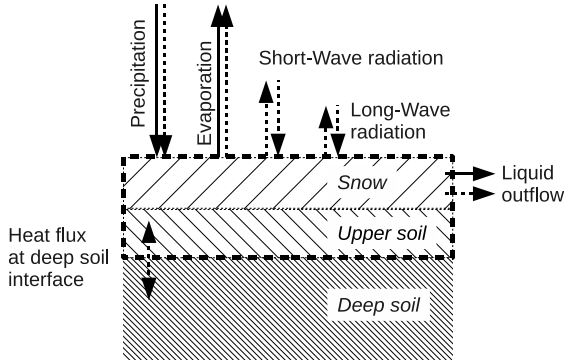


Figure 4.1: Fluxes of mass (solid arrows) and heat (dashed arrows) to be considered when simulating the snow dynamics.

4.1.2.3 Definition of the energy content

The energy content of the snow cover, SEC , can only be defined with respect to some reference. A useful reference state is ice at a temperature of 0°C for which SEC is zero by convention (Tarboton and Luce, 1996). With that reference, the relation between the energy content SEC and the (average) snow temperature T_s follows from the considerations below:

1. Negative values of SEC indicate that SWE consists of solid water only and the snow temperature is negative. The relation between temperature and energy content is then determined by the heat capacity of the ice mass according to Eqn. 4.2 (see Table 4.2 for definition of symbols).

$$\frac{dT_s}{dSEC} = \frac{1}{SWE \cdot \rho_w \cdot C_{ice}} \quad (4.2)$$

With respect to the energy content, it is useful to treat the snow cover and the upper soil up to a certain depth D_s as a single system (dashed box in Fig. 4.1). The upper soil is defined as the layer which thermally interacts with the snow cover on short time scales. Then, Eqn. 4.2 expands to Eqn. 4.3, where D_s (m) represents the depth of the upper soil, ρ_s (kg/m^3) is the soil density and C_s (kJ/kg/K) is the soil's specific heat capacity.

$$\frac{dT_s}{dSEC} = \frac{1}{SWE \cdot \rho_w \cdot C_{ice} + D_s \cdot \rho_s \cdot C_s} \quad (4.3)$$

Then advantage of treating the snow cover and the upper soil as a single system is that the soil energy flux reduces to the long-term average flux at the interface between shallow and deep soil (see Fig. 4.1). This flux is much less variable and may be approximated by a constant.

2. If SEC is zero, the temperature is 0°C and the snow cover still does not contain liquid water as a consequence of the chosen reference.
3. At positive values of SEC , some fraction of SWE exists in liquid form. As long as ice and liquid water coexist, the snow temperature remains at 0°C and all energy input is consumed by the melting process. The energy required to completely melt a snow cover at a temperature of 0°C which consists of solid water only is determined by the ice's heat of fusion (see Table 4.2) and equals (Eqn. 4.4):

$$SWE \cdot \rho_w \cdot H_{ice} \quad (4.4)$$

4. There is a critical value of SEC where all ice was melted and only liquid water is left. The snow has ceased to exist. If more energy is input, the temperature of the liquid water rises above zero according to Eqn. 4.5 (see Table 4.2 for definition of symbols).

$$\frac{dT_s}{dSEC} = \frac{1}{SWE \cdot \rho_w \cdot C_{wat}} \quad (4.5)$$

Based on these considerations, the relation between SEC and T_s can be computed for a snow cover with a given SWE as illustrated in Fig. 4.2.

With the basic relations given by Eqn. 4.2–4.5 we can infer from the energy content SEC two important variables: the temperature T_s of the snow pack and the dimensionless fraction of liquid water SLF .

4.1.2.4 Snow temperature

As the snow temperature is not simulated explicitly, it needs to be inferred from the state variables. Since snow is a good isolator, the snow surface temperature, T_{ss} , is generally different from the depth-averaged snow temperature T_s (Tarboton and Luce, 1996).

Table 4.1: Process matrix of the energy balance snow model describing the dynamics of the state variables. The rate expressions containing state variables, forcings, and parameters are derived in Sec. 4.1.4 & 4.1.5. The stoichiometry factors f_{prec} , f_{subl} , and f_{flow} (kJ/m^3) used to convert between mass and energy are derived in Sec. 4.1.2.6. The (+) indicates that precipitation has an impact on the albedo but this is considered a separate process called 'Albedo evolution' (see Sec. 4.1.3).

Process	Stoichiometry factors			Rate expr.	Rate units
	SEC (kJ/m^2)	SWE (m)	AS (-)		
Short-wave radiation balance	0.001	0	0	R_{netS}	W/m^2
Long-wave radiation balance	0.001	0	0	R_{netL}	W/m^2
Soil heat flux	0.001	0	0	G_{soil}	W/m^2
Sensible heat flux	0.001	0	0	H_{sens}	W/m^2
Precipitation	f_{prec}	1	(+)	M_{prec}	m/s
Sublimation	$-f_{subl}$	-1	0	M_{subl}	m/s
Melt water outflow	$-f_{flow}$	-1	0	M_{flow}	m/s
Albedo evolution	0	0	1	G_{alb}	1/s

Table 4.2: Snow-related physical constants (Tarboton and Luce, 1996; Dyck and Peschke, 1995).

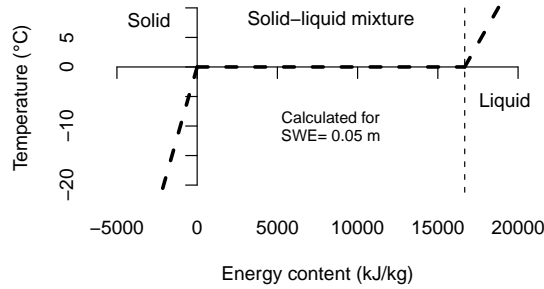


Figure 4.2: Relation between energy content and temperature for a sample snow cover with $SWE=0.05$ m (soil interaction not taken into account). The thin vertical dashed line marks the (theoretical) energy content when the snow cover consists of liquid water only, i. e. when all ice was melted.

Symbol	Value	Unit	Description
ρ_i	≈ 922	kg/m^3	Density of ice
C_{ice}	2.09	kJ/kg/K	Specific heat of ice
H_{ice}	333.5	kJ/kg	Latent heat of ice fusion (melt heat)
E_{ice}	2837	kJ/kg	Latent heat of ice sublimation ($=H_{ice}+E_{wat,0}$)
ρ_w	1000	kg/m^3	Density of water
C_{wat}	4.18	kJ/kg/K	Specific heat of water
$E_{wat,0}$	2503	kJ/kg	Latent heat of water evaporation at 0°C

Depth-averaged temperature Since the snow pack is assumed to be homogeneous, only the depth-averaged value, T_s , is directly accessible through the state variables SEC and SWE . Three cases need to be distinguished (see Sec. 4.1.2.3 for definition of D_s , ρ_s and C_s):

Case 1: ($SEC < 0$)

$$T_s = \frac{SEC}{SWE \cdot \rho_w \cdot C_{ice} + D_s \cdot \rho_s \cdot C_s} \quad (4.6)$$

Case 2: ($0 < SEC < SWE \cdot \rho_w \cdot H_{ice}$)

$$T_s = 0 \quad (4.7)$$

Case 3: ($SEC > SWE \cdot \rho_w \cdot H_{ice}$)

$$T_s = \frac{SEC - SWE \cdot \rho_w \cdot H_{ice}}{SWE \cdot \rho_w \cdot C_{wat} + D_s \cdot \rho_s \cdot C_s} \quad (4.8)$$

The equation for the first case (Eqn. 4.6) directly follows from Eqn. 4.3 by multiplying with a negative ΔSEC . The resulting temperature T_s is negative.

The conditions when Eqn. 4.7 must be used (second case) follow from the definition of SEC and Eqn. 4.4.

The third case (Eqn. 4.8) is considered here only for completeness since it represents the case where all snow became liquid, and T_s actually represents a water temperature.

Surface temperature To compute energy fluxes across the snow-atmosphere interface (outgoing long wave radiation, exchange of sensible heat, etc.), an estimate of the surface temperature T_{ss} is required.

For estimating T_{ss} , Tarboton and Luce (1996) assume that the energy fluxes at the snow surface are in equilibrium. T_{ss} , which controls some of the flux rates, is determined iteratively as the surface temperature where all energy fluxes balance. They also introduce a tuning parameter (snow surface conductance).

To avoid iteration, the very simple approach presented in Eqn. 4.9 is used here to estimate T_{ss} . Therein, TA ($^{\circ}\text{C}$) is the air temperature and μ is a weighting parameter. If $\mu = 0$, the surface temperature T_{ss} is taken to be equal to the depth-averaged temperature T_s and if $\mu = 0.5$, the surface temperature is simply computed as the mean of T_s and TA . Eqn. 4.9 accounts for the fact that T_{ss} cannot become greater than 0°C .

$$T_{ss} = \begin{cases} 0 & \text{if } T_s = 0 \\ \min(0, (1 - \mu) \cdot T_s + \mu \cdot TA) & \text{if } T_s > 0 \end{cases} \quad (4.9)$$

4.1.2.5 Fraction of liquid water

In a melting snow cover, solid and liquid water coexist. To estimate the actual rate of water outflow, the fraction of liquid water, SLF (–), must be known. Since SLF is not simulated explicitly, it needs to be inferred from state variables. Taking into account that $SLF=0$ if $SEC=0$ by definition and that the energy required to completely melt all ice ($SLF=1$) is given by Eqn. 4.4, the liquid fraction can be computed from the energy content SEC as (Eqn. 4.10)

$$SLF = \frac{SEC}{SWE \cdot \rho_w \cdot H_{ice}} \quad (4.10)$$

for $0 \leq SEC \leq SWE \cdot \rho_w \cdot H_{ice}$, i. e. for snow at 0°C . Thus, in practice one should use something like $\min(1, \max(0, SLF))$ if the condition is not checked explicitly. Note that SLF represents a *mass fraction* (Tarboton and Luce, 1996), not a volume fraction. Thus, SLF can also be written as in Eqn. 4.11,

where m_w and m_i represent the masses of water and ice per m^2 respectively.

$$SLF = \frac{m_w}{m_w + m_i} \quad (4.11)$$

Eqn. 4.11 may be transformed into Eqn. 4.10 as follows:

Numerator: As we are dealing with melting snow, the water mass m_w is at 0°C . Due to the definition of the energy content (see Sec. 4.1.2.3), the mass m_w (kg/m^2) can be substituted by SEC/H_{ice} . SEC (kJ/m^2) represents the energy content associated with m_w and H_{ice} is the fusion heat of ice (kJ/kg).

Denominator: The sum $m_w + m_i$ in the denominator of Eqn. 4.11 represents the snow mass per square meter, m_s (kg/m^2). If m_s is written as the product of snow density ρ_{snow} (kg/m^3) and snow height SH (= snow volume per m^2 in meters), it follows from Eqn. 4.1 that the denominator $m_w + m_i$ equals $SWE \cdot \rho_w$.

4.1.2.6 Relations between mass and energy fluxes

In this section, the conversion factors f_{prec} , f_{subl} , and f_{flow} (kJ/m^3) appearing in Table 4.1 are derived. The values of the involved physical constants can be found in Table 4.2.

Precipitation The energy flux ($\text{kJ}/\text{m}^2/\text{s}$) resulting from precipitation input is obtained by multiplying the mass flux (m/s) with f_{prec} (kJ/m^3). For liquid precipitation, f_{prec} is given by Eqn. 4.12 and Eqn. 4.13 applies to solid precipitation (snowfall). Note that precipitation is a water equivalent, thus, the density of water (not the one of ice) must be used when converting from depth (m) to mass (such as kg/m^2).

Case 1: ($TA > T_{crit}$)

$$f_{prec} = \rho_w \cdot C_{wat} \cdot \max(TA, 0) + \rho_w \cdot H_{ice} \quad (4.12)$$

Case 2: ($TA \leq T_{crit}$)

$$f_{prec} = \rho_w \cdot C_{ice} \cdot \min(TA, 0) \quad (4.13)$$

In Eqn. 4.12 and 4.13, TA ($^{\circ}\text{C}$) is the air temperature and T_{crit} ($^{\circ}\text{C}$) is the threshold temperature for rain/snow fall. An approach for mixed precipitation is presented in Tarboton and Luce (1996). The value of f_{prec} computed with Eqn. 4.12 is always positive and it is always negative if Eqn. 4.13 is used. Note that the second

term in Eqn. 4.12 accounts for the fact that the water is liquid and therefore has a positive energy content even at 0°C (see definition of SEC in Sec. 4.1.2.3).

Sublimation The energy flux due to sublimation ($\text{kJ/m}^2/\text{s}$) is obtained by multiplying the corresponding mass flux (m/s) with f_{subl} (kJ/m^3) defined in Eqn. 4.14. The constant E_{ice} integrates the latent heat of both melting and evaporation (see Table 4.2). As heat is lost from the snow pack, the energy flux has a negative sign in Table 4.1.

$$f_{\text{subl}} = \rho_w \cdot E_{\text{ice}} \quad (4.14)$$

Meltwater outflow To obtain the energy flux ($\text{kJ/m}^2/\text{s}$) corresponding to the outflow of water from the snow pack (m/s) one has to multiply the latter by f_{flow} (kJ/m^3) defined in Eqn. 4.15. The expression reflects that the energy of water at 0°C equals H_{ice} as a consequence of the chosen reference for SEC (see Sec. 4.1.2.3). As heat is lost from the snow pack, the energy flux has a negative sign in Table 4.1.

$$f_{\text{flow}} = \rho_w \cdot H_{\text{ice}} \quad (4.15)$$

4.1.3 Simulation of the snow albedo

There are many approaches to estimate the snow albedo AS (–) with different level of sophistication. In general, the albedo is an average value accounting for the reflection of both visible and near infrared solar radiation. After snowfall, AS generally decreases due to various processes such as metamorphosis and pollution of the snow surface. Here, a very simple aging approach cited by Dyck and Peschke (1995) was adopted. The original equation to describe the dependence of AS on the age of the snow surface (Equation 10.40 in Dyck and Peschke, 1995) is a power function (Eqn. 4.16) where AS_{min} is the minimum value that AS approaches after a long time without snowfall and AS_{rng} is the difference between the maximum AS right after snowfall and AS_{min} . Furthermore, Δt is the age of the snow surface and k (1/time) is a rate constant to describe the intensity of the aging process.

For convenience, Eqn. 4.16 was rewritten in an exponential form (Eqn. 4.17) and AS_{rng} was expanded to $(AS_{\text{max}} - AS_{\text{min}})$. In the final rearrangement, the new parameter k_{AS} was introduced which is related to the parameter k of the original power equation (Eqn. 4.16)

by $k_{AS} = -k \cdot \ln(AS_{\text{max}} - AS_{\text{min}})$. Note that reasonable values of AS are < 1 why $\ln(AS_{\text{max}} - AS_{\text{min}})$ is always negative and the minus sign is required to define k_{AS} as a positive constant.

$$\begin{aligned} AS &= AS_{\text{min}} + AS_{\text{rng}}^{(1+\Delta t \cdot k)} \\ &= AS_{\text{min}} + AS_{\text{rng}} \cdot AS_{\text{rng}}^{\Delta t \cdot k} \\ &= AS_{\text{min}} + AS_{\text{rng}} \cdot \exp(\ln(AS_{\text{rng}}^{\Delta t \cdot k})) \\ &= AS_{\text{min}} + AS_{\text{rng}} \cdot \exp(\Delta t \cdot k \cdot \ln(AS_{\text{rng}})) \\ &= AS_{\text{min}} + (AS_{\text{max}} - AS_{\text{min}}) \cdot e^{-k_{AS} \cdot \Delta t} \end{aligned} \quad (4.16) \quad (4.17)$$

The advantage of Eqn. 4.17 over the original power function (Eqn. 4.16) is the much simpler derivative with respect to time which is given in Eqn. 4.18. Note that the definition of AS (Eqn. 4.17) was used to simplify the derivative and that, in this way, the surface age (Δt) was eliminated from the expression.

$$\begin{aligned} \frac{dAS}{dt} &= (AS_{\text{max}} - AS_{\text{min}}) \cdot e^{-k_{AS} \cdot \Delta t} \cdot (-k_{AS}) \\ &= (AS - AS_{\text{min}}) \cdot (-k_{AS}) \end{aligned} \quad (4.18)$$

Considering that the snow surface is renewed when new snow falls, the process rate G_{alb} (1/s) controlling the albedo (see Table 4.1) may be expressed by Eqn. 4.19.

$$G_{\text{alb}} = \begin{cases} (AS_{\text{max}} - AS) & \text{if snowing} \\ k_{AS}(TA) \cdot (AS_{\text{min}} - AS) & \text{else} \end{cases} \quad (4.19)$$

where $X = 1$ if $((PI > 0) \& (TA > T_{\text{crit}}))$ and $X = 0$ otherwise. Note that the applied value of the rate constant k_{AS} depends on whether the air temperature is above or below 0 °C (Dyck and Peschke, 1995). Thus, G_{alb} is affected by both the precipitation intensity PI and air temperature TA . In the current model version, the albedo is independent of the snow height, i. e. there is no reduction when the snow cover becomes shallow.

Recommended values of the parameters are given in Table 4.3. A synthetic example illustrating the dynamics of the albedo in response to precipitation and temperature is shown in Fig. 4.3.

Table 4.3: Parameters controlling the snow albedo based on [Dyck and Peschke \(1995\)](#). With respect to k_{AS} , the factor $1/86400$ converts from $1/d$ to $1/s$ and the term $\ln(AS_{max} - AS_{min})$ accounts for the structural difference between Eqn. 4.17 and Eqn. 4.16.

Symbol	Units	Value
AS_{min}	–	0.35–0.4
AS_{max}	–	0.75–0.9
$k_{AS}(TA \geq 0)$	$1/s$	$-0.12/86400 \cdot \ln(AS_{max} - AS_{min})$
$k_{AS}(TA < 0)$	$1/s$	$-0.05/86400 \cdot \ln(AS_{max} - AS_{min})$

4.1.4 Energy flux rates

4.1.4.1 Short-wave radiation balance

The short-wave net radiation (or short-wave radiation balance), R_{netS} (W/m^2) is computed from Eqn. 4.20

$$R_{netS} = SR \cdot (1 - AS) \quad (4.20)$$

where SR is the incoming solar (i. e. short-wave) radiation (W/m^2) and AS (–) is the corresponding albedo of the snow surface (see Sec. 4.1.3). If measured values of SR are unavailable, they can be estimated as described in [Tarboton and Luce \(1996\)](#) or [Dyck and Peschke \(1995\)](#). No corrections for slope and aspect are made here as it is assumed that the effects level out for larger areas. If the model is applied locally, slope and aspect might need to be taken into account by reducing/amplifying the measured (or computed) solar radiation for a horizontal surface.

The presence of a dense vegetation cover (coniferous forest) may considerably reduce the amount of incoming short-wave radiation. An ad-hoc approach to estimate the corrected incoming short-wave radiation SR' due to shadowing is presented in Eqn. 4.21

$$SR' = SR \cdot \left(1 - \frac{LAI}{LAI_{r0}}\right) \quad (4.21)$$

where LAI is the leaf-area index (m^2/m^2) and LAI_{r0} is an empirical parameter. Conceptually, LAI_{r0} represents the leaf-area index where short-wave radiation is extincted completely. According to [Ludwig and Bremicker \(2006\)](#), a reduction of incoming short-wave by 30% can be assumed for coniferous forest. Assuming a leaf-area index for coniferous forest of 11

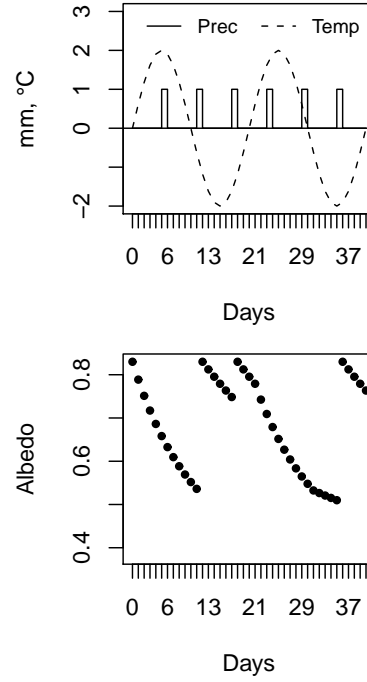


Figure 4.3: Synthetic example illustrating the dynamics of the albedo as affected by temperature and precipitation. Snowfall was assumed at temperatures below $0^\circ C$. For AS_{min} and AS_{max} , the means of the ranges given in Table 4.3 were used.

([Ludwig and Bremicker, 2006](#), page 11), this results in $LAI_{r0} \approx 36$.

4.1.4.2 Long-wave radiation balance

The long-wave radiation balance R_{netL} (W/m^2) is the difference between the incoming long-wave radiation emitted from clear sky and clouds, R_{inL} , and the long-wave emission of the snow pack, R_{outL} (Eqn. 4.22).

$$R_{netL} = R_{inL} - R_{outL} \quad (4.22)$$

According to the Stefan-Boltzmann equation (Eqn. 4.23), emissions R are proportional to the fourth power of temperature T (here in $^\circ C$), with σ being the Stefan-Boltzmann constant ($=5.67e-08 W/m^2/K^4$) and ε being the dimensionless emissivity (range 0–1 with 1 for a black body).

$$R = \varepsilon \cdot \sigma \cdot (T + 273.15)^4 \quad (4.23)$$

Outgoing part The emission of the snow pack, R_{outL} (W/m^2), can directly be computed from Eqn. 4.23 substituting T by the snow surface temperature T_{ss} (see Eqn. 4.9). The emissivity of snow is about $\varepsilon=0.82$ for old snow and $\varepsilon=0.99$ for fresh snow (Dyck and Peschke, 1995). A pragmatic way to account for the age of the snow pack is to relate ε to the dynamically computed albedo AS (see Sec. 4.1.3) as in Eqn. 4.24.

$$\varepsilon = \varepsilon_{min} + (\varepsilon_{max} - \varepsilon_{min}) \cdot \frac{AS - AS_{min}}{AS_{max} - AS_{min}} \quad (4.24)$$

Incoming part Note: The following section is based on the German wikipedia site for the term 'Atmosphärische Gegenstrahlung' as this was the most transparent and concise source of information.

The incoming long-wave R_{inL} is harder to estimate. Generally, it is distinguished between clear-sky emissions ($R_{inL,cs}$) and emissions by clouds ($R_{inL,cl}$). A transparent formulation is given by Eqn. 4.25 where $R_{inL,cs}$ and $R_{inL,cl}$ are estimated individually and FC represents the degree of cloud cover (range 0–1). It is (legitimately) assumed that long-wave emissions mainly stem from the lower atmosphere (whose state is approximately known from ground measurements).

$$R_{inL} = (1 - FC) \cdot R_{inL,cs} + FC \cdot R_{inL,cl} \quad (4.25)$$

For the cloud cover FC (–), measured values must be used or FC needs to be estimated from a comparison of actual solar radiation to the theoretical maximum value depending on the day of the year and the latitude. However, the latter approach can only yield daily estimates of FC as it does not work during nighttime.

Incoming part (Clear sky emissions) The clear sky radiation $R_{inL,cs}$ appearing in Eqn. 4.25 is computed from the Stefan-Boltzmann equation (Eqn. 4.23) substituting T by the air temperature TA and using a value of the emissivity ε representative for a clear sky. Hock (2005) lists various empirical formulas for estimation of the clear-sky ε based on atmospheric temperature and/or vapor pressure. Some formulas are compared in Fig. 4.4.

Here, we selected the simple formula developed by Brunt (Eqn. 4.26) which estimates the clear-sky ε as a

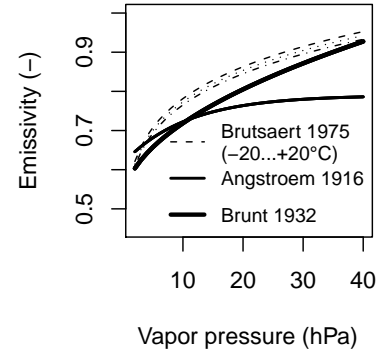


Figure 4.4: Comparison of different empirical formulas for clear sky emissivity.

function of the vapor pressure e in hPa (see Hock, 2005, p.373).

$$\varepsilon = 0.51 + 0.066 \cdot \sqrt{e} \quad (4.26)$$

Incoming part (Cloud emissions) Finally, the long-wave emissions of the clouds ($R_{inL,cl}$ in Eqn. 4.25) are also computed using Eqn. 4.23. The clouds are treated as a black body, thus ε is set to 1. A reasonable estimate of the clouds' bottom-side temperature is the dew point temperature T_{dew} ($^{\circ}\text{C}$). T_{dew} represents the temperature to which a parcel of air with a specific content of vapor must be cooled, for water vapor to condense. Thus, T_{dew} is the temperature at which air with a specific vapor content becomes saturated. T_{dew} can be computed by rearranging the Magnus-Equation (Eqn. 4.35) for the temperature T (Eqn. 4.27). The rearranged Eqn. 4.35 yields the temperature at which, for a given vapor pressure, saturation would occur. Thus, the actual vapor pressure e (not E) must be inserted in the rearranged Eqn. 4.35. If, as usual, only relative humidity and temperature are given, the value of e must be obtained from Eqn. 4.34 with E being computed with Eqn. 4.35 (now without rearrangement).

Thus, the dewpoint temperature T_{dew} follows from Eqn. 4.27 with e being computed from RH (%) and TA

(°C) after Eqn. 4.35. Results for a range of temperatures and relative humidities are presented in Fig. 4.5.

$$T_{dew} = \begin{cases} \frac{237.3 \cdot \log_{10}(e/6.11)}{7.5 - \log_{10}(e/6.11)} & \text{over water} \\ \frac{265.5 \cdot \log_{10}(e/6.11)}{9.5 - \log_{10}(e/6.11)} & \text{over ice} \end{cases} \quad (4.27)$$

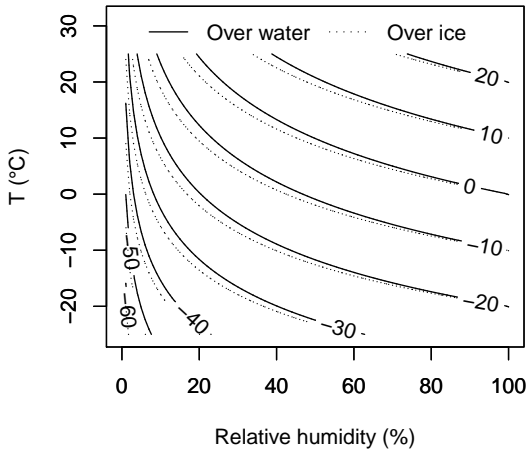


Figure 4.5: Dewpoint temperature as a function of temperature and relative humidity as computed with Eqn. 4.27.

4.1.4.3 Soil heat flux

The soil heat flux G_{soil} (W/m²) is, in this model, the long-term average flux at the interface between upper and deep soil (recall Sec. 4.1.2.3). G_{soil} is taken as zero if not known (Tarboton and Luce, 1996).

4.1.4.4 Sensible heat flux

The flux of sensible heat, H_{sens} (W/m²), is assumed to be proportional to the gradient of temperature between atmosphere (TA) and snow surface (T_{ss} , see Eqn. 4.9) as expressed by Eqn. 4.28. In this equation, D is a turbulent transfer coefficient (m/s), and ρ_{air} (kg/m³) and C_{air} (kJ/kg/K) represent the density and the specific heat capacity of air, respectively. This expression is

equivalent to Equation 34 in Tarboton and Luce (1996) or Equation 10.43 in Dyck and Peschke (1995).

$$H_{sens} = D \cdot \rho_{air} \cdot C_{air} \cdot 10^3 \cdot (TA - T_{ss}) \quad (4.28)$$

The value of the air specific heat capacity is $C_{air} = 1.005$ kJ/kg/K (Tarboton and Luce, 1996). The density of air ρ_{air} (kg/m³) is estimated from Eqn. 4.29 (see Equation 4.9 in Dyck and Peschke, 1995) that represents the ideal gas law (PA : air pressure in hPa, TA : air temperature in °C, specific gas constant for dry air: 0.287 kJ/kg/K, base of the Celsius-scale: 273.15 K).

$$\rho_{air} = \frac{PA \cdot 0.1}{0.287 \cdot (273.15 + TA)} \quad (4.29)$$

The values of C_{air} and ρ_{air} relate to dry air. However, the error in pressure due to neglect of moisture is rather low. Even at saturation, the vapor pressure is in the order of 0.5–2.5 % of the air pressure only for temperatures between 0–25 °C (see Fig. 4.6). The error in the estimate of the specific heat capacity is small as well. The value is about 1.005 kJ/kg/K for dry air (Tarboton and Luce, 1996) and about 1.013 kJ/kg/K for moist air (Dyck and Peschke, 1995, page 188, Eqn. 11.15).

The turbulent transfer coefficient D (m/s) in Eqn. 4.28 is a calibration parameter. Several approaches to estimate D do exist (e. g. Dyck and Peschke, 1995; Tarboton and Luce, 1996) making assumptions on the stability of the atmosphere and introducing other unknown parameters. Here, as in Knauf (1980), a simple approach is used that assumes a linear dependence of D on the wind speed WS in m/s according to Eqn. 4.30. The empirical coefficients a_0 and a_1 are dimensionless and must be determined by calibration.

$$D = a_0 + a_1 \cdot WS \quad (4.30)$$

4.1.5 Mass flux rates

4.1.5.1 Precipitation

The mass flux due to precipitation, M_{prec} (m/s), is computed from the precipitation intensity in units of mm/ Δt by Eqn. 4.31 where Δt is the length of the time step in seconds (e. g. $\Delta t = 3600$ for hourly precipitation data).

$$M_{prec} = \frac{PI}{10^3 \cdot \Delta t} \quad (4.31)$$

The corresponding energy fluxes are given by Eqn. 4.12 & 4.13, respectively.

4.1.5.2 Sublimation

The mass flux due to sublimation, M_{subl} (m/s) is proportional to gradient of vapor pressure between the air and the snow surface as expressed by Eqn. 4.32. In this expression, D is a turbulent transfer coefficient (m/s), ρ_{air} and ρ_w (kg/m³) represent the densities of air and water. The symbols q and q_s denote the specific humidities (–) above and at the snow surface, respectively. This expression is equivalent to Equation 35 in Tarboton and Luce (1996) or Equation 10.44 in Dyck and Peschke (1995) (with changed sign) after multiplication with the density of water ρ_w to obtain the mass flux in kg/m²/s.

$$M_{subl} = D \cdot \frac{\rho_{air}}{\rho_w} \cdot (q_s - q) \quad (4.32)$$

Only positive values of M_{subl} are considered. The density of (dry) air ρ_{air} is estimated from Eqn. 4.29 (Sec. 4.1.4.4). The specific humidity (–) can be computed from vapor pressure e and air pressure PA (both in hPa) according to Eqn. 4.33 (see Equation 4.10 in Dyck and Peschke, 1995).

$$q = \frac{0.622 \cdot e}{PA - 0.378 \cdot e} \quad (4.33)$$

Note that a commonly used approximation of Eqn. 4.33 is $q \approx 0.622 \cdot e/PA$ (Dyck and Peschke, 1995). This approximation is used, for example, by Tarboton and Luce (1996) in the derivation of their Equation 42. Note that they also substitute the pressure PA by the product of temperature, air density, and the dry air gas constant according to the ideal gas law.

The vapor pressure e (hPa) is derived from the relative humidity RH (%) by Eqn. 4.34 taking into account the vapor pressure at saturation E which is a function of temperature T .

$$e = \frac{RH}{100} \cdot E(T) \quad (4.34)$$

E is commonly estimated with the Magnus equation (Eqn. 4.35, Fig. 4.6) given by Dyck and Peschke (1995). The temperature T is the air temperature in °C.

$$E(T) = \begin{cases} 6.11 \cdot 10^{\frac{7.5 \cdot T}{237.3 + T}} & \text{over water} \\ 6.11 \cdot 10^{\frac{9.5 \cdot T}{265.5 + T}} & \text{over ice} \end{cases} \quad (4.35)$$

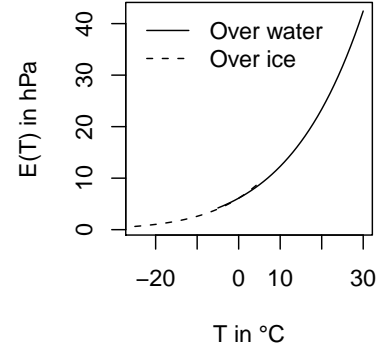


Figure 4.6: Saturation vapor pressure over water and ice as a function of temperature (Magnus formula, Eqn. 4.35).

When computing the input values for Eqn. 4.32, the saturation vapor pressure over ice (2nd form of Eqn. 4.35) must be used. When calculating the specific humidity of the atmosphere (q), one uses measured values of the air temperature, relative humidity, and air pressure in Eqn. 4.33 & 4.34. When computing the specific humidity at the snow surface (q_s), it is commonly assumed that the air is saturated at the surface temperature (Tarboton and Luce, 1996). Thus, one has to use $RH = 100$ and $T = T_{ss}$ in Eqn. 4.34 (see Eqn. 4.9 for the surface temperature T_{ss}).

For the turbulent transfer coefficient D (m/s), the same value is assumed as for the transfer coefficient of sensible heat (see Eqn. 4.30 in Sec. 4.1.4.4).

4.1.5.3 Melt water outflow

The mass flux due to meltwater outflow, M_{flow} (m/s) equals the snow pack's actual hydraulic conductivity (Male and Gray, 1981, cited in Tarboton and Luce (1996)). The actual hydraulic conductivity depends on both the saturated hydraulic conductivity $k_{sat,snow}$ (m/s) and the availability of liquid water expressed by the relative saturation RSS (–) according to Eqn. 4.36 (see Illangasekare et al., 1990).

$$M_{flow} = k_{sat,snow} \cdot RSS^3 \quad (4.36)$$

The dimensionless relative saturation RSS is defined as the relative saturation in excess of water retained

by capillary forces (Illangasekare et al., 1990; Tarboton and Luce, 1996) and can be computed as:

$$RSS = \frac{\text{liquid vol.} - \text{capillary retention vol.}}{\text{pore vol.} - \text{capillary retention vol.}} \quad (4.37)$$

Tarboton and Luce (1996) relate the capillary retention volume to the water equivalent of the solid matrix given by $SWE \cdot (1 - SLF)$. Thus, the whole Eqn. 4.37 needs to be divided by this expression. For the single terms we obtain:

Capillary retention volume

$$= \frac{\text{capillary retention volume}}{SWE \cdot (1 - SLF)}$$

$$= SCR = \text{const.}$$

Tarboton and Luce (1996) suggest a value of 0.05 for the newly introduced constant SCR .

Liquid volume

$$= \frac{\text{liquid water volume}}{SWE \cdot (1 - SLF)}$$

$$= \frac{SWE \cdot SLF}{SWE \cdot (1 - SLF)}$$

$$= \frac{SLF}{1 - SLF}$$

Pore volume

$$= \frac{\text{pore volume}}{SWE \cdot (1 - SLF)}$$

$$= \frac{\text{snow volume} - \text{solid water volume}}{SEC \cdot (1 - SLF)}$$

$$= \frac{\left(\frac{\text{mass of snow}}{\rho_{snow}} \right) - \left(\frac{\text{mass of ice}}{\rho_i} \right)}{SEC \cdot (1 - SLF)}$$

$$= \frac{\left(\frac{SWE \cdot \rho_w}{\rho_{snow}} \right) - \left(\frac{SEC \cdot (1 - SLF) \cdot \rho_w}{\rho_i} \right)}{SEC \cdot (1 - SLF)}$$

$$= \frac{1}{1 - SLF} \cdot \frac{\rho_w}{\rho_{snow}} - \frac{\rho_w}{\rho_i}$$

Collecting together all terms, Eqn. 4.37 becomes Eqn. 4.38.

$$RSS = \frac{\left(\frac{SLF}{1 - SLF} \right) - SCR}{\left(\frac{1}{1 - SLF} \cdot \frac{\rho_w}{\rho_{snow}} \right) - \left(\frac{\rho_w}{\rho_i} \right) - SCR} \quad (4.38)$$

Eqn. 4.38 is identical to Equation 48 in Tarboton and Luce (1996) except for the term $1/(1 - SLF)$ in the denominator. The reason is that, although not explicitly stated, Tarboton and Luce (1996) define ρ_{snow} in their equation 48 to be the *dry snow density*, $\rho_{snow,dry}$, which, as opposed to the common snow density ρ_{snow} , relates only for the mass of solid water to the snow volume and thus neglects the mass of liquid water (see Equation 7 in Morris and Kelly, 1990).

Recalling Eqn. 4.11 from Sec. 4.1.2.5, the equality between $(1 - SLF) \cdot \rho_{snow}$ and $\rho_{snow,dry}$ can be demonstrated

$$\begin{aligned} \rho_{snow,dry} &= \frac{m_i}{v_s} \\ &= \frac{m_i \cdot m_s}{v_s \cdot m_s} \\ &= \rho_{snow} \cdot \frac{m_i}{m_s} \\ &= \rho_{snow} \cdot \frac{m_s - m_w}{m_s} \\ &= \rho_{snow} \cdot \left(1 - \frac{m_w}{m_s} \right) \\ &= \rho_{snow} \cdot (1 - SLF) \end{aligned}$$

where m_i , m_w , and m_s (kg) represent masses of ice (solid), water (liquid), and snow (mixture of solid and liquid), respectively, and v_s (m^3) is the corresponding snow volume. Using $\rho_{snow,dry}$, Eqn. 4.38 may be rewritten as Eqn. 4.39 which is identical to Equa-

tion 48 in [Tarboton and Luce \(1996\)](#). They suggest for $\rho_{snow,dry}$ a value of 450 kg/m³.

$$RSS = \frac{\left(\frac{SLF}{1 - SLF} \right) - SCR}{\left(\frac{\rho_w}{\rho_{snow,dry}} \right) - \left(\frac{\rho_w}{\rho_i} \right) - SCR} \quad (4.39)$$

All in all, the rate of melt water outflow M_{flow} is controlled by the three free parameters listed in [Table 4.4](#).

Table 4.4: Parameters controlling the rate of meltwater outflow. Approximate values in brackets after [Tarboton and Luce \(1996\)](#).

Symbol	Units	Description
$k_{sat,snow}$	m/s	Saturated hydraulic conductivity. To be calibrated.
SCR	–	Capillary retention volume as a fraction of the solid water equivalent. [≈ 0.05].
$\rho_{snow,dry}$	kg/m ³	Snow dry density [≈ 450].

Table 4.5: Calibrated parameters of the energy balance snow model based on daily data from two sites in Germany (Fichtelberg and Kahler Asten).

Parameter	Value	Corresp. eqn.(s)
T_{crit}	0.2	Eqn. 4.12
μ	0.35	Eqn. 4.9
a_0	0.002	Eqn. 4.30
a_1	0.0008	Eqn. 4.30
ε_{min}	0.84	Eqn. 4.24
ε_{max}	0.99	Eqn. 4.24
$\rho_{snow,dry}$	450	Eqn. 4.39
$k_{sat,snow}$	4.0e-05	Eqn. 4.36
SCR	0.05	Eqn. 4.39
AS_{min}	0.55	Eqn. 4.17
AS_{max}	0.88	Eqn. 4.17
$k_{AS}(TA \geq 0)$	1.11e-06	Eqn. 4.17
$k_{AS}(TA < 0)$	4.62e-07	Eqn. 4.17
D_s	0.1	Eqn. 4.3
ρ_s	1300	Eqn. 4.3
C_s	2.18	Eqn. 4.3

4.2 Degree-day method

This method is currently *not* implemented in an any **echse**-based hydrological models.

4.1.6 Test application

The energy balance model has been tested on daily data from two mountains in Germany. The two sites are 'Kahler Asten' (Lat: 51.1814, Lon: 8.4897, Elevation: 839 m) and 'Fichtelberg' (Lat: 50.4294, Lon: 12.9553, Elevation: 1213 m). Note that coordinates are in decimal degrees.

The required meteorological data were supplied by the German Weather Service (DWD) free of charge via the 'WEBVERDIS' interface. The data are in daily resolution and some post-processing was necessary to identify gaps and to remove duplicate records. Based on the data from the two mentioned sites, a common parameter set has been identified ([Table 4.5](#)) by carrying out a sequence of Monte-Carlo simulations with successive narrowing of the sampling ranges.

A comparison of the observed and simulated snow water equivalent for the two test sites is provided in [Figs. 4.7 & Fig. 4.8](#). Note that only a selection of the data was used for model calibration. In particular, the focus was put on the melting phase since this is of special interest for flood forecasting.

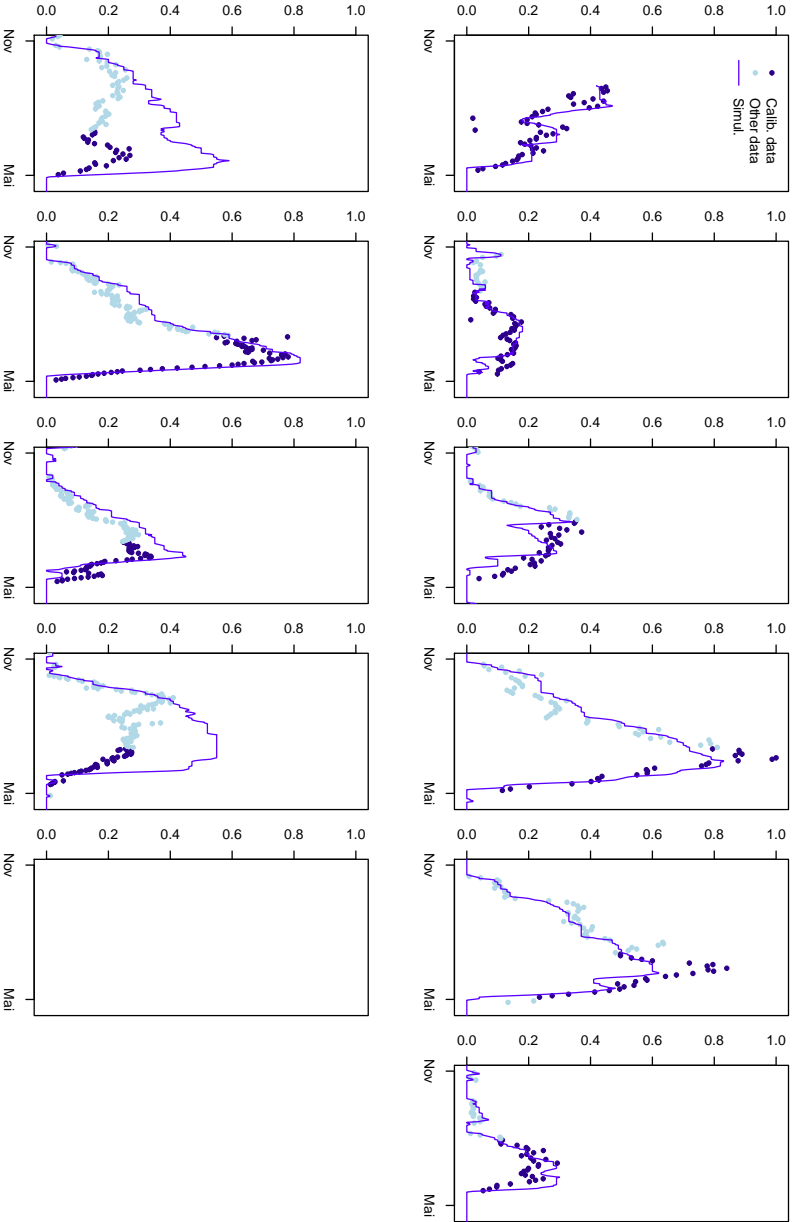


Figure 4.7: Observed and simulated snow water equivalent at DWD station 'Fichtelberg'.

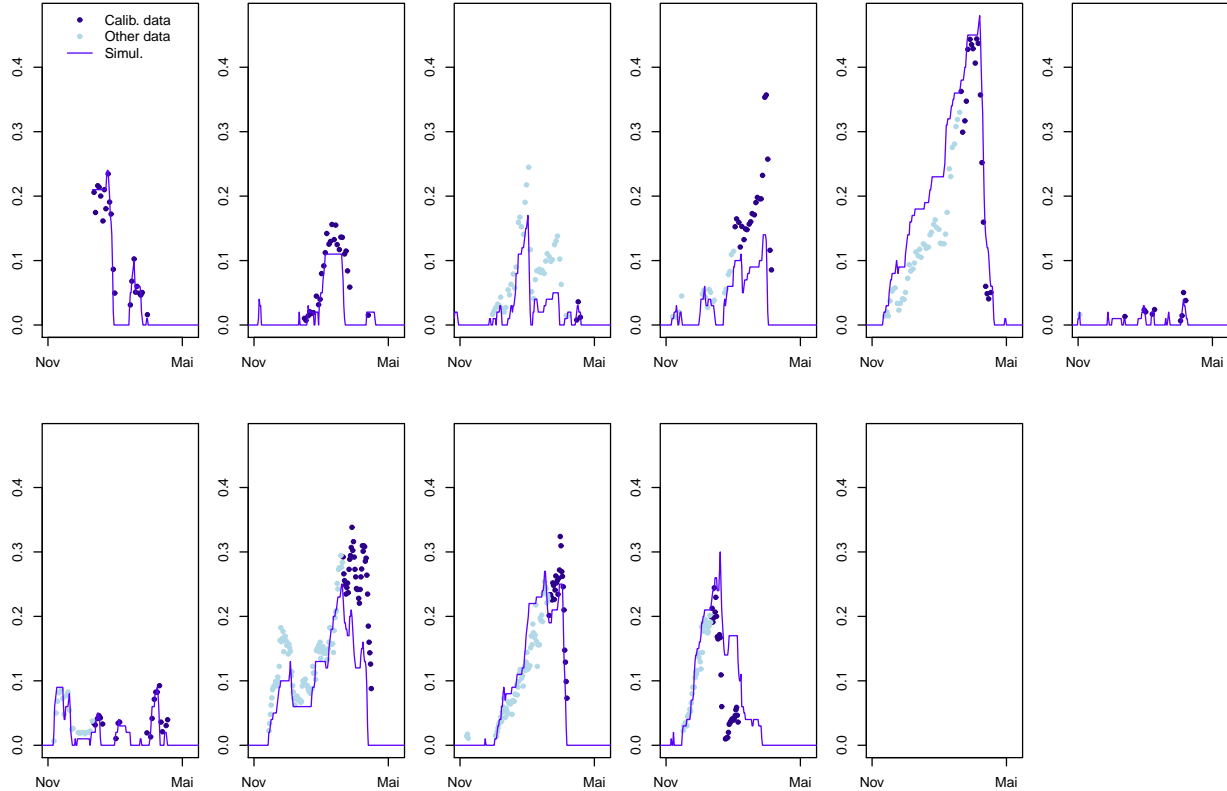


Figure 4.8: Observed and simulated snow water equivalent at DWD station 'Kahler Asten'.

Chapter 5

Runoff generation

5.1 Introduction

To avoid confusion, it is important to distinguish between the terms *runoff generation* and *runoff concentration*. As *runoff generation*, we understand the transformation of water input (rain, snow melt) into runoff *at the local scale*, i. e. at every single point of a catchment. In contrast to that, the term *runoff concentration* describes the transport of the locally generated runoff to the catchment's outlet (or the nearest river).

In some cases, the strict separation of the two terms is really pragmatic. However, it provides a clear and quite useful concept for hydrological catchment modeling.

5.2 Simple four components model

5.2.1 Processes and equations

The four components runoff generation model described here is based on the concepts used in the LAR-SIM¹ model [Ludwig and Bremicker \(2006\)](#). Originally, most equations were first presented by [Todini \(1996\)](#).

The runoff generation model is built upon the water balance of a soil column (Fig. 5.1) which can be expressed by Eqn. 5.1

$$\frac{d\theta}{dt} = \frac{WS - r_{surf} - r_{pref} - r_{int} - r_{base} - r_{evap}}{D} \quad (5.1)$$

with

θ	(-)	Soil water content as m ³ /m ³
WS	(m/s)	Rate of water supply (see Eqn. 5.2)
r_{surf}	(m/s)	Rate of surface runoff
r_{pref}	(m/s)	Rate of quick sub-surface runoff (preferential flow)
r_{int}	(m/s)	Rate of slow sub-surface runoff (interflow)
r_{base}	(m/s)	Rate of deep percolation (rate of ground water recharge)
r_{evap}	(m/s)	Rate of evapo(transpi)ration
D	(m)	Depth (thickness) of soil column.

The relevant thickness of the soil column D is equivalent to the rooted depth. Soil water at greater depths is assumed (1) to be unavailable for evapotranspiration and (2) not to contribute to lateral runoff processes.

Snow coverage of the soil column is assumed to be either 0 or 100%, i. e. partial covering is *not* simulated. As long as no snow is present, the rate of water supply to the soil column is the same as the intensity of precipitation, PI . Once a snow cover exists, all precipitation is trapped in the snow and the rate of water supply is controlled by the melt rate, r_{melt} (Eqn. 5.2). Both PI and r_{melt} are in units of m/s.

$$WS = \begin{cases} r_{melt} & \text{if snow cover is present} \\ PI & \text{else} \end{cases} \quad (5.2)$$

In the presented four components model, the generation of direct runoff² is bound to the existence of (local) soil saturation. Thus, the model accounts for surface runoff due to infiltration excess but *not* for Hortonian surface runoff.

¹Model variant '4Q-KOMP mit A2'

²Runoff being quickly generated in response to water input.

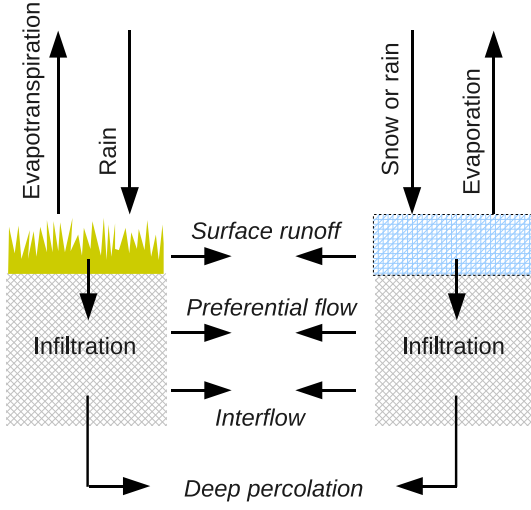


Figure 5.1: Water fluxes with respect to a soil column with (right) and without snow cover (left).

Following to the Xinanjiang approach (Zhao et al., 1980), the fraction of saturated areas f_{sat} in a catchment can be estimated from the area-integrated relative saturation of the soil S which is the ratio of the current and maximum soil water content θ and θ_{max} , respectively (Eqns. 5.3 and 5.4). The rationale of the Xinanjiang model is a positive correlation between the catchment's average wetness, represented by the relative filling of the soil reservoir and the proportion of saturated areas. In other words, the occurrence of local saturation is assumed to increase as the catchment's average wetness becomes higher.

$$S = \frac{\theta}{\theta_{max}} \quad (5.3)$$

$$f_{sat} = 1 - (1 - S)^\beta \quad (5.4)$$

The shape of the relation between S and f_{sat} is controlled by a dimensionless empirical parameter β . The effect of different values of β is illustrated in Fig. 5.2. A linear relation is assumed in the case $\beta = 1$. Note that only values of $\beta \leq 1$ are physically reasonable.

The amount of direct runoff h_d (in meters) is computed as a function of the fraction of saturated areas f_{sat} according to Eqn. 5.5

$$h_d = \begin{cases} I - (W_m - W) + W_m \cdot x^{\beta+1} & \text{if } (x > 0) \\ I - (W_m - W) & \text{if } (x \leq 0) \end{cases}$$

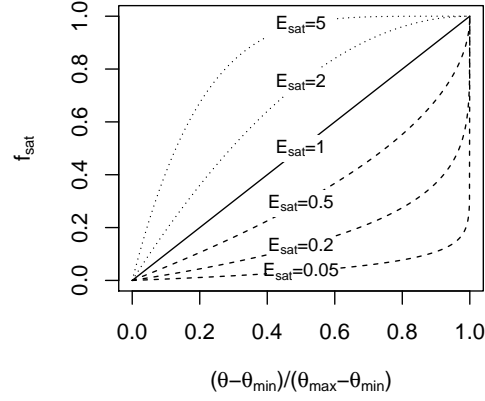


Figure 5.2: Influence of the empirical parameter β on the relation between the catchment-integrated relative filling of the soil reservoir (x-axis) and the fraction of saturated areas f_{sat} (y-axis). Only values of $\beta \leq 1$ are physically reasonable.

with

$$x = \left(1 - \frac{W}{W_m}\right)^{\left(\frac{1}{\beta+1}\right)} - \frac{I}{(1 + \beta) \cdot W_m} \quad (5.5)$$

and I being the total water input in a time step ($I = WS \cdot \Delta t$), W being the amount of water in the modeled soil column ($W = \theta \cdot D$) and W_m being the maximum capacity of the soil column ($W_m = \theta_{max} \cdot D$), all in units of meters. The derivation of this expression can be found in Todini (1996) but it has to be noted that in this publication some signs are incorrect. The corrected version is presented in Bremicker et al. (2006), for example. The relation between h_d and I according to Eqn. 5.5 is illustrated in Fig. 5.3 for fix values of W and W_m . A retention effect is visible for small to moderate water inputs. For water inputs considerably higher than the initial storage capacity of the soil, the relation between h_d and I becomes linear.

The model described here distinguished two components of direct runoff which differ with respect to retention characteristics. They may be considered as surface runoff and quick subsurface runoff through preferential flow paths. The proportion of the two components is controlled by a threshold value thr_{surf} in units of m/s.

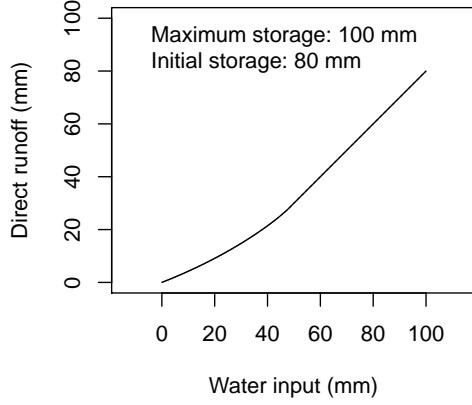


Figure 5.3: Direct runoff computed with Eqn. 5.5 for example values of soil storage and water input.

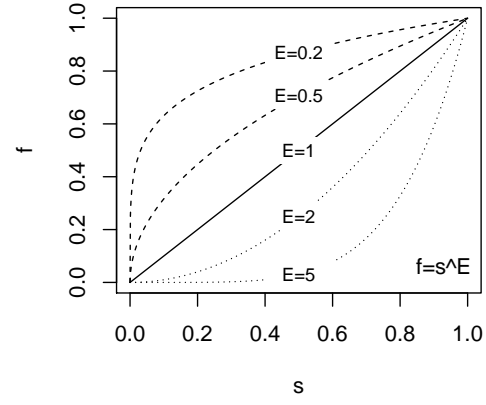


Figure 5.4: Effect of the exponent E in a formula $f = s^E$ for s in range $[0,1]$.

The rates of surface runoff and quick subsurface runoff are computed according to Eqn. 5.6 and Eqn. 5.7

$$r_{surf} = \max \left(0, \frac{h_d}{\Delta t} - thr_{surf} \right) \quad (5.6)$$

$$r_{pref} = \frac{h_d}{\Delta t} - r_{surf} \quad (5.7)$$

Thus, if the rate of direct runoff production $h_d/\Delta t$ is below the threshold thr_{surf} , only subsurface runoff is generated. Otherwise, surface runoff is generated from the excessive water. Note that the settings $thr_{surf} = 0$ or $thr_{surf} \rightarrow \infty$ effectively result in a model with only 3 runoff components.

The generation of the slow runoff components is closely linked to the relative saturation of the soil S (Eqn. 5.3). The rate of interflow runoff is computed by Eqn. 5.8 using three empirical parameters. Here, b_{int} represents a maximum rate of interflow runoff generation corresponding to total saturation of the soil. The actual rate, r_{int} , decreases at lower values of the soil saturation. If the saturation falls below a threshold level S_{int} , no interflow runoff is generated at all. The shape of the soil moisture dependence is controlled by the empirical exponent E_{int} whose effect is illustrated in Fig. 5.4 (argument s represents the fractional expression of Eqn. 5.8). The higher the value of the empirical exponent, the wetter the soil needs to be for interflow

runoff becoming an important component. At very low values of E_{int} , interflow runoff is produced almost at the maximum rate b_{int} , as soon as the soil saturation exceeds the threshold S_{int} . As in LARSIM, the parameter E_{int} is treated as a constants with a value of 1.5 (Bremicker et al., 2006).

$$r_{int} = \begin{cases} b_{int} \cdot \left(\frac{S - S_{int}}{1 - S_{int}} \right)^{E_{int}} & \text{if } S > S_{int} \\ 0 & \text{if } S \leq S_{int} \end{cases} \quad (5.8)$$

The rate of groundwater recharge (or base flow runoff), r_{base} , is computed by Eqn. 5.9 which is conceptually identical to Eqn. 5.8. Here, b_{base} is the maximum rate of groundwater recharge which corresponds to a saturated soil. If the relative saturation of the soil falls below S_{base} , the rate of groundwater recharge becomes zero. The shape of the dependence between r_{base} and S is controlled by the empirical exponent E_{base} . Again, the effect of this exponent can be seen from Fig. 5.4 (argument s represents the fractional expression of Eqn. 5.9). As in LARSIM, the parameters S_{base} and E_{base} are treated as constants with values of 0.05 and 1, respectively (Bremicker et al., 2006). Thus, only b_{base} remains as a calibration parameter.

$$r_{base} = \begin{cases} b_{base} \cdot \left(\frac{S - S_{base}}{1 - S_{base}} \right)^{E_{base}} & \text{if } S > S_{base} \\ 0 & \text{if } S \leq S_{base} \end{cases} \quad (5.9)$$

Of course, the theory described so far is only applicable to areas where soil water storage occurs. For areas covered by water or impervious surfaces, the rate of surface runoff r_{surf} equals the rate of rainfall or snow melt, respectively.

5.2.2 Combination with other models

Depending on the model's purpose and local conditions, the described runoff generation model has to be augmented with

- a model to compute snow storage and melt,
- a model to estimate evapotranspiration,
- an approach for precipitation correction (if not done externally).

5.2.3 Mathematical solution

Eqn. 5.1 is an ordinary differential equation. Depending on the use of the model, a more or less sophisticated numerical solution has to be adopted. If computation times are critical (e. g. in operational models), a simple 1st order numerical solution may be preferable. Then, however, it needs special efforts to prevent unstable or unphysical solutions. In particular, in the absence of appropriate correction terms, a 1st order solution of Eqn. 5.1 may yield a computed soil moisture θ which is negative.

5.2.4 Implementation

Table 5.1 relates the identifier names used in the model implementation (names of state variables and parameters) to the symbols used in the process equations (Sec. 5.2.1). Additional information that may be helpful when calibrating a model without any prior knowledge of parameter values is given in Sec. 5.2.5.

5.2.5 Hints for application

The parameter b_{base} specifies the rate of deep percolation under the conditions of a fully saturated soil

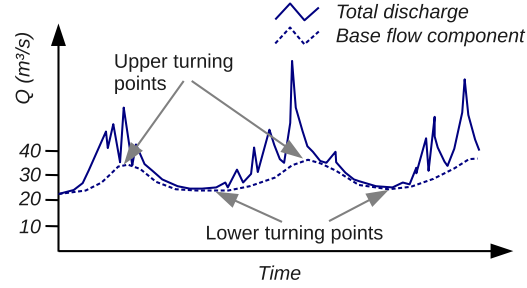


Figure 5.5: Discharge hydrograph with manually separated base flow component.

(Eqn. 5.9). At a first glance, it seems as if b_{base} could be estimated from the soil's saturated hydraulic conductivity k_f . However, at high values of the soil moisture, the other runoff components are also active and, typically, these other components are much more effective in draining the soil. Consequently, we can expect $b_{base} \ll k_f$.

A more promising approach to estimate b_{base} relies on the analysis of a discharge hydrograph (Fig. 5.5). In this figure, an approximate hydrograph of the base flow component was added. It can be drawn by hand as a smooth line connecting the annual minimum values (low flows) also touching the minima during the rainy season. Obviously, the hydrograph of the base flow component has, like any periodic function, two types of turning points. For convenience, we focus on the lower turning points here. They are easier to identify from the data without the need for any drawing, actually.

In the following we assume that the base flow component is equivalent to the outflow from a conceptual ground water reservoir. For simplicity, we may consider a linear reservoir described by Eqns. 6.1 & 6.2 (see page 57). From the differential equation, we find that, at the mentioned turning points, the derivative of the storage volume with respect to time becomes zero, hence the rates of inflow and outflow are equal. Consequently, the *base flow rate* at the turning points in a plot like Fig. 5.5 directly yields an estimate of the *rate of ground water recharge*, r_{base} , at the respective point in time.

The relation between the actual rate of ground water recharge r_{base} and the model parameter b_{base} is given by Eqn. 5.9. This can be rearranged and r_{base} can be substituted by $A \cdot Q_{base}$ where A is the size of the catchment in units of m^2 and Q_{base} is the base flow component in $\text{m}^3 \text{s}^{-1}$ (Eqn. 5.10). Using the fixed val-

Table 5.1: Symbols used in the process equations (Sec. 5.2.1), corresponding identifiers, and hints for calibration.

Symbol	Identifier	Units	Typical values	Details
θ	wc	–	–	Computed state variable
D	soildepth	m	Rooted depth	–
θ_{max}	wc_max	–	0.4–0.5	Table 9.3 on page 78
β	exp_satfrac	–	0.01–1	See Fig. 5.2
thr_{surf}	thr_surf	m/s	–	Values of 0 or near ∞ result in a 3 components model (see Eqns. 5.6 & 5.7).
S_{int}	relsat_inter	–	0.5 – 0.8	Number between 0 and 1.
r_{int}	rate_inter	m/s	example: 1.e-07	Depends on hydraulic conductivity
r_{base}	rate_base	m/s	example: 1.e-08	Depends on hydraulic conductivity

ues of S_{base} and E_{base} mentioned in Sec. 5.2.1, we end up with Eqn. 5.11.

$$b_{base} = \frac{Q_{base}}{A} \cdot \left(\frac{S - S_{base}}{1 - S_{base}} \right)^{-E_{base}} \quad (5.10)$$

$$= \frac{Q_{base}}{A} \cdot \left(\frac{0.95}{S - 0.05} \right) \quad (5.11)$$

In order to calculate b_{base} from Eqn. 5.11 we have to supply an estimate of the soil saturation S at the respective point in time (i. e. the analyzed turning point). For the lower turning points, a reasonable guess can be obtained from the soil water content at the wilting point. For a silty soil, for example, the saturation S would be ≈ 0.2 for a soil moisture at the wilting point of 0.1 and a maximum water content of 0.48 (see Table 9.3 on page 78).

The value of b_{base} obtained from the hydrograph analysis is a crude estimate. However, it might help in the definition of a proper search range for b_{base} in the context of automatic model calibration.

5.3 Process-based approaches

In contrast to the simple conceptual four components model of Sec. 5.2 the present section focuses on a process-based description of runoff generation. That means, each process of runoff generation, viz. infiltration into the soil, and vertical and horizontal soil water movement, shall be explicitly calculated. Together with evapotranspiration, interception, and snow storage and melt, which are described in independent chapters, this implicitly leads essentially to the same runoff components mentioned in Sec. 5.2.

Note that the term *process-based* refers to the explicit treatment of physical processes which are, however, often calculated using more or less empirical relationships as a detailed physical description is often not possible.

5.3.1 Soil water movement

In the following, ECHSE's process implementations of infiltration and soil water movement shall be described.

5.3.1.1 Infiltration

Infiltration is the process of water uptake by the soil surface. The amount of water that can infiltrate is determined by the infiltration capacity of the soil which depends on soil texture properties and the current moisture state.

In the following the infiltration calculation approaches implemented in ECHSE are presented. They are accessible by calling the infiltration function and selecting the specific method via a choice parameter. The function's input is presented and shortly described in Table 5.2. It returns the actual infiltration flux averaged over the simulation time step in [m s^{-1}]. The equations presented in the following refer to the infiltration capacity, i.e. the maximum possible infiltration flux f_{max} . The actual amount of infiltration f_{act} is then derived by considering the incoming surface water flux for infiltration R_f :

$$f_{act} = \min(R_f, f_{max}) \quad (5.12)$$

That means, the nonlinear infiltration process over the simulation time step is averaged to obtain a rate of volume change suitable for easy updating of the model's state variables defined in the respective model

engine.

Usage

```
infiltration(ch_inf,input,wc,wc_sat,  
ksat,delta_t,na_val,  
Hort_ini,Hort_end,Hort_k,  
Phil_s,Phil_a,Phil_cal,  
suc)
```

Table 5.2: Argument list for ECHSE’s master function infiltration in the order of occurrence (check the source code for the case of unreported changes!).

Symbol	Identifier	Unit	Explanation	Comment
General input and parameters				
–	ch_inf	–	Choice flag for infiltration method	1: Horton’s equation 2: Philip’s equation 3: Green-Ampt two-stage model for layered soil
R_f	input	m s^{-1}	Surface water flux for infiltration	Typically precipitation, reduced by interception plus interception precipitation, plus snow melt plus lateral surface water inflow
θ	wc	$\text{m}^3 \text{m}^{-3}$	Actual volumetric water content of top soil	–
θ_s	wc_sat	$\text{m}^3 \text{m}^{-3}$	Volumetric water content at saturation of top soil	–
k_f	ksat	m s^{-1}	Saturated hydraulic conductivity	–
Δt	delta_t	s	Time step length	Temporal resolution of the model; use ECHSE’s internal parameter! (only argument for the <code>simulate</code> method, cf. Kneis (2012b))
–	na_val	–	Numeric value treated as <i>not available</i> (NA)	Input quantities having the specified value will be internally treated as NA (e.g. for input checks)
Horton’s equation specific parameters				
f_i	Hort_ini	m s^{-1}	Initial infiltration rate	Parameter for Horton’s equation; should be estimated from infiltration experiments or calibrated
f_e	Hort_end	m s^{-1}	Final infiltration rate	Parameter for Horton’s equation; should be estimated from infiltration experiments or calibrated
β	Hort_k	m s^{-1}	Decay constant	Parameter for Horton’s equation describing infiltration decay from f_i to f_e over time; should be estimated from infiltration experiments or calibrated
Philip’s equation specific parameters				
S	Phil_s	$\text{m s}^{-1/2}$	Sorptivity	Parameter for Philip’s equation; should be estimated from infiltration experiments or calculated from soil parameters, see Sec. 5.3.1.1

Continued on next page.

Continued from previous page.

A	Phil_a	m s^{-1}	Parameter	Parameter for Philip's equation; should be estimated from infiltration experiments or estimated from k_f and k_A , see Sec. 5.3.1.1
k_A	Phil_cal	–	Calibration parameter	Calibration parameter for Philip's equation; for estimation of A , in the range of [0.2..1.0], see Sec. 5.3.1.1
Green-Ampt specific parameters				
ψ_f	suc	m	Capillary suction at the wetting front	Soil-specific parameter, can be derived by pedotransfer functions; note that unit [m] is approximately equal to 100 hPa

Horton's equation The infiltration model of Horton is a famous and simple empirical relationship and already applied for a long time (Horton, 1933). It is based on the observation that the infiltration capacity f during an event exponentially declines since onset of the storm (time t) from an initial value f_i approaching a constant value f_e whereas the shape of the decline is defined by a shape parameter β (Horton, 1939):

$$f = f_e + (f_i - f_e)e^{-\beta t} \quad (5.13)$$

Integration leads to the potentially cumulated infiltration:

$$F = f_e t + \frac{1}{\beta}(f_i - f_e)(1 - e^{-\beta t}) \quad (5.14)$$

The parameters are empirical and to be derived from infiltration experiments. However, for specific soil types values are reported in the literature that could be used (e.g. Maidment (1993)).

Note that this equation should be applied to a single event whereas a typical application within ECHSE at discrete time steps would treat each call to the infiltration function as individual event. Soil moisture is not explicitly accounted for. You should therefore **not** use this approach in a typical continuous discrete time step application but apply it only to a single event! A further assumption is that incoming surface water flux for infiltration is at all times larger than the infiltration capacity. Recovery of infiltration capacity after an rainfall event is also not accounted for.

Philip's equation Philip's equation was directly derived from Richards equation (i.e. Darcy's law combined with the continuity equation) of flow through porous media. It was developed from the vertical description of flow assuming a homogeneous semi-infinite medium with constant initial soil moisture content and excess water available at the surface. The partial differential equation was approximated by a power series in $t^{1/2}$ whereas only the first two terms were considered as important and rearranged gave the simplified physically-based empirical equations for (potential) infiltration flux f and the cumulated infiltration F as (Philip, 1957a,b):

$$f = \frac{1}{2}St^{-1/2} + A \quad (5.15)$$

and

$$F = St^{1/2} + At \quad (5.16)$$

with

- t Time since start of infiltration event (s)
- S Sorptivity, see text ($\text{m s}^{-1/2}$)
- A Parameter proportional (but not equal to) saturated hydraulic conductivity, see text (m s^{-1})

For small t the first term of the equation is dominant, simulating horizontal water movement as function of $t^{1/2}$ and sorptivity. The latter was the most dominant quantity of the first term in the derivation of the equation where Philip (1957b) interpreted the physical meaning as being "*a measure of the capillary uptake or removal of water*". As it hence embraces both adsorption and desorption the more general term *sorptivity* was chosen for the parameter. It is a property of the medium, depending on soil texture and initial soil moisture content, and should be derived from experiments. However, there also exist some relations to soil properties. Currently implemented in ECHSE is an approach which already appeared in Green and Ampt (1911) (though not under the term *sorptivity* which was defined by Philip (1957b)) as given by Stewart et al. (2013):

$$S = \sqrt{2k_f(\theta_s - \theta)\psi_f} \quad (5.17)$$

Usage

sorptivity(wc, wc_sat, ksat, suc)

with

- θ Actual volumetric water content of top soil, wc ($\text{m}^3 \text{m}^{-3}$)
- θ_s Volumetric water content at saturation of top soil, wc_sat ($\text{m}^3 \text{m}^{-3}$)
- ψ_f Capillary suction at the wetting front; soil-specific parameter, can be derived by pedotransfer functions; suc (m); **note** that unit is approximately equal to 100 hPa

k_f Saturated hydraulic conductivity, k_{sat} (m s^{-1})

This function is called internally if, when calling the `infiltration` function, `sorptivity` (`Phil_s`) was set to NA (`na_val`). [Stewart et al. \(2013\)](#) also gives a better approximation of sorptivity which is, however, much more complicated and requires to solve an integral and was thus not yet implemented in ECHSE.

For growing t the second term becomes more and more dominant as, when the soil becomes more saturated, gravitation is dominant over capillary pressure. It is clear that for $t \rightarrow \infty$ the infiltration rate approximates the saturated hydraulic conductivity k_f . Due to the power series approximation in the derivation of the equation, however, parameter A can be related but is not equal to k_f . This also implies that the equation fails for large t (in a test study in [Philip \(1957b\)](#) the error for 10^6 s, i.e. about 11.5 days, was 5 %). Ideally, this parameter should as well be estimated from infiltration experiments. However, if the parameter (`Phil_a`) is set to NA (`na_val`) when calling `infiltration` it is approximated from k_f (as, e.g., in [Kreye et al. \(2010\)](#)):

$$A = k_f k_A \quad (5.18)$$

with k_A being a parameter roughly in the the range of [0.2..1.0] that should be calibrated.

Green-Ampt two-stage approach for homogeneous layered soil The approach implemented in ECHSE is based on the approach used in the WASA ([Güntner, 2002](#)) and WaSiM-ETH ([Schulla, 1997](#)) models which build upon the semi-physical suction gradient-based method of [Green and Ampt \(1911\)](#) and the extended two-stage model for layered soils. In the German language community this approach is often referred to [Peschke \(1977, 1987\)](#) whereas the oldest publications of this method I could so far (Feb. 2016) find are [Mein and Larson \(1971, 1973\)](#). See also common text books such as [Dyck and Peschke \(1995\)](#) or [Chow et al. \(1988\)](#) for an English version.

First the refillable porosity is calculated:

$$n_r = \theta_s - \theta \quad (5.19)$$

with

n_r Refillable porosity (–)
 θ Actual volumetric water content of top soil, w_c ($\text{m}^3 \text{m}^{-3}$)
 θ_s Volumetric water content at saturation of top soil, w_{c_sat} ($\text{m}^3 \text{m}^{-3}$)

and if the soil is saturated, i.e. if $n_r = 0$, the function will return an infiltration rate equal to saturated hydraulic conductivity k_f . If the soil is not saturated and the incoming water flux is less than or equal to k_f , all the incoming water may infiltrate over the simulation time step and no saturated of the soil surface will occur. If the incoming water flux, however, is larger than k_f the approach implies a sharp wetting front evenly propagating through the soil. Initiation of infiltration is largely dominated by the matric potential. With successive wetting infiltration approaches k_f and the process is maintained by gravitation. The part above the wetting front is assumed to be at saturation whereas antecedent soil moisture is assumed for the soil below. The depth of the wetting front at the point of saturation of soil surface can be calculated using the following relation:

$$D_{wet} = \frac{\psi_f}{R_f/k_f - 1} \quad (5.20)$$

with

D_{wet} Depth of wetting front at saturation (m)
 ψ_f Capillary suction at the wetting front; soil-specific parameter, can be derived by pedotransfer functions; suc (m); **note** that unit is approximately equal to 100 hPa
 R_f Surface water flux for infiltration (precipitation, reduced by interception plus interception precipitation, plus snow melt plus lateral surface water inflow), `input` (m s^{-1})
 k_f Saturated hydraulic conductivity, k_{sat} (m s^{-1})

which leads to the total amount of potentially infiltrated water at saturation:

$$F_s = D_{wet} n_r \quad (5.21)$$

and the time until saturation (also referred to as *ponding time*):

$$t_{sat} = \frac{F_s}{R_f} \quad (5.22)$$

with

F_s Amount of infiltrated water at saturation (m)

t_{sat} Time until saturation occurs (s)

If t_{sat} is larger than the simulation time step no saturation will occur and actual infiltration rate equals incoming water flux at the soil surface, i.e. no surface runoff will be generated and all water at the surface infiltrates. Otherwise water can infiltrate until t_{sat} . After that, infiltration rate decreases approaching k_f and ponding of the soil surface (i.e. generation of surface runoff) occurs. The accumulated amount of potential infiltration at the end of the simulation time step can be calculated by iteratively solving the following equation (for deviation see, e.g., Schulla (1997) or Chow et al. (1988)):

$$F_{\Delta t} = k_f(\Delta t - t_{sat}) + n_r \psi_f \cdot \ln \left(\frac{F_{\Delta t} + n_r \psi_f}{F_s + n_r \psi_f} \right) + F_s \quad (5.23)$$

with

$F_{\Delta t}$ Potential amount of infiltrated water at the end of the simulation time step (m)

Δt Time step length, `delta_t`, internal variable of `simulate` method (s)

For the iteration the absolute error as break condition was defined to be smaller than 0.0001 and as initial condition half of the input still left for infiltration was defined (note that a mathematically more sound method such as *Newton iteration* might be more efficient):

$$F_{\Delta t, init} = \frac{R_f(\Delta t - t_{sat})}{2} + F_s \quad (5.24)$$

Note that the depth of the wetting front might be greater than the depth of the considered soil horizon! This should be accounted for within the model engine

when calling the infiltration routine (e.g. by comparing refillable porosity of the soil horizon with the amount of infiltration derived from the infiltration function and distributing excess infiltration water to the next horizon(s)).

Furthermore, note the following underlying assumptions:

- Homogeneous soil without macropores and preferential flow
- Continuous evenly distributed incoming surface water flux over the simulation time step
- Soil surface is completely wet
- No soil compaction or erosion from rain drops
- No shrinkage or swelling of soil
- Soil Matrix initially is uniformly dry with a specific water content
- Distinct wetting front during infiltration
- Wetting front suction constant over time and space
- Soil behind wetting front is uniformly wet with constant hydraulic conductivity

5.3.1.2 Percolation

Percolation (as defined herein) is the downward vertical movement of water through the soil column. It is caused by gravity and, by definition, may only occur if the current water content (θ) of the considered soil element is above field capacity (θ_{fc}), i.e. if there is excess water available that is not hold against gravity within the soil element by the matric potential.

Storage routing approach In ECHSE a simple storage routing approach was integrated following the implementation in the WASA model as described by Güntner (2002), similar to the approach in SWAT (Neitsch et al., 2011). The amount of water available for percolation (SW_{perc} in [m]) is calculated by:

$$SW_{perc} = \begin{cases} 0 & \text{if } \theta \leq \theta_{fc} \\ D_{hor}(\theta - \theta_{fc}) & \text{otherwise} \end{cases} \quad (5.25)$$

The unsaturated hydraulic conductivity (k_u in $[\text{m s}^{-1}]$), following the *Van Genuchten* approach (Maidment, 1993):

$$k_u = k_f \left(\frac{\theta - \theta_r}{\theta_s - \theta_r} \right)^{1/2} \left\{ 1 - \left[1 - \left(\frac{\theta - \theta_r}{\theta_s - \theta_r} \right)^{1/m} \right]^m \right\}^2 \quad (5.26)$$

leads to an estimation of the travel time (TT in $[\text{s}]$) of the excess water through the soil column (i.e. the retention constant of the storage approach):

$$TT = \frac{SW_{perc}}{k_u} \quad (5.27)$$

and, finally, the percolation rate (q_{perc} in $[\text{m s}^{-1}]$) can be obtained from the storage approach:

$$q_{perc} = SW_{perc} \left[1 - \exp\left(\frac{-\Delta t}{TT}\right) \right] / \Delta t \quad (5.28)$$

usage

`percolation(wc, hor_depth, wc_fc, wc_sat, wc_res, ksats, pores_ind, delta_t)`

with

D_{hor}	Thickness of current soil column, <code>hor_depth</code> (m)
θ	Actual volumetric water content of the current soil column, <code>wc</code> ($\text{m}^3 \text{m}^{-3}$)
θ_{fc}	Volumetric water content at field capacity of the current soil column, <code>wc_fc</code> ($\text{m}^3 \text{m}^{-3}$)
θ_r	Residual volumetric water content of the current soil column, <code>wc_res</code> ($\text{m}^3 \text{m}^{-3}$)
θ_s	Volumetric water content at saturation of the current soil column, <code>wc_sat</code> ($\text{m}^3 \text{m}^{-3}$)
m	Parameter: $m = \frac{\lambda}{\lambda+1}$
λ	Pore-size index, <code>pores_ind</code> (-)
k_f	Saturated hydraulic conductivity, <code>ksats</code> (m s^{-1})

Δt Time step length, `delta_t`, internal variable of `simulate` method (s)

5.3.1.3 Lateral subsurface flow

Lateral subsurface flow is the horizontal flow of water through the soil column. As percolation it is caused by gravity and, by definition, may only occur if the current water content (θ) of the considered soil element is above field capacity (θ_{fc}), i.e. if there is excess water available that is not hold against gravity within the soil element by the matric potential. This further implies that lateral subsurface flow only occurs if the soil profile is inclined.

Darcy-based approach A simple method to quantify lateral subsurface outflow from the soil element is to apply Darcy's law for saturated flow as done by Güntner (2002). Lateral flow thereby may occur only if the actual water content of the soil is above field capacity. If this is the case, within the approach first the excess water depth ready for lateral redistribution is calculated as:

$$d_s = D_{hor} \frac{\theta - \theta_{fc}}{\theta_s - \theta_{fc}} \quad (5.29)$$

with

d_s	Depth of excess water depth in the soil (m)
D_{hor}	Thickness of current soil column, <code>hor_depth</code> (m)
θ	Actual volumetric water content of the current soil column, <code>wc</code> ($\text{m}^3 \text{m}^{-3}$)
θ_{fc}	Volumetric water content at field capacity of the current soil column, <code>wc_fc</code> ($\text{m}^3 \text{m}^{-3}$)
θ_s	Volumetric water content at saturation of the current soil column, <code>wc_sat</code> ($\text{m}^3 \text{m}^{-3}$)

Lateral outflow is then calculated following Darcy's equation whereas the flow gradient is determined by the inclination of the soil column:

$$Q_{lat} = A_{flow} k_{fs} \quad (5.30)$$

with

Q_{lat}	Lateral outflow rate from the soil element ($\text{m}^3 \text{s}^{-1}$)
A_{flow}	Flow's cross section area (m^2)
s	Slope gradient of the hillside, s_{slope} (m m^{-1})
k_f	Saturated hydraulic conductivity, k_{sat} (m s^{-1})

whereas the flow's cross section area can be determined from the width of the soil unit (the length perpendicular to hillside inclination) and d_s :

$$A_{flow} = l_{width} d_s = \frac{A_{soil}}{l_{slope}} d_s \quad (5.31)$$

with

l_{width}	Width of the soil unit, perpendicular to hillside inclination (m)
A_{soil}	Surface area of the soil element (m^2)
l_{slope}	Sloplength, i.e. length of soil element in (average) flow direction; parameter that can be derived from terrain analysis, e.g. via GIS, <code>sloplength</code> (m)

Normalizing by A_{soil} finally gives:

$$q_{lat} = \frac{d_s}{l_{slope}} k_f s \quad (5.32)$$

Usage

```
latflow(hor_depth, wc, wc_fc,
        wc_sat, ksat, sloplength, slope)
```

Note that q_{lat} in Eqn. 5.32 is **not** equal to the *Darcy flux* (although it has the same units of a velocity)!

Furthermore, the approach implies several assumptions that usually cannot be fulfilled:

- Darcy's equation requires saturation whereas herein soil moisture must only exceed field capacity
- Pressure gradient is equal to hillside inclination
- Water flow occurs only in a well-separated part of the soil (where $\theta > \theta_{fc}$)
- The soil element is rectangularly shaped

When deriving l_{slope} it should be noted that common GIS tools usually calculate the sloplength for an entire hillslope and thus has to be reduced to the soil element if the hillslope contains several soil units, e.g. by multiplying the hillslope's sloplength by the areal fraction of the respective soil unit, depending on your landscape discretization scheme.

5.3.2 Runoff generation

Runoff directly deviates from the processes of infiltration and soil water movement described above. It can be roughly divided into the components *surface* runoff, *subsurface* runoff, and *groundwater* runoff (or *base-flow*). However, no clear definitions exist. E.g., in the four components approach introduced in Sec. 5.2 subsurface runoff is divided into a quick and a slow component. Inferring runoff from the process rates is part of the model engine development and no function will be presented here. A suggestion is to define each runoff component as a state variable and update the state variables based on summation of process rates. Runoff concentration at the watershed outlet or at the river can then be treated separately (see Chap. 6).

In the following, some brief guidelines of how to obtain runoff components shall be given.

5.3.2.1 Surface runoff

Surface runoff can be obtained from infiltration. If the rate of incoming water (precipitation, reduced by interception plus interception precipitation, plus snow melt plus lateral surface water inflow) exceeds the infiltration capacity the resulting excess water is laterally distributed as surface runoff (commonly referred to as *infiltration-excess* or *Hortonian* runoff). I.e. it is the difference between input and the output of the function `infiltration`.

On the other hand, if water at the surface cannot infiltrate due to saturation of the soil the occurring runoff in this case is typically called *saturation-excess* runoff. To account for natural heterogeneity of soil moisture it is possible to calculate the areal fraction of saturation of

a soil unit, e.g. as in the WASA model (Güntner, 2002) using:

$$a_{sat} = \begin{cases} a_1 & \text{if } \theta \leq \theta_{c,1} \\ a_1 + (a_2 - a_1)(1 - \frac{\theta_{c,2} - \theta}{\theta_{c,2} - \theta_{c,1}}) & \text{if } \theta_{c,1} < \theta \leq \theta_{c,2} \\ a_2 + (a_3 - a_2)(1 - \frac{\theta_{c,3} - \theta}{\theta_{c,3} - \theta_{c,2}}) & \text{if } \theta_{c,2} < \theta \leq \theta_{c,3} \\ a_3 + (a_4 - a_3)(1 - \frac{\theta_{c,4} - \theta}{\theta_{c,4} - \theta_{c,3}}) & \text{if } \theta_{c,3} < \theta \leq \theta_{c,4} \\ a_4 + (a_5 - a_4)(1 - \frac{\theta_{c,5} - \theta}{\theta_{c,5} - \theta_{c,4}}) & \text{if } \theta_{c,4} < \theta \leq \theta_{c,5} \\ a_5 & \text{if } \theta > \theta_{c,5} \end{cases}$$

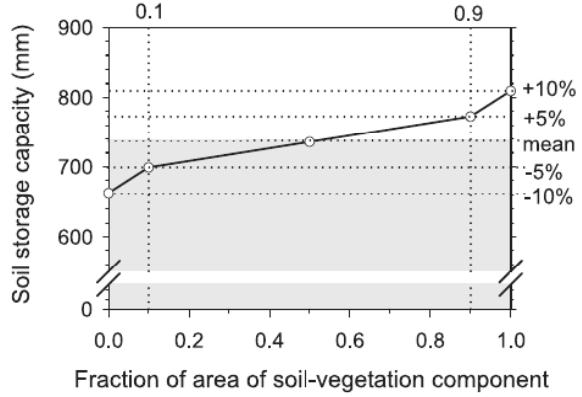
(5.33) **Figure 5.6:** Example for the computation of saturated fraction of a soil unit from actual water content as given by Eqn. 5.33. Graphic copied from Güntner (2002). Units shown deviate from Eqn. 5.33!

usage

f_saturation(wc, wc_sat, var1, var2, var3, var4, var5, frac1, frac2, frac3, frac4, frac5)

with

- a_{sat} Areal fraction of saturation of the soil unit ($\text{m}^2 \text{m}^{-2}$)
- θ Depth-weighted average of actual volumetric water content of the soil profile, wc ($\text{m}^3 \text{m}^{-3}$)
- θ_s Depth-weighted average of volumetric water content at saturation of the soil profile, wc_{sat} ($\text{m}^3 \text{m}^{-3}$)
- $\theta_{c,1}$ $\theta_s c_{var,1}$; first parts of the soil unit become saturated, should be greater than field capacity, var1 (-)
- $\theta_{c,2}$ $\theta_s c_{var,2}$, second node, var2 (-)
- $\theta_{c,3}$ $\theta_s c_{var,3}$, about half the soil is saturated, var3 (-)
- $\theta_{c,4}$ $\theta_s c_{var,4}$, fourth node, var4 (-)
- $\theta_{c,5}$ $\theta_s c_{var,5}$, soil is saturated, $c_{var,5} > c_{var,4} > c_{var,3} > c_{var,2} > c_{var,1}$, var5 (-)
- a_1 Areal fraction of first node point; typically zero, frac1 ($\text{m}^2 \text{m}^{-2}$)
- a_2 Areal fraction of second node point, frac2 ($\text{m}^2 \text{m}^{-2}$)
- a_3 Areal fraction of third node point; typically 0.5, frac3 ($\text{m}^2 \text{m}^{-2}$)
- a_4 Areal fraction of fourth node point, frac4 ($\text{m}^2 \text{m}^{-2}$)



a_5 Areal fraction of fifth node point; typically one, frac5 ($\text{m}^2 \text{m}^{-2}$)

See Fig. 5.6 for an illustration of the function. Based on the specified node points (varN define the ordinate and fracN the abscissa of the diagram, respectively) the saturated areal fraction of the soil element is linearly interpolated between the node points based on the current soil moisture state.

When using function f_saturation saturation excess flow can be determined by multiplying incoming surface water flux with the saturated areal fraction of the soil. The remaining part can be given to the infiltration routine. If f_saturation is not used saturation excess surface runoff occurs only when the soil is completely saturated (you should check that before calling infiltration in order to be able to deviate the two types of surface runoff).

5.3.2.2 Subsurface runoff

Subsurface runoff within the physical based approach can be directly determined from lateral excess runoff (i.e. simply the output of function latflow). Further discrimination between a faster (e.g. preferential flow) and slower component is so far not possible.

5.3.2.3 Groundwater runoff

Groundwater runoff (or *baseflow* although in some definitions this also includes slow subsurface runoff) can

be deviated from function `percolation`. It is simply the percolation from the deepest soil horizon. To account for travel time through an unsaturated zone below the soil profile a storage routing approach could be applied before adding the percolation output to the groundwater storage.

5.4 Contributions and TODOs

The following work still has to be done or issues need to be resolved:

- Add more approaches, e.g.
 - Better approximation of sorptivity and suction at wetting front ([Stewart et al., 2013](#))
 - Horton: account for soil moisture state and discrete time steps/intermittent rainfall (promising approaches: [Ludwig et al. \(2010\)](#); [Bauer \(1974\)](#); [Green \(1986\)](#); [Rossman and Huber \(2016\)](#))
- Create separate function to calculate unsaturated hydraulic conductivity and matric potential with several alternatives (so far only *Van Genuchten* considered; could be extended by, e.g., *Brooks and Corey* and/or *Campbell*, [Maidment \(1993\)](#))
- Include macro pore/preferential flow
- Include capillary rise
- Account for ponding of soil profile from lower layers
- Somehow possible to include the Richards equation? Must be solved numerically, I think each soil layer would have to be somehow subdivided into smaller instances during solving...

Chapter 6

Runoff concentration

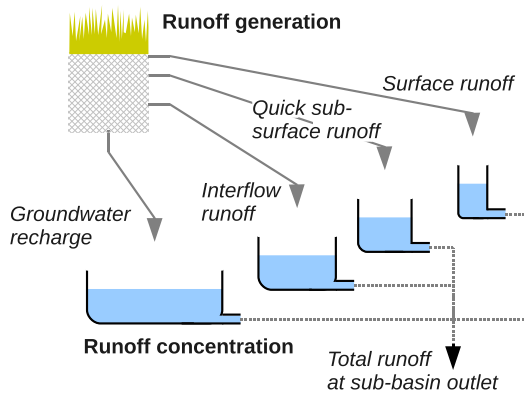


Figure 6.1: Parallel storage model for the case of four runoff components.

6.1 Introduction

The term *runoff concentration* describes the transport of the locally generated runoff (see Chap. 5) to the catchment's outlet or the nearest river. In general, the description of water transport covers the phenomena of translation and retention.

6.2 Parallel storage model

6.2.1 Processes and equations

In the parallel storage model, it is assumed that runoff concentration can be computed separately for the individual runoff components. For each component, translation and retention is simulated by means of a simple reservoir model. The cumulated runoff from the parallel reservoirs finally represents the sub-basins total runoff (Fig. 6.1).

Following the approach used in LARSIM (Ludwig and Bremicker, 2006), all reservoirs depicted in Fig. 6.1 are of the linear type. Thus, in addition to the mass balance (Eqn. 6.1), the linear relation of Eqn. 6.2 applies to each reservoir.

$$\frac{dv}{dt} = q_{in} - q_{out} \quad (6.1)$$

v	Storage volume	L^3
q_{in}	Inflow rate	L^3/T
q_{out}	Outflow rate	L^3/T

$$q_{out} = \frac{1}{k} \cdot v \quad (6.2)$$

k	Retention constant	T
-----	--------------------	---

Eqns. 6.1 and 6.2 can be combined and integrated over time using the substitution method. Assuming that the inflow rate q_{in} is constant over a discrete time step, the integration yields Eqn. 6.3 as the solution for the storage volume.

$$v(t_0 + \Delta t) = (v(t_0) - q_{in} \cdot k) \cdot e^{(-\Delta t/k)} + q_{in} \cdot k \quad (6.3)$$

$v(t_0)$	Initial storage at	L^3
Δt	Length of time step	T

The only parameters in this runoff concentration model are the values of the retention constants k (one for each reservoir shown in Fig. 6.1). Regarding these constants, we can formulate two expectations:

1. Larger values of k result in a higher retention effect and thus in a more delayed input-output reaction (Fig. 6.2). Consequently, we expect the highest k value for the groundwater reservoir while the smallest k value corresponds to the reservoir describing the concentration of surface runoff.

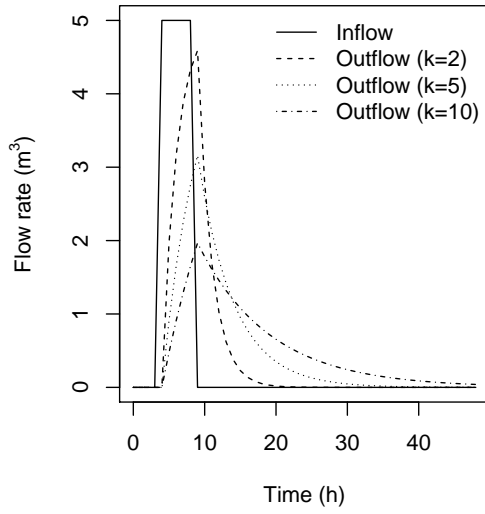


Figure 6.2: Outflow hydrographs from a single linear reservoir for an identical input signal but different storage constants k (hours).

2. Furthermore, it seems legitimate to assume a relation between the k values and the characteristics of a sub-basin. In particular, we expect smaller retention constants in regions with steep hill slopes, dense drainage networks, and for sub-basin of compact shape.

To take these two aspect into account, it is convenient to define the retention constants as in Eqns. 6.4 to 6.7.

$$\text{Surface runoff:} \quad k = S_{surf} \cdot CTI \quad (6.4)$$

$$\text{Preferential flow:} \quad k = S_{pref} \cdot CTI \quad (6.5)$$

$$\text{Interflow:} \quad k = S_{inter} \cdot CTI \quad (6.6)$$

$$\text{Base flow:} \quad k = S_{base} \cdot CTI \quad (6.7)$$

Here, S_{surf} , S_{pref} , S_{inter} , and S_{base} are dimensionless calibration parameters, fulfilling $S_{surf} < S_{pref} < S_{inter} < S_{base}$ (recall 1st point of above enumeration). Furthermore, CTI is an indicator of the sub-basin's runoff concentration characteristics having the dimension of a time (2nd point of above enumeration). For estimating the CTI different approaches do exist. In LARSIM (Ludwig and Bremicker, 2006), for example, an empirical formula derived by Kirpich (1940) is used. This one computes the CTI from the average length

and slope of the major reach(es) in a sub-basin. Alternatively, a CTI can be derived by analysis of a digital elevation model. This approach is described in the documentation of the **topocatch** preprocessor (see Kneis, 2012a).

See Sec. 6.2.4 for the relation between the k values and the half-life time τ .

The inflow rate q_{in} (m³/s) appearing in Eqns. 6.1 to 6.3 is generally obtained by multiplying the runoff rate (m/s) by the contributing area (m²). For the reservoir describing the concentration of surface runoff, q_{in} is usually composed of the runoff generated on saturated soils, water surfaces, and also impervious surfaces.

6.2.2 Mathematical solution

In each time step, the storage of the four reservoirs is updated based on Eqn. 6.3 using the individual inflow rates and retention constants (Eqns. 6.4 to 6.7). The total outflow from a sub-basin is then obtained as the sum of the outflow rates from the four linear reservoirs.

Note that, if Eqn. 6.2 is applied to the already updated storage volumes, the computed outflow rates are *instantaneous values* which correspond to the *end* of a time step. To ensure conservation of mass, these rates should not be directly used as inputs for a downstream model (usually a flow routing model). Instead, *time-step averaged* outflow rates must be passed to the downstream model. For each reservoir, the time-step averaged outflow rates are obtained from the discrete version of the mass balance equation (recall Eqn. 6.1) as shown in Eqn. 6.8.

$$\overline{q_{out}} = q_{in} - \frac{v(t_0 + \Delta t) - v(t_0)}{\Delta t} \quad (6.8)$$

$\overline{q_{out}}$	Time-step averaged outflow rate	L ³ /T
q_{in}	Inflow rate (constant over Δt)	L ³ /T
$v(t_0)$	Initial storage volume	L ³
$v(t_0 + \Delta t)$	Storage at end of time step	L ³

6.2.3 Implementation

Table 6.1 relates the identifier names used in the model implementation (names of state variables and parameters) to the symbols used in the process equations (Sec. 6.2.1).

Table 6.1: Symbols used in the process equations (Sec. 6.2.1) and corresponding identifiers.

Symbol	Identifier	Units	Details
v (surface runoff)	vol_surf	m ³	Storage volume of surface runoff reservoir
v (preferential flow)	vol_pref	m ³	Storage volume of preferential flow reservoir
v (interflow)	vol_inter	m ³	Storage volume of interflow reservoir
v (baseflow)	vol_base	m ³	Storage volume of baseflow reservoir
S_{surf}	str_surf	sec	Retention constant of surface runoff reservoir
S_{pref}	str_pref	sec	Retention constant of preferential flow reservoir
S_{inter}	str_inter	sec	Retention constant of interflow reservoir
S_{base}	str_base	sec	Retention constant of baseflow reservoir

6.2.4 Hints for application

As with all state variables, initial values must be assigned to the storage volumes listed in Table 6.1. These values are generally unknown and cannot be derived from observation data. Therefore, a widely used approach is to simply guess the initial values and to allow for a rather long 'warm-up' period of the model (several years). If boundary condition data are available for a limited period of time only, one should run a sequence of warm-up simulations. Guessed initial values are used only in the first run. In all later runs, the model is initialized with the final state of the previous run. The success of the latter strategy can be checked, for example, by plotting some simulated hydrographs. If the differences between the hydrographs of consecutive runs becomes negligible, the desired equilibrium of the storage volumes has been reached. However, even then, the initial part of a simulated time series should not be compared to observations because the initial state is still a (refined) guess.

The retention constants listed in Table 6.1 need to be identified by calibration. The values depend on the characteristics of the modeled basin, the model's resolution, as well as on the definition of the used concentration time index, CTI (see Eqns. 6.4 to 6.7). When calibrating the retention constants, one should keep in mind that a particular parameter set is reasonable only if $S_{surf} < S_{pref} < S_{inter} < S_{base}$ (see Sec. 6.2.1 for details).

The time for model calibration can be reduced (and the overall chance of success can be increased), if prior knowledge on the magnitude of the retention constants is available. If a calibrated model for another nearby basin is available, one could try to adopt the values used in this model as initial guesses. However, this will only work if the basins' characteristics in terms of climate,

geomorphology, and land-use are really comparable. Furthermore, the two models must also be comparable with respect to the spatial and temporal discretization.

If another model for a nearby basin is not available or the mentioned conditions are not met, one can try to infer estimates of the retention constants from observed discharge hydrographs. For that purpose, one has to analyze the shape of stream flow recessions using the theory of the single linear reservoir.

Substituting the volume v in Eqn. 6.3 using Eqn. 6.2 yields an equation to predict the future outflow of a linear reservoir using a known initial outflow rate (Eqn. 6.9).

$$q_{out}(t_0 + \Delta t) = (q_{out}(t_0) - q_{in}) \cdot e^{(-\Delta t/k)} + q_{in} \quad (6.9)$$

During recession some time after a flow peak, we can assume that the outflow from the reservoir is much higher than the inflow. Assuming zero inflow, Eqn. 6.9 simplifies to Eqn. 6.10

$$q_{out}(t_0 + \Delta t) = q_{out}(t_0) \cdot e^{(-\Delta t/k)} \quad (6.10)$$

which can then be solved for the storage constant k (Eqn. 6.11). Note that all values appearing at the right hand side of this equation are easily obtained from a hydrograph plot (Fig. 6.3).

$$k = \frac{\Delta t}{\ln(q_{out}(t_0)/q_{out}(t_0 + \Delta t))} \quad (6.11)$$

When using Eqn. 6.11 to estimate the model parameters S_{surf} , S_{pref} , S_{inter} , and S_{base} , one must take Eqn. 6.4–6.7 into account. Thus, the values of k computed from Eqn. 6.11 have to be divided by the concentration time index CTI in order to obtain the desired values of S_{surf} , S_{pref} , S_{inter} , and S_{base} .

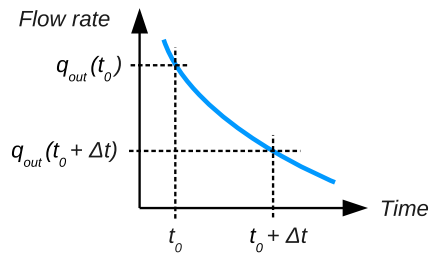


Figure 6.3: Analysis of the recession following a flow peak.

In practice, the estimation of the storage constants is complicated by the fact that multiple runoff components contribute to stream flow at the same time. Thus, to estimate the value of a particular constant, one has to consider a recession which is likely to be *dominated* by the corresponding process. For example, S_{pref} and possibly S_{surf} (and possibly S_{inter}) are likely to control the steep part of the recession after major events. To identify S_{base} , however, one needs analyze long-lasting recessions, preferably at the end of a rainy season.

In general, the obtained values for S_{surf} , S_{pref} , S_{inter} , and S_{base} should be considered as rough estimates only. It is recommended to refine the estimates during calibration.

Chapter 7

Channel flow

7.1 Introduction

This chapter describes approaches to the simulation of open channel flow. In a dynamic model, we generally deal with unsteady flow conditions. One can distinguish between two basic concepts:

Hydrodynamic approach Such models are based on a solution of the St. Venant equations, expressing the conservation of momentum and mass. The solution of these (possibly simplified) partial differential equations requires rather expensive numerical methods.

Hydrological approaches Such models still consider the principle of mass conservation (continuity equation). However, in contrast to hydrodynamic models, they do not account for the conservation of momentum or energy but rely on empirical relations between channel storage and flow.

In hydrological catchment models, hydrological approaches are widely because they are easier to implement and allow for fast computations based on analytical solutions. Prominent examples include:

- the single reservoir approach,
- the Muskingum method,
- the method of Kalinin-Miljukov (Nash's cascade).

The approach(es) described below apply to a single reach. Here, a reach is defined as a river section of a constant geometry (i. e. cross-section and slope). In hydrological catchment modeling for larger areas, cross-section and slope data are usually scarce and a constant geometry is therefore assumed between the neighbored junctions along a river. Then, a reach is practically identical to the river section between two junctions.

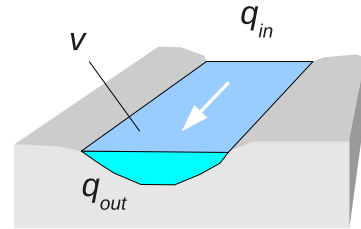


Figure 7.1: Sketch of a reach with storage volume v , and the rates of in- and outflow (q_{in} , q_{out}).

7.2 Single reservoir approach

7.2.1 Processes and equations

In this approach, a reach (Fig. 7.1) is treated as a single reservoir. Considering the principle of mass conservation, the storage volume v (m^3) is related to the rates of inflow q_{in} and outflow q_{out} (both in m^3/s) by the continuity equation Eqn. 7.1.

$$\frac{dv}{dt} = q_{in} - q_{out} \quad (7.1)$$

To simulate the dynamics of v for a given inflow rate, the continuity equation must be complemented by a second equation relating q_{out} to v . In the case of a linear reservoir, for example, this missing relation is given by Eqn. 7.2 where k is a retention constant with the dimension of a time. The advantage of this linear relation is that it allows for an analytical solution of Eqn. 7.1.

$$q_{out} = \frac{1}{k} \cdot v \quad (7.2)$$

Assuming that the inflow rate q_{in} is constant over a discrete time step of length Δt , combining Eqn. 7.1

and 7.2 and subsequent integration using the substitution method yields Eqn. 7.3.

$$v(t_0 + \Delta t) = (v(t_0) - q_{in} \cdot k) \cdot e^{(-\Delta t/k)} + q_{in} \cdot k \quad (7.3)$$

$$\begin{array}{ll} v(t_0) & \text{Initial storage at} \quad L^3 \\ \Delta t & \text{Length of time step} \quad T \end{array}$$

A slightly advanced version of the linear reservoir model is obtained if the inflow rate q_{in} is allowed to vary linearly with time. Then, the modified continuity equation is given by Eqn. 7.4

$$\frac{dv}{dt} = q_{in,0} + (q_{in,1} - q_{in,0}) \cdot t - q_{out} \quad (7.4)$$

where $q_{in,0}$ and $q_{in,1}$ represent an initial and final inflow rate, respectively. After combining Eqn. 7.4 with Eqn. 7.2, the integration yields Eqn. 7.5

$$\begin{aligned} v(t_0 + \Delta t) = & v(t_0) \cdot x + \frac{a \cdot (x - 1)}{b^2} \\ & + \frac{q_{in,0} \cdot (x - 1) - a \cdot \Delta t}{b} \end{aligned} \quad (7.5)$$

with the abbreviations

$$a = (q_{in,1} - q_{in,0}) / \Delta t$$

$$b = -1/k$$

$$x = e^{(-\Delta t/k)}$$

and

$$q_{in,0} = q_{in}(t_0)$$

$$q_{in,1} = q_{in}(t_0 + \Delta t)$$

This equation is also used in the LARSIM model (same as Equation 3.54 in Ludwig and Bremicker, 2006).

Unfortunately, for natural channels, the relation between q_{out} and v is typically non-linear and Eqn. 7.2 is therefor not applicable. However, the analytical solution of the linear reservoir equation (Eqns. 7.3 or 7.5) is very attractive to use because of its low computational cost. A common solution to this problem is the idea of

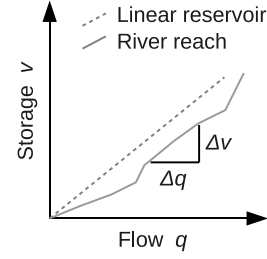


Figure 7.2: Relation between storage volume v and outflow rate q_{out} for a linear reservoir and a river reach.

a locally-linear reservoir. In this concept, the analytical solution of the linear reservoir equation is still used but the retention constant k is allowed to depend on the storage volume v (or the outflow rate q_{out}).

According to Eqn. 7.2, the retention constant of a linear reservoir is given by Eqn. 7.6

$$k = \frac{v}{q_{out}} \quad (7.6)$$

Similarly, for the locally-linear reservoir, the retention constant is given by Eqn. 7.7

$$k = \frac{\Delta v}{\Delta q_{out}} \quad (7.7)$$

Thus, the retention constant k still equals the slope of the relation between v and q_{out} (Fig. 7.2).

For channels of known geometry, the relation between q_{out} to v (Fig. 7.2) can be derived from a rating curve, i. e. corresponding observations of flow rates and water levels (the latter being convertible to storage volumes). Since the vast majority of simulated reaches in a hydrological model is ungaged, rating curves are not practically available and need to be estimated. This is usually done by applying Manning's equation (Eqn. 7.8).

$$q(h) = \frac{1}{n} \cdot \sqrt{S_f} \cdot R(h)^{2/3} \cdot A(h) \quad (7.8)$$

q	Flow rate	m^3/s
S_f	Slope of the energy grade line	–
R	Hydraulic radius	m
A	Wet cross-section area	m^2
h	Water level	m
n	Manning's n (parameter)	Non-physical

Considering that the storage volume v in a uniform reach equals $A \cdot L$ (L : length of the channel), Eqn. 7.8 can be used to tabulate corresponding pairs of v and q_{out} and thus also $k(q_{out})$ or $k(v)$, respectively (recall Eqn. 7.7). The required information are:

- The functions $A(h)$ and $R(h)$. They can easily be computed from the x-section's geometry (table of offsets and corresponding elevations).
- The roughness parameter n . Tables and empirical formulas exist to estimate this value from channel properties. It can also be fitted by steady flow modeling.
- The slope of the energy grade line S_f . In practice, only the slope of the channel bottom S_0 is constant and known. It can be measured in the field or has to be gathered from a digital elevation model (with subsequent quality checks).

7.2.2 Mathematical solution

Governing equation

In each time step, the storage v is updated using Eqn. 7.5. The applied retention constant is an average value (\bar{k}) taking into account the initial storage volume, the initial inflow rate, and the inflow rate at the end of the time step (Eqn. 7.9)

$$\bar{k} = \frac{k(q_{in}(t_0)) + k(q_{in}(t_0 + \Delta t)) + k(v(t_0))}{3} \quad (7.9)$$

with all k values taken from the $\Delta v / \Delta q$ relation (Eqn. 7.7).

To apply Eqns. 7.5 and 7.9, the inflow rates corresponding to the begin and the end of a time step, $q_{in}(t_0)$ and $q_{in}(t_0 + \Delta t)$, must be known.

Inflow rates

Problems with conservation of mass may arise from using $q_{in}(t_0)$ and $q_{in}(t_0 + \Delta t)$ together with the assumption of a linear variation over Δt when simulating multiple reaches in series. This is due to the fact that the outflow from a reach – and thus the inflow of the downstream reach – varies exponentially rather than linearly (see Eqn. 7.3 & 7.5). To allow for a proper mass balance (priority) while also taking into account the variation in the inflow rate (secondary objective), the model uses as input

1. the rate at the end of the time step, $q_{in}(t_0 + \Delta t)$.
2. the average inflow rate for the time step, $\overline{q_{in}}$.

Then, the inflow rate at the begin of the time step, $q_{in}(t_0)$ is estimated from these two values using

$$q_{in}(t_0) = \max(0, 2 \cdot \overline{q_{in}} - q_{in}(t_0 + \Delta t))$$

and subsequently applying the correction

$$q_{in}(t_0 + \Delta t) = 2 \cdot \overline{q_{in}} - q_{in}(t_0)$$

The latter correction is necessary to account for the mass balance in those cases where the 2nd argument of $\max()$ is negative and $q_{in}(t_0)$ is therefor set to zero. These are cases where the value of the average inflow rate is incompatible with the assumption of a linear variation over Δt .

Outflow rates

Using the concept of the linear reservoir, the outflow rate at the end of the time step is computed from Eqn. 7.10.

$$q_{out}(t_0 + \Delta t) = \frac{1}{\bar{k}} \cdot v(t_0 + \Delta t) \quad (7.10)$$

The time-step averaged outflow rate is calculated using Eqn. 7.11, which is a discrete version of the mass balance equation.

$$\overline{q_{out}} = \frac{v(t_0) - v(t_0 + \Delta t)}{\Delta t} + \overline{q_{in}} \quad (7.11)$$

7.2.3 Hints for application

In hydrological catchment modeling, data on the geometry of river cross-sections are usually scarce. The **topocatch** software (Kneis, 2012a) contains methods to estimate the x-section characteristics for all reaches in a river basin using survey data from a limited number of sites only. Basically, these methods perform a spatial regionalization of the functions $A(h)$ and $R(h)$. It then applies Eqn. 7.8 to generate a table of corresponding storage volumes and outflow rates, allowing for look-up of the retention constant (Eqn. 7.7).

Chapter 8

Evaporation from Water Surfaces

8.1 Introduction

This chapter introduces evaporation models. The approach(es) can be used to estimate the water losses associated with evaporation from lake, reservoir, and river surfaces.

8.2 Makkink model

The Makkink model is a simple empirical equation to estimate evaporation using a minimum set of input data, namely short wave radiation and air temperature. It has been derived for the Netherlands. Using convenient units, the basic equation is (Eqn. 8.1)

$$e = c \cdot \frac{s}{s + \gamma} \cdot \frac{R_{inS}}{1000 \cdot E_{wat} \cdot \rho_w} + b \quad (8.1)$$

with	
e	Makkink reference evaporation (m/s)
s	Slope of the curve of saturation water vapor pressure (kPa / K)
γ	Psychrometric constant (kPa / K)
R_{inS}	Incoming short-wave radiation (W/m ²)
E_{wat}	Latent heat of water evaporation (kJ/kg).
ρ_w	Density of water (≈ 1000 kg/m ³).
c	Empirical factor (–).
b	Empirical correction term (m/s).

One should realize that only the incoming short-wave radiation is used in Eqn. 8.1, thus other terms of the energy balance, such as reflection (albedo), long wave emissions, and heat storage are all neglected.

For the dimensionless term $s/(s + \gamma)$ Yao (2009) present a convenient approximation based on the air temperature TA in units of °C (Eqn. 8.2). The error from using this approximation is $\pm 4\%$ for temperatures

Table 8.1: Makkink evaporation (mm/day) for different values of temperature (°C) and daily-average short-wave radiation (W/m²). The empirical parameters were set to $c = 0.61$ and $b = -0.012/100/86400$.

	Temperature (°C)					
Radiation (W/m ²)	5	10	15	20	25	30
50	0.40	0.47	0.53	0.59	0.66	0.72
100	0.93	1.05	1.18	1.31	1.43	1.56
150	1.45	1.64	1.83	2.02	2.21	2.41
200	1.98	2.23	2.48	2.73	2.99	3.25

between 4 and 30 °C and about 7 % at 0 °C when compared to the equations for separate estimation of s and γ given in Hiemstra and Sluiter (2011).

$$\frac{s}{s + \gamma} \approx 0.439 + 0.01124 \cdot TA \quad (8.2)$$

The latent heat of water evaporation E_{wat} (kJ/kg) can be estimated from the water temperature T (°C) using Eqn. 8.3 (Hiemstra and Sluiter, 2011). Since water temperature data are usually unavailable, the air temperature TA must be used as a substitute for T .

$$E_{wat} = 2501 - 2.375 \cdot T \quad (8.3)$$

For the two empirical parameters, Winter et al. (1995) report values of $c = 0.61$ and $b = -0.012/100/86400$ (unit of b converted from cm/d to m/s). Hiemstra and Sluiter (2011) suggest $c = 0.65$ and $b = 0$ but their report does not explicitly focus on evaporation from water surfaces.

Table 8.1 provides some results of the application of Eqn. 8.1 for selected temperatures and short-wave radiation inputs.

Chapter 9

Evapotranspiration

9.1 Introduction

This chapter describes approaches to model evapotranspiration. Two distinct calculation procedures exist:

1. Computation of a *potential* evapotranspiration rate et_{pot} . This represents the maximum possible rate in the absence of water stress. It is basically limited by energy supply.
2. Estimation of the *actual* evapotranspiration rate et_{act} taking into account the properties of vegetation and the limitation by a soil moisture deficit.

Over past decades a large number of approaches has been developed, ranging from simple empirical to complex process-based ones. For a review of the historical development of both scientific knowledge and modeling of evapotranspiration the reader is referred to [Shuttleworth \(2007\)](#).

Each of the functions introduced in the next sections can be called independently. However, to have a greater flexibility 'master functions' were defined taking all possible input variables and parameters, and a choice flag (in a model application this would preferably be a `sharedParamNum`) internally calling the desired method with all relevant inputs. Note that, in general, all inputs have to be given but can be set to a dummy value in case it is not needed for the desired method. The master function `et_pot` calculates *potential* evapotranspiration whereas `et_act` calculates the *actual* value. The output unit is, as commonly done in ECHSE, defined following the international SI system: $[m\ s^{-1}]$. This can be adapted in the implementation of your model engine. E.g., to derive a *sum* of evapotranspiration instead of an average *flux* over the simulation time step multiply by `delta_t` (in [s]) and by 1000 to get [mm]. Tables [9.1](#) and [9.2](#) list all input variables for the master

functions in the order of occurrence (however, you are advised to look into the source code in case changes have not yet been included into the documentation!).

If the functions are called with hourly time steps it may happen that negative evapotranspiration is calculated due to a negative energy balance (outgoing energy predominates incoming energy). This can be interpreted as dew formation. However, so far this process is not explicitly considered and the result of every evapotranspiration routine is limited to zero as lower boundary.

In the following the procedures so far incorporated in ECHSE shall be briefly described. Note that many approaches make use of meteorological quantities and relationships which are independently described in [Chap. 10](#).

Table 9.1: Argument list for ECHSE's master function `et_pot` in the order of occurrence (check the source code for the case of unreported changes!).

Symbol	Identifier	Unit	Explanation	Comment
Common meteorological variables				
TA	<code>temper</code>	$^{\circ}\text{C}$	Mean air temperature over time step	Mandatory; estimated from TA_{min} and TA_{max} if it is missing
TA_{min}	<code>temp_min</code>	$^{\circ}\text{C}$	Minimum air temperature within time step	Currently only used to estimate TA if it is missing
TA_{max}	<code>temp_max</code>	$^{\circ}\text{C}$	Maximum air temperature within time step	Currently only used to estimate TA if it is missing
R_{inS}	<code>glorad</code>	W m^{-2}	Incoming short-wave radiation	Needed for energy balance based approaches; commonly measured but can be estimated from <code>radex</code> , <code>sundur</code> , <code>cloud</code> , <code>lat</code> , <code>doy</code> , <code>radex_a</code> , and <code>radex_b</code> , Sec. 10.5.1
RH	<code>rhum</code>	%	Relative humidity of air	Calculation of vapor pressure
WS	<code>wind</code>	m s^{-1}	Wind speed averaged over time step	Estimation of <i>aerodynamic resistance</i> , see Sec. 9.3.2
PA	<code>apress</code>	hPa	Air pressure at location	Estimation of γ and ρ_{air} ; can also be estimated from <code>elev</code> , Sec. 10.3.1
n	<code>sundur</code>	h	Measured sunshine duration over time step	Calculation of R_{inS} in case it is missing
FC	<code>cloud</code>	%	Percentage of cloudiness	Not yet fully incorporated but included in the interface (use a dummy value)!
Common site-specific parameters				
φ	<code>lat</code>	dec. $^{\circ}$	Latitude	Needed for calculation of R_{ex} and R_{inS} ; use positive values for northern and negative values for southern hemisphere
L_m	<code>lon</code>	dec. $^{\circ}$	Longitude	Currently only needed to calculate R_{ex} at hourly resolution; defined as degrees west of Greenwich meridian, e.g. Greenwich: 0° , New York: 75° , Berlin: 346.5°
h	<code>elev</code>	m	Elevation above sea level	Needed for calculation of PA and $R_{inS,cs}$
Quantities of energy balance (commonly calculated internally)				
R_{ex}	<code>radex</code>	W m^{-2}	Extraterrestrial radiation	Needed for energy balance based approaches; usually calculated from <code>lat</code> and <code>doy</code> (daily resolution) or <code>lat</code> , <code>doy</code> , <code>hour</code> , <code>utc_add</code> , and <code>L_m</code> (hourly resolution), Sec. 10.4.4

Continued on next page.

Continued from previous page.

$R_{inS,cs}$	glorad_max	W m^{-2}	Incoming short-wave radiation under clear sky	Needed for energy balance based approaches to calculate the cloudiness correction factor; usually calculated from radex and radex_a, radex_b or elev Sec. 10.5.2
R_{net}	H_net	W m^{-2}	Net incoming short-wave + long-wave radiation	Needed for energy balance based approaches; usually calculated from a range of meteorological variables and parameters, see Sec. 10.5.6
$R_{net,soil}$	H_soil	W m^{-2}	Net incoming short-wave + long-wave radiation directly at soil surface	Needed for energy balance in SW approach (Sec. 9.2.2.3)
R_{netL}	H_long	W m^{-2}	Net incoming long-wave radiation	Needed for energy balance based approaches; usually calculated from a range of meteorological variables and parameters, see Sec. 10.5.5
G_{soil}	soilheat	W m^{-2}	Soil heat flux	Needed for energy balance based approaches; usually calculated, see Sec. 10.5.7; in SW calculated from $R_{net,soil}$ instead of R_{net}
G_{total}	totalheat	W m^{-2}	Heat flux into soil AND storage of physical and biochemical energy in vegetation and atmosphere below measurement height	Needed for energy balance in SW approach (Sec. 9.2.2.3); so far calculated just as G_{soil} from R_{net}
Meteorological parameters				
z_t	h_tempMeas	m	Measurement height of air temperature	Calculation of aerodynamic resistance, see Sec. 9.3.2; usually 2 m
z_h	h_humMeas	m	Measurement height of relative humidity	Calculation of aerodynamic resistance, see Sec. 9.3.2; usually 2 m
z_w	h_windMeas	m	Measurement height of wind speed	Calculation of aerodynamic resistance, see Sec. 9.3.2; usually 2 m
$\varepsilon_a, \varepsilon_b$	emis_a, emis_b	–	Emissivity parameters	See Sec. 10.5.3
f_a, f_b	fcorr_a, fcorr_b	–	Cloudiness coefficients	Parameters for calculation of f , see Sec. 10.5.4
a_s, b_s	radex_a, radex_b	–	Ångström coefficients	Calculation of R_{inS} and $R_{inS,cs}$, see Sections 10.5.1, 10.5.2
c_d, c_n	f_day, f_night	–	Coefficients for soil heat flux calculation	Calculation of G_{soil} , see Sec. 10.5.7
Vegetation and land-cover parameters and variables				
c_{Makk}	crop_makk	–	Crop factor <i>Makkink</i>	Calculation of land-cover specific et_{pot} after <i>Makkink</i> , cf. Sec. 9.3.1.1

Continued on next page.

Continued from previous page.

c_{FAO}	crop_faoref	–	Crop factor <i>FAO reference</i>	Calculation of land-cover specific et_{pot} following <i>FAO reference evaporation model</i> , cf. Sections 9.2.2.2, 9.3.1.1; simply set it to one if you want the reference evaporation
h_{cano}	cano_height	m	Canopy height	Calculation of <i>aerodynamic resistance</i> , cf. Sec. 9.3.2
LAI	lai	$m^2 m^{-2}$	Leaf area index	Calculation of <i>resistances</i> , cf. Sec. 9.3.2
μ	alb	–	Albedo	Calculation of energy balance (R_{net}), see Sec. 10.5.6
ϵ	ext	–	Canopy's extinction coefficient	Extinction of incoming radiation by canopy expressed by the <i>Beer-Lambert law</i> ; needed for calculation of canopy surface resistance, see Sec. 9.3.2
$r_{l,min}$	res_leaf_min	$s m^{-1}$	Minimum stomatal resistance of a single leaf	Species-specific parameter; value gets up-scaled to whole canopy for calculation of canopy surface resistance, see Sec. 9.3.2
ρ_s	soil_dens	$kg m^{-3}$	Bulk density of soil	Calculation of soil's <i>surface resistance</i> ; only for approaches explicitly accounting for surface resistance of soil, see Sec. 9.3.2.2
g_{srad}	glo_half	$W m^{-2}$	Short-wave radiation at which stomatal conductance is half of its maximum	Species-specific parameter for calculation of canopy resistance, see Eqn. 9.29
r_b	res_b	$s m^{-1}$	Mean boundary layer resistance	Parameter bulk boundary layer aerodynamic resistance of vegetative elements in the canopy; for two-layer approaches, see Sec. 9.3.2.1
c_d	drag_coef	–	Effective value of mean drag coefficient of vegetative elements	Parameter for calculation of aerodynamic resistance using approach of Shuttleworth and Gurney (1990) , see Sec. 9.3.2
$z_{r,s}$	rough_bare	m	Roughness length of bare soil	Parameter for calculation of aerodynamic resistance, see Sec. 9.3.2
n	eddy_decay	–	Eddy diffusivity decay constant	Parameter for calculation of aerodynamic resistance using approach of Shuttleworth and Wallace (1985) , see Sec. 9.3.2
$k_{rss,a}, k_{rss,b}$	rss_a, rssb	–	Parameters for calculation of soil surface resistance	Empirical parameters for calculation of soil surface resistance (needed for two-layer approaches) following Domingo et al. (1999) , see Sec. 9.3.2

Continued on next page.

Continued from previous page.

Computational parameters				
doy	doy	–	Day of the year (Julian day)	Calculation of R_{inS} and R_{ex}
h	hour	–	Hour of day	Value in the range of $\{0..23\}$; only needed for calculation of hourly values of R_{ex}
a_{UTC}	utc_add	h	Deviation of local time zone from UTC	Value in the range of $\{-12..14\}$; can vary over the year due to daylight saving time; only needed for calculation of hourly values of R_{ex}
–	na_val	–	Numeric value treated as <i>not available</i> (NA)	Input quantities having the specified value will be internally treated as NA (e.g. for input checks)
Δt	delta_t	s	Time step length	Temporal resolution of the model; use ECHSE's internal parameter! (only argument for the <code>simulate</code> method, cf. Kneis (2012b))
Choice flags				
–	choice	–	Choice of potential evapotranspiration model	1: Makkink 11: Penman-Monteith 12: FAO reference evaporation
–	ch_rcs	–	Choice of canopy stomatal resistance model	See Sec. 9.3.2
–	ch_roughLen	–	Choice for calculation of roughness length	For calculation of aerodynamic resistance, Sec. 9.3.2
–	ch_plantDispl	–	Choice for calculation of displacement height	For calculation of aerodynamic resistance, Sec. 9.3.2
–	ch_gloradmax	–	Choice for calculation of $R_{inS,cs}$	See Sec. 10.5.2

Table 9.2: Arguments for ECHSE's master function `et_act` **in addition** to those for `et_pot` listed in Table 9.1 (check the source code for the case of unreported changes!).

Symbol	Identifier	Unit	Explanation	Comment
θ_{top}	wc_vol_top	$\text{m}^3 \text{m}^{-3}$	Volumetric water content of the top-most soil horizon	Needed for estimation of resistance against soil evaporation (Sec. 9.3.2.2)
θ_{root}	wc_vol_root	$\text{m}^3 \text{m}^{-3}$	Volumetric water content of the root zone	Needed for estimation of soil moisture factor (Sec. 9.3.1.2) or resistance against plant transpiration (Sec. 9.3.2.2)
θ_s	wc_sat	$\text{m}^3 \text{m}^{-3}$	Volumetric water content at saturation of the root zone	Needed for estimation of resistance against plant transpiration (Sec. 9.3.2.2)
θ_{pwp}	wc_pwp	$\text{m}^3 \text{m}^{-3}$	Volumetric water content of the root zone at permanent wilting point	Needed for estimation of soil moisture factor (Sec. 9.3.1.2)

Continued on next page.

Continued from previous page.

θ_r	wc_res	$\text{m}^3 \text{m}^{-3}$	Residual volumetric water content of the root zone	Needed for estimation of resistance against plant transpiration (Sec. 9.3.2.2)
θ_{etmax}	wc_etmax	$\text{m}^3 \text{m}^{-3}$	Parameter giving the minimum volumetric water content for actual evapotranspiration to be equal to the potential one	Needed for estimation of soil moisture factor (Sec. 9.3.1.2); typically $\frac{\theta_{etmax}}{\theta_{fc}}$ is a value of [0.5..0.8] with θ_{fc} being <i>field capacity</i>
h_b	bubble	hPa	Bubbling pressure of the root zone	Needed for estimation of resistance against plant transpiration (Sec. 9.3.2.2); Parameter can be derived by pedotransfer functions; note that unit [hPa] is approximately equal to [cm of water]
λ	pores_ind	–	Pore-size-index of the root zone	Needed for estimation of resistance against plant transpiration (Sec. 9.3.2.2); Parameter can be derived by pedotransfer functions
$\psi_{s,min}$	wstressmin	hPa	Capillary suction at minimum water stress (stomata completely open)	Needed for estimation of resistance against plant transpiration (Sec. 9.3.2.2); Species-specific plant parameter; note that unit [hPa] is approximately equal to [cm of water]
$\psi_{s,max}$	wstressmax	hPa	Capillary suction at maximum water stress (total stomata closure, wilting point)	Needed for estimation of resistance against plant transpiration (Sec. 9.3.2.2); Species-specific plant parameter; note that unit [hPa] is approximately equal to [cm of water]
a_{vap}	par_stressHum	hPa^{-1}	Empirical parameter	Needed for calculation of water vapor deficit stomatal conductance stress factor (Sec. 9.3.2.2)

9.2 Models

9.2.1 Empirical equations

9.2.1.1 Makkink model

The Makkink model is simple approach to estimate potential evaporation using only temperature (`temper`), downward short-wave radiation (`glorad`), and air pressure (`apress`; or estimated from elevation, see Sec. 10.3.1) as predictors. The approach is discussed in detail by [de Bruin \(1987\)](#); [Feddes \(1987\)](#); [Hiemstra and Sluiter \(2011\)](#).

Using convenient units, the basic equation without an additive empirical constant (see [de Bruin, 1987](#)) is Eqn. 9.1

$$et_{pot} = c \cdot \frac{s}{s + \gamma} \cdot \frac{R_{inS}}{1000 \cdot E_{wat} \cdot \rho_w} \quad (9.1)$$

usage

`et_pot_makkink(glorad, temper, apress, cropfactor)`

with

et_{pot}	Makkink reference crop-evaporation (m/s)
s	Slope of the curve of saturation water vapor pressure (kPa / K); see Sec. 10.3.5
γ	Psychrometric constant (kPa / K); see Sec. 10.3.9
R_{inS}	Incoming short-wave radiation (W/m ²); see Sec. 10.5.1
E_{wat}	Latent heat of water evaporation (kJ/kg); see Sec. 10.3.8
ρ_w	Density of water (≈ 1000 kg/m ³)
1000	Factor to convert kJ into J
c	Dimensionless empirical constant, $c=0.65$

Note that, to derive et_{pot} for a specific site with certain land-cover, Eqn. 9.1 still has to be multiplied by a crop factor (`cropfactor`, see Sec. 9.3.1.1). Accounting for soil moisture deficit will finally lead to *actual* evapotranspiration et_{act} (see Sec. 9.3.1.2).

9.2.2 Process-based approaches

9.2.2.1 Penman-Monteith equation

The famous equation of *Penman-Monteith* is a widely used physically-based approach of modelling evapotranspiration. That means, in contrast to purely empirical approaches, it explicitly simulates the governing

physical processes whereas the individual components, however, might still rely on empirical relationships.

The formula takes into account the energy available for evapotranspiration in the canopy and the vapor pressure deficit. It further incorporates resistance to evapotranspiration due to (a) stomatal resistance of the canopy, i.e. the movement of water through the stomata of leaves controlled by the plant, termed *surface resistance*, and (b) the transfer of water vapor from the surface of evapotranspiration into the atmosphere by turbulent diffusion, termed *aerodynamic resistance*, which is controlled by wind speed and the roughness of the surface. In analogy to *Ohm's law* applied in electrotechnic the resistances are treated as a network of resistances connected in series.

The *Penman-Monteith* equation further relies on the *big leaf* simplification, i.e. the vegetation canopy is treated as a single big leaf, and the vegetation being uniformly distributed over the area of interest neglecting evaporation from bare soil. The relation should therefore be applied only at sites of uniform crop vegetation with closed canopy. Over forests and sites of heterogeneous and/or sparse (natural) vegetation with exposed soil the *big leaf* approach would be inoperative.

More detailed information on the model can be obtained from textbooks, e.g. [Maidment \(1993\)](#) or [Dyck and Peschke \(1995\)](#). The formula is:

$$et_{pot} = \frac{1}{E_{wat}} \left[\frac{s(R_{net} - G_{soil}) + \rho_{air} C_{air} (E - e) / r_{aa}}{s + \gamma(1 + r_{cs} / r_{aa})} \right] \quad (9.2)$$

usage

`etp_penmon(lambda, delta, H_net, G, rho_air, ez_0, ez, gamma, r_c, r_a)`

with

et_{pot}	Potential evapotranspiration under given meteorological and land-cover conditions assuming unlimited water supply (m/s)
E_{wat}	Latent heat of water evaporation; see Sec. 10.3.8

s	Slope of the curve of saturation water vapor pressure; see Sec. 10.3.5
R_{net}	Incoming net (short- and long-wave) radiation; see Sec. 10.5.6
G_{soil}	Soil heat flux; see Sec. 10.5.7
ρ_{air}	Density of air; see Sec. 10.3.12
C_{air}	Specific heat of moist air; see Sec. 10.2
E	Water vapor pressure at saturation; see Sec. 10.3.2
e	Water vapor pressure; see Sec. 10.3.3
γ	Psychrometric constant; see Sec. 10.3.9
r_{aa}	Aerodynamic resistance; see Sec. 9.3.2
r_{cs}	Canopy surface resistance; see Sec. 9.3.2

`apress, delta, H_net, G, ez_0, ez, h_windMeas, delta_t)`

with

et_{ref}	FAO reference evaporation (m s^{-1})
TA	Air temperature ($^{\circ}\text{C}$)
WS	Wind speed (m s^{-1})
s	Slope of the curve of saturation water vapor pressure; see Sec. 10.3.5
R_{net}	Incoming net (short- and long-wave) radiation; see Sec. 10.5.6
G_{soil}	Soil heat flux; see Sec. 10.5.7
E	Water vapor pressure at saturation; see Sec. 10.3.2
e	Water vapor pressure; see Sec. 10.3.3
γ	Psychrometric constant; see Sec. 10.3.9

9.2.2.2 FAO reference evaporation

The *Food and Agricultural Organization of the United Nations (FAO)* published guidelines for the computation of crop water requirements by estimation of evapotranspiration based on the *Penman-Monteith* equation which are freely accessible online via <http://www.fao.org/docrep/X0490E/x0490e00.htm>.

For simplification and generalization a so-called *reference crop* was defined, a hypothetical well-watered and uniform grass vegetation of 0.12 m height with a fixed *surface resistance* of 70 s m^{-1} and an albedo of 0.23. For the calculation of potential evapotranspiration for that reference vegetation (et_{ref} in m s^{-1}), the so-called *FAO reference evaporation*, two approaches for daily and hourly time steps, respectively, have been adopted and implemented into ECHSE:

$$et_{ref,d} = \frac{0.408s(R_{net} - G_{soil}) + \gamma \frac{900}{TA+273} WS(E - e)}{s + \gamma(1 + 0.34WS)} \quad (9.3)$$

$$et_{ref,h} = \frac{0.408s(R_{net} - G_{soil}) + \gamma \frac{37}{TA+273} WS(E - e)}{s + \gamma(1 + 0.34WS)} \quad (9.4)$$

usage

`etp_penmon_ref(temper, wind,`

This simplified approach can be used if necessary data to apply Eqn. 9.2 are not available. However, to actually derive the potential evapotranspiration for your location you still need to multiply the result with a land-cover specific *crop factor* (cf. Sec. 9.3.1.1).

Note that applying this simplified relation may result in some errors due to the amount of implicit assumptions. Especially when hourly values are calculated the presumed constant value of *surface resistance* over the whole day may lead to underprediction over daytime and overpredictions over nighttime where errors should compensate one another when summed over the day.

Note that internal adjustments are applied which are not shown in the presented equations to derive the mentioned units from the reported units of input variables.

9.2.2.3 Shuttleworth-Wallace

The model of *Shuttleworth and Wallace (1985)* (henceforth also termed **SW model**) is an enhancement of the *Penman-Monteith* equation (Sec. 9.2.2.1). It relaxes the *big leaf* assumption by an advanced resistance scheme to better account for a clumped vegetation containing patches of bare soil. The model is thus suitable for application in semi-arid environments and over agricultural fields containing sparse crops without a closed canopy. Yet it should be not applied at forest sites.

The approach uses a one-dimensional model of energy partition into a part for closed vegetation and bare soil, respectively. It further introduces additional resistances to account for the resistance of soil against evaporation. Transpiration from the canopy et_c (in $[\text{m s}^{-1}]$)

and evaporation from bare soil et_s (in $[m\ s^{-1}]$) can then be separately calculated as:

$$et_s = \frac{1}{E_{wat}} \left[\frac{sA_s + \rho_{air}C_{air}D_0/r_{sa}}{s + \gamma(1 + r_{ss}/r_{sa})} \right] \quad (9.5)$$

usage

```
et_sw_soil(lambda,delta,H_soil,
soilheat,rho_air,D_0,gamma,
r_ss,r_sa)
```

$$et_c = \frac{1}{E_{wat}} \left[\frac{s(A - A_s) + \rho_{air}C_{air}D_0/r_{ca}}{s + \gamma(1 + r_{cs}/r_{ca})} \right] \quad (9.6)$$

usage

```
et_sw_cano(lambda,delta,H_net,
H_soil,totalheat,soilheat,
rho_air,D_0,gamma,r_cs,r_ca)
```

with

E_{wat}	Latent heat of water evaporation; see Sec. 10.3.8
s	Slope of the curve of saturation water vapor pressure; see Sec. 10.3.5
A_s	Total energy available at soil surface: $A_s = R_{net,soil} - G_{soil}$
A	Total energy available at measurement height (above canopy): $A = R_{net} - G_{total}$
R_{net}	Incoming net (short- and long-wave) radiation; see Sec. 10.5.6
$R_{net,soil}$	Incoming net (short- and long-wave) radiation hitting the soil surface
G_{soil}	Soil heat flux; see Sec. 10.5.7
G_{total}	Heat flux into soil AND vegetation
ρ_{air}	Density of air; see Sec. 10.3.12
C_{air}	Specific heat of moist air; see Sec. 10.2
D_0	Vapor pressure deficit at canopy source height
γ	Psychrometric constant; see Sec. 10.3.9
r_{ca}	Bulk boundary layer resistance of the vegetative elements in the canopy; see Sec. 9.3.2
r_{cs}	Canopy surface resistance; see Sec. 9.3.2
r_{sa}	Aerodynamic resistance between soil and canopy source height; see Sec. 9.3.2
r_{ss}	Surface resistance of soil; see Sec. 9.3.2

To calculate the vapor pressure deficit at canopy source height D_0 either measurements of air temperature and relative humidity at canopy source height have to be given (D_0 can then be calculated as described in Sec. 10.3.4) or from the energy balance whereas the total latent heat flux ($E_{wat}et$) has already to be known:

$$D_0 = D + \frac{r_{aa}}{\rho_{air}C_{air}} [sA - (s + \gamma)E_{wat}et] \quad (9.7)$$

usage

```
vapPressDeficit_canopy(H_net,
totalheat,gamma,delta,lambda,
vapPressDeficit,r_aa,et_total,
rho_air)
```

with

et	Total evapotranspiration, i.e. $et_s + et_c$
r_{aa}	Aerodynamic resistance between canopy source height and reference level; see Sec. 9.3.2
D	Vapor pressure deficit at reference/measurement height ; see Sec. 10.3.4

Shuttleworth and Wallace (1985) also present a set of formulas to calculate total evapotranspiration where D_0 was eliminated:

$$et = \frac{1}{E_{wat}} [C_c PM_c + C_s PM_s] \quad (9.8)$$

where PM_c and PM_s are terms for transpiration from canopy and evaporation from soil, respectively, which are calculated following Penman-Monteith:

$$PM_c = \frac{sA + (\rho_{air}C_{air}D - sr_{ca}A_s)/(r_{aa} + r_{ca})}{s + \gamma[1 + r_{cs}/(r_{aa} + r_{ca})]} \quad (9.9)$$

$$PM_s = \frac{sA + [\rho_{air}C_{air}D - sr_{sa}(A - A_s)]/(r_{aa} + r_{sa})}{s + \gamma[1 + r_{ss}/(r_{aa} + r_{sa})]}$$

with the coefficients:

$$C_c = \frac{1}{1 + R_c R_a / R_s (R_c + R_a)} \quad (9.11)$$

$$C_s = \frac{1}{1 + R_s R_a / R_c (R_s + R_a)} \quad (9.12)$$

and:

$$R_a = (s + \gamma) r_{aa} \quad (9.13)$$

$$R_c = (s + \gamma) r_{sa} + r_{ss} \quad (9.14)$$

$$R_s = (s + \gamma) r_{ca} + r_{cs} \quad (9.15)$$

usage

```
et_sw(lambda, delta, H_net, H_soil,
totalheat, soilheat, rho_air, ez_0,
ez, gamma, r_cs, r_ca, r_ss, r_sa, r_aa)
```

Thus, if you want to obtain canopy transpiration and soil evaporation separately, first apply Eqns. 9.8 to 9.15 to obtain total et , use this to calculate D_0 using Eqn. 9.7, and finally calculate et_c and et_s using Eqns. 9.6 and 9.7, respectively.

9.3 Actual vs. potential evapotranspiration

To calculate *actual* evapotranspiration two distinct approaches are included in ECHSE. The first calculates *potential* evapotranspiration which is then reduced depending on *crop factors* and a *soil moisture factor* considering the current soil moisture state. This approach is described in Sec. 9.3.1 and is applied to all empirical models described in Sec. 9.2.1 and to the FAO reference evaporation. The second approach is more physically based by incorporating the current soil moisture state in the calculation of *surface resistances* (see Sec. 9.3.2).

(9.10) 9.3.1 Reduction functions

In the approaches described here, the rate of real evapotranspiration et_{act} is computed by multiplying the potential rate et_{pot} with dimensionless correction factors. Typically, these factors account for

- the different transpiration characteristics of the actual vegetation as compared to the reference vegetation to which et_{pot} refers (usually short grass). These factors are known as *crop factors* (Sec. 9.3.1.1).
- the reduction of plant transpiration due to soil moisture limitation (Sec. 9.3.1.2).

9.3.1.1 Crop factors

For some equations to estimate et_{pot} , an extensive set of crop factors has been established based on empirical research. The values vary between different crops and also account for the different stages of plant grow, i. e. seasonality. For the Makkink model (Sec. 9.2.1.1), crop factors can be found in Feddes (1987). Guidelines on crop coefficients can also be obtained from the FAO, together with their approach on reference evaporation included in ECHSE and described in Sec. 9.2.2.2, freely accessible online via <http://www.fao.org/docrep/X0490E/x0490e00.htm>.

For wider applicability, it is desirable to derive the crop factors from other easily available data. A potential candidate is the leaf-area index LAI . Based on figure Fig. 9.1, an approximate relation between the crop factor of the Makkink model and the LAI can be derived:

$$\text{crop factor} \approx 0.14 \cdot LAI + 0.4 \quad (9.16)$$

Note that, following the conventional definition of et_{pot} , the crop factor should take a value of one for the reference crop (typically actively growing grass of 12 cm height with unlimited water supply). Assuming that the corresponding LAI is about 5 (see, e. g. Misra and Misra, 1981) or (Bremicker et al., 2006, page 11), the simplest linear approach would be:

$$\text{crop factor} \approx 0.2 \cdot LAI \quad (9.17)$$

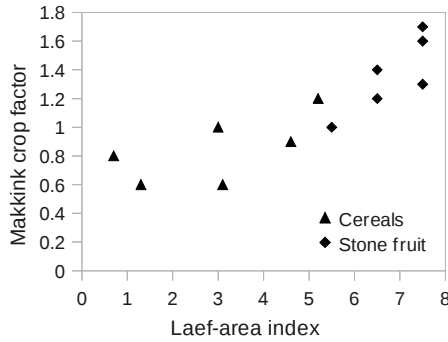


Figure 9.1: Relation between the crop factor (for Makkink model) and the leaf-area index (m^2/m^2) for two selected crops. Crop factors and the corresponding values of LAI were taken from Feddes (1987) and Ludwig and Bremicker (2006), respectively.

This equation, however, implies that evapotranspiration from bare soil is zero. In reality, a non-zero intercept is more plausible.

During calibration of a hydrological model for the Upper Neckar Basin (Germany), the relation shown in Eqn. 9.18 was identified. It yielded the best result for a larger part of the catchment (gage Kirchzellinsfurt, 2300 km^2). The optimum parameters for smaller sub-basins were similar. The assumed LAI of grassland vegetation in that model was 5.

$$\text{crop factor} \approx 0.16 \cdot \text{LAI} + 0.2 \quad (9.18)$$

Note that so far the master functions for evapotranspiration et_{pot} and et_{act} simply take the crop factor as input. It has to be determined during the pre-processing or within your model engine. So far, none of the aforementioned methods is included in the process definitions.

9.3.1.2 Soil moisture factor

A widely used scheme to account for the limitation of real evapotranspiration by soil moisture is illustrated in Fig. 9.2. This approach uses two empirical constants rs_{etmin} and rs_{etmax} representing threshold values of relative soil saturation. For very dry soil with relative saturation between 0 and rs_{etmin} , real evapotranspiration is zero. For wet conditions with relative saturation between rs_{etmax} and 1, the rate of real evapotranspiration et_{act} is equal to the potential rate et_{pot} . For intermediate conditions, et_{act} is assumed to vary linearly

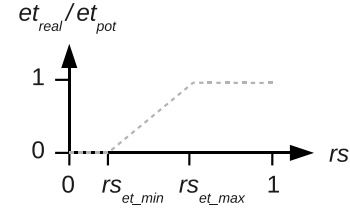


Figure 9.2: Ratio of real to potential evapotranspiration $et_{\text{act}}/et_{\text{pot}}$ as a function of relative soil saturation rs .

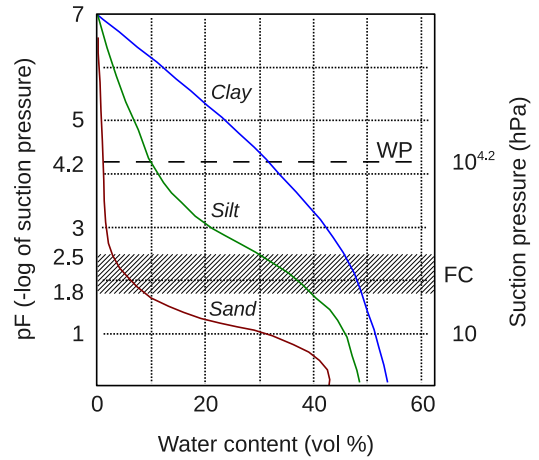


Figure 9.3: Typical relation between water content and suction pressure for different soil types. The permanent wilting point is defined as $pF=4.2$ (≈ 1500 kPa). The hatching marks the typical range of the field capacity found in soils. Adapted from Scheffer and Schachtschabel (1998).

with soil saturation (i. e. soil moisture). Mathematically, this is expressed by:

$$\frac{et_{\text{act}}}{et_{\text{pot}}} = \min \left(1, \max \left(0, \frac{rs - rs_{\text{etmin}}}{rs_{\text{etmax}} - rs_{\text{etmin}}} \right) \right) \quad (9.19)$$

In this definition, the relative soil saturation rs is the quotient of the current soil water content θ and the soil-specific maximum value θ_{max} . Thus, the two parameters rs_{etmin} and rs_{etmax} take values in range 0 to 1. A reasonable estimate for rs_{etmin} can be obtained from data on the water content at the wilting point. This value varies considerably between soil types as illustrated in Fig. 9.3.

Table 9.3: Characteristic values of the soil water content θ and corresponding estimates of model parameters derived from Fig. 9.3.

Soil	θ_{max}	θ at pF=2.5	θ at pF=4.2	r_{setmax}	r_{setmin}
Sand	0.43	0.03	0.02	< 0.07	0.05
Silt	0.48	0.3	0.1	< 0.63	0.21
Clay	0.53	0.46	0.32	< 0.86	0.6

Some characteristic values of soil water content (based on Fig. 9.3) and the corresponding estimates of model parameters are presented in Table 9.3.

Note that this approach is automatically applied to all empirical approaches (Sec. 9.2.1) and the FAO reference evaporation when calling `et_act`. r_{setmin} is automatically set to permanent wilting point (θ_{pwp}) and r_{setmax} is a calibration parameter (θ_{etmax}) but should take a value such that $\frac{\theta_{etmax}}{\theta_{fc}}$ is a value of [0.5..0.8] with θ_{fc} being field capacity.

9.3.2 Resistances

During the diffusion of water vapor through air several factors hinder the water molecules on their way. These factors are commonly called *resistances* and are, in analogy to *Ohm's law*, generally defined as *resistance* = *water vapor gradient/water vapor flux*. Depending on the modeling approach several sources of resistance to evapotranspiration can be defined and related to each other (cf. Sections 9.2.2.1, 9.3). In analogy to electrotechnic the resistances are treated as a network connected in series or parallel.

In the following several resistances including their modeling approaches implemented in ECHSE shall be introduced.

9.3.2.1 Aerodynamic resistances

Wind blowing over a rough surface (e.g. soil or the top of a vegetation canopy) induces *turbulence*, i.e. an ill-defined yet coherent movement of air. Turbulence is a much more efficient transport mechanism than molecular diffusion for water molecules through the air. It causes a vertical exchange of moist air above a vaporizing surface with drier air from higher levels of the atmosphere. This mechanism is controlled by *atmospheric resistance*.

In a Penman-Monteith model this type of resistance induced by the atmosphere is the only form of resistance that is accounted for. In the SW approach it is split into resistance to water transfer between canopy source height and reference height (r_{aa}), bulk boundary layer resistance within the canopy (r_{ca}), and aerodynamic resistance between the substrate surface and reference height over bare soil (r_{sa}).

Aerodynamic resistance between canopy and reference level – r_{aa} When applying Penman-Monteith the following equation is commonly used to calculate *aerodynamic resistance* (r_{aa}) assuming a logarithmic wind profile and a neutral atmospheric layering (Maidment, 1993; Dyck and Peschke, 1995):

$$r_{aa} = \frac{\ln[(z_w - d)/z_{om}] \ln[(z_h - d)/z_{ov}]}{\kappa^2 WS} \quad (9.20)$$

usage

```
res_aero(ch_plantDispl, ch_roughLen,
h_windMeas, h_humMeas, h_tempMeas,
wind, cano_height, rough_bare,
lai, drag_coef)
```

with

WS Horizontal wind speed
 z_w Measurement height of horizontal wind speed
 z_h Measurement height of humidity
 d Displacement height of the vegetation, see Sec. 10.6.1
 z_{om} Roughness length for sensible heat flux, see Sec. 10.6.2
 z_{ov} Roughness length for latent heat flux, see Sec. 10.6.2
 κ Von Kármán constant, see Table 10.1

In the presentation paper of their evapotranspiration model Shuttleworth and Wallace (1985) present an approach using the same underlying theory but with a more detailed description of the decay of eddy diffusion integrated from the top of canopy (meaning $(d + z_{om})$) to reference height of meteorological measurements (z_w):

$$r_{aa} = \frac{\ln[(z_w - d)/z_{om}]}{\kappa^2 W S} + \frac{h_{cano}}{n(h_{cano} - d)} \left[\exp[n(1 - (d + z_{om})/h_{cano})] - 1 \right] \quad (9.21)$$

usage

```
res_aa(wind, h_windMeas, cano_height,
h_plantDispl, rough_len, eddy_decay)
```

with

h_{cano} Vegetation canopy height
 n Eddy diffusivity decay constant; [Shuttleworth and Wallace \(1985\)](#) use a value of 2.5

Aerodynamic resistance between the substrate and canopy source height – r_{sa} This resistance can be, in principle, described as above. However, eddy diffusion is integrated from the soil surface (meaning the roughness length of bare soil ($z_{r,s}$), a parameter commonly set to 0.01) to the top of the canopy (meaning ($d + z_{om}$)) ([Shuttleworth and Wallace, 1985](#); [Shuttleworth and Gurney, 1990](#)):

$$r_{sa} = \frac{\ln[(z_w - d)/z_{om}]}{\kappa^2 W S} \frac{h_{cano}}{n(h_{cano} - d)} \left[\exp[n(1 - z_{r,s}/h_{cano})] - \exp[n(1 - (d + z_{om})/h_{cano})] \right] \quad (9.22)$$

usage

```
res_sa(wind, h_windMeas, cano_height,
h_plantDispl, rough_len, eddy_decay,
rough_bare)
```

Bulk boundary layer resistance of the vegetative elements in the canopy – r_{ca} After water molecules left a leaf through the leaf's stomata they have to pass a laminar boundary layer within the vegetation canopy before they enter the free and turbulent air. Within this boundary layer air is moving slowly resulting in a poorly mixed and saturated state and, thus, forming a resistance to water vapor movement.

While Penman-Monteith does not explicitly account for this kind of resistance it is directly accounted for in the SW approach. Here it simply varies inversely with the Leaf Area Index (LAI) and depends on the parameter of mean boundary layer resistance of per unit area of vegetation (r_b) which [Shuttleworth and Wallace \(1985\)](#) considered to be of minor significance and set to 25 s m^{-1} based on field studies:

$$r_{ca} = \frac{r_b}{2LAI} \quad (9.23)$$

usage

```
res_ca(lai, res_b)
```

9.3.2.2 Surface resistances

Bulk stomatal resistance of the canopy – r_{cs} The process of plant transpiration is mainly caused by the diffusion of water molecules through openings in the leaves, the so-called *stomata*. The process can be actively influenced by the plant by closing or opening the stomata depending on the current conditions. The resulting resistance against transpiration is called *stomatal resistance*.

The *minimum* resistance in case of unlimited water supply is a species-dependent parameter ($r_{l,min}$). The *actual* resistance depends on the degree of stress the plant currently experiences. In ECHSE it is calculated following the frequently applied approach of [Jarvis \(1976\)](#):

$$r_{l,act} = r_{l,min} \frac{1}{\Phi_{stress}} \quad (9.24)$$

usage

```
res_stom_leaf(res_leaf_min, cond_rad,
cond_co2, cond_temp, cond_vap,
cond_water)
```

Here Φ_{stress} is the combined stress factor, a value in the range of zero (maximum stress) to one (no stress).

It is the product of independent stress factors, viz. radiation, CO_2 , temperature, vapor pressure deficit, and soil water stress. The factors are of varying importance, depend on species and environmental conditions, and no generally accepted approaches for their calculation exist. ECHSE so far incorporates approaches for the calculation of soil water stress (Φ_{wat}) and the vapor pressure deficit stress factor (Φ_{vap}). The other factors are so far neglected, partly because they were not yet relevant (this approach was herein so far only applied for NE Brazil where temperature stress was assumed negligible) or because the effects are still heavily debated (CO_2 and radiation stress). It should further be noted that in the model of Jarvis (1976) all stress factors are implicitly assumed to be independent of each other which is not necessarily the case.

To calculate soil water stress first the current capillary suction (ψ) is calculated following the relationships of Van Genuchten as given in Maidment (1993):

$$\psi = \left[\frac{1}{\left(\frac{\theta_{root} - \theta_r}{\theta_s - \theta_r} \right)^{\frac{1}{m}} - 1} \right]^{\frac{1}{\lambda+1}} h_b \quad (9.25)$$

and finally, similar to an approach by Hanan and Prince (1997):

$$\Phi_{wat} = \begin{cases} 1 & \text{if } \psi < \psi_{s,min} \\ 1 - \frac{\psi - \psi_{s,min}}{\psi_{s,max} - \psi_{s,min}} & \text{if } \psi_{s,min} \leq \psi < \psi_{s,max} \\ 0.01 & \text{if } \psi \geq \psi_{s,max} \end{cases} \quad (9.26)$$

usage

```
stress_soilwater(wc, wc_sat, wc_res,
bubble, pores_ind, wstressmin,
wstressmax)
```

with

θ_{root} Actual volumetric water content of the root zone
 θ_r Residual volumetric water content of the root zone

θ_s Volumetric water content at saturation of the root zone
 m Parameter: $m = \frac{\lambda}{\lambda+1}$
 λ Pore-size index
 h_b Bubbling capillary pressure
 $\psi_{s,min}$ Capillary suction at minimum water stress (stomata completely open)
 $\psi_{s,max}$ Capillary suction at maximum water stress (total stomata closure, wilting point)

Note that Eqn. 9.25 is only a simplification and does not account for hysteresis (i.e. different matric potential to soilwater content relationships during wetting and drying, respectively). Furthermore, the calculation is strongly parameterization dependent.

For stress resulting from vapor pressure deficit (Φ_{vap}) Jarvis (1976) assume a linear empirical relationship of increasing plant stress with increasing deficit (D) depending on a species-specific parameter (a_{vap} ; see Jarvis (1976) and Hanan and Prince (1997) for example values):

$$\Phi_{vap} = \frac{1}{1 + a_{vap}D} \quad (9.27)$$

usage

```
stress_humidity(vap_deficit,
par_stressHum)
```

Note that D in Eqn. 9.27 has to be determined **within** the canopy. This is often neglected due to a lack of data. However, as D outside the canopy (where measurements are commonly taken) certainly is much larger than within the canopy the resulting error is not necessarily negligible.

After computing the combined stress factor (Φ_{stress}) and the *actual* surface resistance of a single leaf ($r_{l,act}$) using Eqn. 9.24 the bulk surface resistance of the whole canopy still has to be obtained. In ECHSE two approaches are incorporated. The first ($ch_rcs = 1$) is a simple relationship depending on the actual leaf area index (LAI) only (Shuttleworth and Wallace, 1985):

$$r_{cs} = \frac{r_{l,act}}{2LAI} \quad (9.28)$$

A second and physically more meaningful but also more parameter intensive approach (`ch_rcs = 2`) was adopted from [Saugier and Katerji \(1991\)](#):

$$r_{cs} = \frac{r_{l,act}\epsilon}{\ln\left[\frac{q_{srad} + \epsilon R_{ins}}{q_{srad} + \epsilon R_{ins} \exp(-\epsilon LAI)}\right]} \quad (9.29)$$

usage

```
res_cs(ch_rcs, lai, res_ST,
ext, glorad, glo_half)
```

with

R_{ins} Incoming short-wave radiation (above canopy)
 ϵ Canopy extinction coefficient
 q_{srad} Solar radiation for which stomatal conductance is half of its maximum value

Surface resistance of the substrate – r_{ss} In analogy to leaves the evaporating soil constitutes a resistance against evaporation as well. With decreasing soil water content the soil dries out from the top. Thus, water molecules have to move through pores with poorly mixed and possibly well saturated air before they reach the well-mixed atmosphere.

So far only a very simple empirical relationship is integrated in ECHSE derived from [Domingo et al. \(1999\)](#):

$$r_{ss} = k_{rss,a} \theta_g^{k_{rss,b}} \quad (9.30)$$

usage

```
res_ss(soilwat_grav, rss_a, rss_b)
```

with

θ_g **Gravimetric** soil water content; can be estimated from soil water content of the top-most horizon (θ_{top}), density of water (1000 kg m^{-3}), and bulk density (ρ_s):
 $\theta_g = \frac{\theta_{top} \cdot 1000}{\rho_s}$
 $k_{rss,a}, k_{rss,b}$ Empirical parameters

[Domingo et al. \(1999\)](#) report values of $k_{rss,a} = 15.4$ and $k_{rss,b} = -0.76$ for bare soil, and $k_{rss,a} = 37.5$ and $k_{rss,b} = -1.23$ under shrub vegetation in SE Spain, respectively.

9.4 Contributions and TODOs

So far ECHSE incorporates only a few approaches compared to the large number of, especially, empirical approaches that exist. Contributions are very welcome and can be easily made. Use the following workaround:

1. Write a function for the approach into the processes source code file `hydro/evap/et_approaches.h`
2. Make the approach accessible via the master functions `et_pot` (file: `hydro/evap/et_pot.h`) and `et_act` (file: `hydro/evap/et_act.h`); extent the input argument lists if necessary
3. Update the documentation using the latex file: `echse_doc/engines/chapters/part_processes/evapotranspiration/evapotranspiration.tex`
4. Open a pull request on github for the process update (https://github.com/echse/echse_engines) and the update of the documentation (https://github.com/echse/echse_doc)

The following work still has to be done or issues need to be resolved:

- Add more approaches (especially empirical approaches, e.g. Haude, Hargreaves, Priestly-Taylor, Turc, etc.)
- Implement an approach for estimation of the crop factor, e.g. following the descriptions of Sec. 9.3.1.1 or using the FAO guidelines, Part B and C: <http://www.fao.org/docrep/x0490e/x0490e00.htm>
- Complete approaches for soil stress factor estimation and / or implement more or better approaches (Sec. 9.3.2.2)
- Add more or better (physically-based?) approaches for estimation of soil surface resistance (Sec. 9.3.2.2)
- Add more or better approaches to estimate the soil moisture factor (Sec. 9.3.1.2)
- Implement pedotransfer functions to estimate soil parameters from more readily available texture parameters (simplifies the pre-processing)

- Explicitly consider dew formation (negative values of evapotranspiration over nighttime). So far the function's outputs are simply limited to zero as lower boundary to prevent negative evapotranspiration values.

Chapter 10

Meteorological quantities

10.1 Introduction

In this chapter important meteorological quantities and relationships shall be introduced and described. These are mostly used for the calculation of evapotranspiration (Chap. 9) and the energy balance based snow simulation (Chap. 4).

To directly include the functions and constants into your self-defined model code add `meteo/meteo.h` and `meteo/meteo_const.h` to your auxiliary source code file `userCode_*_aux.cpp`.

see, e.g., https://en.wikipedia.org/wiki/Barometric_formula):

$$PA = 1013.25 \cdot \left[1 - \frac{0.0065 \cdot h}{293} \right]^{5.255} \quad (10.1)$$

Usage: `apress_simple(elev)`

Please note that this is only a rough estimation of atmospheric pressure which should only be used if your target variable (e.g. evapotranspiration) is not very sensitive to pressure values!

10.2 Important constants

Table 10.1 lists all important (hydro-) meteorological, mathematical, and physical constants used in ECHSE with their respective symbols used in this manual, identifiers in the source code, numerical values (precision shown as implemented in ECHSE), units, a short explanation, and a reference.

10.3 Hydro-meteorological quantities

10.3.1 Atmospheric pressure – PA

If no values of atmospheric pressure are given it is possible to assess it from elevation above sea level of your location using the common *barometric formula*. Assuming a temperature lapse rate of -0.0065 K m^{-1} , standard pressure at sea level (1013.25 hPa), a temperature of 20°C at sea level, and the air behaving as an ideal gas one obtains the simplified formula as implemented in ECHSE calculating the air pressure (PA in [hPa]) at altitude above sea level (h , `elev` in [m]) (for derivation

10.3.2 Saturation vapor pressure – E

To calculate saturation vapor pressure a number of different approaches exist using air temperature as dependent variable and assuming standard atmospheric conditions. However, Fig. 10.1 shows that the differences between four tested methods are negligible. In ECHSE the *Magnus formula* (sometimes also called *Magnus-Tetens* or *August-Roche-Magnus* formula) as given by [Dyck and Peschke \(1995\)](#) is implemented whereas separate approaches can be selected for calculations of water and ice surfaces, respectively.

Over water:

$$E_w = 6.11 \cdot 10^{\frac{7.5 \cdot TA}{237.3 + TA}} \quad (10.2)$$

Usage: `satVapPress_overWater(temp)`

Over ice:

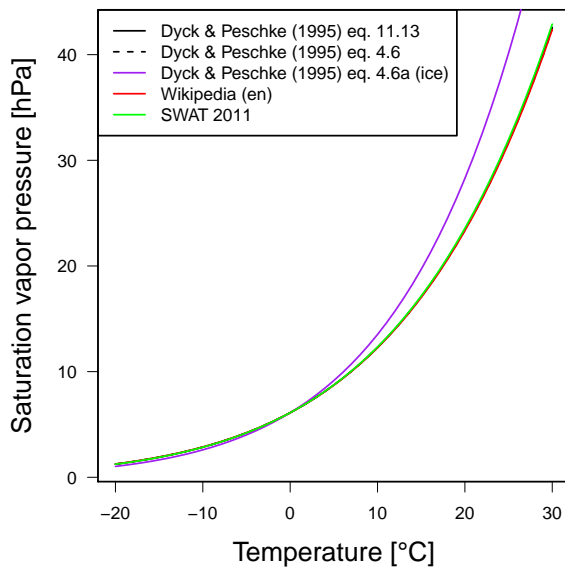
$$E_i = 6.11 \cdot 10^{\frac{9.5 \cdot TA}{265.5 + TA}} \quad (10.3)$$

Usage: `satVapPress_overIce(temp)`

E_w and E_i are given in [hPa] and air temperature TA (`temp`) in $^\circ\text{C}$ is used.

Table 10.1: Constants defined and used in ECHSE.

Symbol	Identifier	Value	Unit	Explanation	Reference
T_{deg_K}	T_DEG_K	273.15	–	Conversion term [°C] to [K] and vice versa	Any textbook
σ	SIGMA	$5.670\,373 \times 10^{-8}$	$\frac{W}{m^2 K^4}$	Stefan-Boltzmann constant; respect units!	Any textbook
π	Pi	3.141592653589793	–	Pi number	Any textbook
R_{SC}	SOLAR_C	1360.8	$\frac{W}{m^2}$	Solar constant; respect units!	Kopp and Lean (2011) (new, revised value!)
M_a	M_DA	$28.965\,46 \times 10^{-3}$	$\frac{kg}{mol}$	Molar mass of dry air	Picard et al. (2008)
M_w	M_W	$18.015\,28 \times 10^{-3}$	$\frac{kg}{mol}$	Molar mass of water	Picard et al. (2008)
R	R	8.314	$\frac{J}{mol K}$	Molar gas constant	Mohr and Taylor (2005)
κ	KARMAN	0.41	–	Von Kármán constant; range of 0.36 to 0.43, 0.41 frequently used in textbooks etc.	Neitsch et al. (2011)
C_{air}	SPHEATMOIST 1012		$\frac{J}{kg K}$	Specific heat of moist air under typical room conditions	https://en.wikipedia.org/wiki/Heat_capacity

**Figure 10.1:** Comparison of different approaches for the calculation of saturated water vapor pressure obtained from Dyck and Peschke (1995); Neitsch et al. (2011), and https://en.wikipedia.org/wiki/Clausius-Clapeyron_relation.

10.3.3 Vapor pressure – e

As the relative humidity RH (`relhum`) of air is defined as the proportion of actual water vapor pressure e to saturated water vapor pressure E (both in [hPa]), the former can be easily derived from measurements of air temperature TA (`temp`; in [°C] to estimate E) and RH in [%]:

$$e = \frac{E(TA) \cdot RH}{100} \quad (10.4)$$

Usage:

```
vapPress_overWater(temp, relhum)
vapPress_overIce(temp, relhum)
```

To get a higher accuracy, if applying Eqn. 10.4 on a daily time step, it is advised to use paired values of TA and RH as input, e.g. minimum RH and maximum TA of a day or maximum RH and minimum TA , as these typically occur simultaneously. Using daily averaged values induces a higher uncertainty due to the non-linearity of $E(TA)$.

10.3.4 Vapor pressure deficit – D

In ECHSE water vapor pressure deficit in [hPa], i.e. $E(TA) - e$ (cf. Sections 10.3.2 10.3.3), can be directly computed from air temperature (TA , $temp$ in [°C]) and relative humidity (RH , $relhum$ in [%]).

Usage:

```
vapPressDeficit_overWater(temp, relhum)
vapPressDeficit_overIce(temp, relhum)
```

10.3.5 Slope of the saturation vapor pressure curve – s

The slope of the saturation vapor pressure temperature curve (s in [hPa K⁻¹]; in a more general sense also known as *Clausius-Clapeyron* relation) is derived by differentiation of the saturation vapor pressure E with respect to air temperature TA ($temp$). Dyck and Peschke (1995) derived the following equation by differentiation of the *Magnus formula* (cf. Sec. 10.3.2) which is implemented in ECHSE (TA in [°C]):

$$s = \frac{4098 \cdot E(TA)}{(237.3 + TA)^2} \quad (10.5)$$

Usage: `slopeSatVapPress(temp)`

Note that herein the temperature dependence of latent heat of evaporation of water is neglected which should, however, be sufficient within the general purpose of evapotranspiration calculation (see Wikipedia for more information: https://en.wikipedia.org/wiki/Clausius-Clapeyron_relation).

10.3.6 Dew point temperature – T_{dew}

TODO

10.3.7 Specific humidity – q

Specific humidity (q , dimensionless) is the ratio of mass of water in a parcel of air to the total mass. Dyck and Peschke (1995) give the following simplified equation depending on vapor pressure (e , $vapPress$ in [hPa]; cf. Sec. 10.3.3) and air pressure (PA , $pressAir$ in [hPa]; cf. Sec. 10.3.1) only:

$$q = \frac{0.622 \cdot e}{PA - 0.378 \cdot e} \quad (10.6)$$

Usage: `specificHumidity(pressAir, vapPress)`

10.3.8 Latent heat of water evaporation – E_{wat}

Latent heat of water evaporation, or heat equivalent of water, (E_{wat} in [kJ kg⁻¹]) is a function of temperature (TA , $temp$ in [°C]) and can be derived from the following empirical formula (Dyck and Peschke, 1995):

$$E_{wat} = 2501 - 2.37 \cdot TA \quad (10.7)$$

Usage: `latentHeatEvap(temp)`

Note that for sublimation and deposition from and into ice a different formula must be used (not yet included in ECHSE).

10.3.9 Psychrometric constant – γ

The psychrometric constant (γ in [hPa K⁻¹]) relates the partial pressure of water in the air to temperature. It depends on atmospheric pressure (PA , $airpress$ in [hPa]) and heat equivalent of water E_{wat} , which in turn depends on air temperature (TA , $temp$ in [°C]; cf. Sec. 10.3.8), as boundary conditions, and the constants ratio of molecular weight of water vapor to that of dry air and specific heat of air at constant pressure. In summarized form, it can be eventually calculated using the following relation (Dyck and Peschke, 1995):

$$\gamma = 0.016286 \frac{PA}{E_{wat}(TA)} \quad (10.8)$$

Usage: `psychroConst(temp, airpress)`

10.3.10 Mole fraction of water vapor – x_v

The mole fraction of water vapor is a dimensionless number meaning the amount of water vapor in air. Following the definition from the *International Committee for Weights and Measures CIPM-81/91* its realization in ECHSE is:

$$x_v = RH \cdot (1.00062 + 3.14 \times 10^{-8} \cdot PA + 5.6 \times 10^{-7} \cdot TA^2)$$

$$\frac{E(TA)}{PA} \quad (10.9)$$

Usage:

`moleFrac_waterVap (airpress, temp, relhum)`

Where $RH/relhum$ means relative humidity in [%], $PA/airpress$ is air pressure in [hPa], and E is saturation vapor pressure in [hPa] depending on air temperature ($TA, temp$ in [°C]; cf. Sec. 10.3.2). **Note** that these units are needed for input, internal conversions are applied that are not shown here.

10.3.11 Compressibility factor – Z

The compressibility factor (dimensionless) is used to calculate the density of moist air. The ECHSE implementation follows the definition from the *International Committee for Weights and Measures CIPM-81/91* taking into account air pressure ($PA, airpress$ in [hPa]), temperature ($TA, temp$ in [°C]), and relative humidity ($RH, relhum$ in [%]) (**NOTE:** Units shown are needed for input, internal conversions are applied that are not shown here):

$$Z = 1 - \frac{PA}{T_{deg_K} + TA} + \frac{PA^2}{(T_{deg_K} + TA)^2} \cdot (d + ex_v^2) \quad (10.10)$$

Usage: `f_compress (airpress, temp, relhum)`
Where:

$$a_0 = 1.58123 \times 10^{-6} \text{ K Pa}^{-1}$$

$$a_1 = -2.9331 \times 10^{-8} \text{ Pa}^{-1}$$

$$a_2 = 1.1043 \times 10^{-10} \text{ K}^{-1} \text{ Pa}^{-1}$$

$$b_0 = 5.707 \times 10^{-6} \text{ K Pa}^{-1}$$

$$b_1 = -2.051 \times 10^{-8} \text{ Pa}^{-1}$$

$$c_0 = 1.9898 \times 10^{-4} \text{ K Pa}^{-1}$$

$$c_1 = -2.376 \times 10^{-6} \text{ Pa}^{-1}$$

$$d = 1.83 \times 10^{-11} \text{ K}^2 \text{ Pa}^{-2}$$

$$e = -0.765 \times 10^{-8} \text{ K}^2 \text{ Pa}^{-2}$$

For x_v see Sec. 10.3.10 and for T_{deg_K} see Sec. 10.2.

10.3.12 Density of moist air – ρ_{air}

To calculate the density of moist air (ρ_{air} in [kg m^{-3}]) the most recent version of the formula from the *International Committee for Weights and Measures (CIPM)*, published and analyzed by [Picard et al. \(2008\)](#), is incorporated in ECHSE:

$$\rho_{air} = \frac{PA \cdot M_a}{Z \cdot R \cdot (T_{deg_K} + TA)} \left[1 - x_v \left(1 - \frac{M_w}{M_a} \right) \right] \quad (10.11)$$

Usage:

`densityMoistAir (airpress, temp, relhum)`

Air pressure ($PA, airpress$ in [hPa]), temperature ($TA, temp$ in [°C]), and relative humidity ($RH, relhum$ in [%]) have to be given. For derivation of Z , and x_v see Sections 10.3.11, and 10.3.10, respectively. For the constants M_a, M_w, R , and T_{deg_K} see Sec. 10.2.

10.4 Astronomical quantities

10.4.1 Solar declination – δ

Solar declination (δ in [rad]) is the angle between the rays of the Sun and a plane of the Earth's equator. It varies roughly between 23.5° on June solstice and -23.5° on December solstice caused by the Earth's axial tilt. In ECHSE incorporated is an approximation as used in the SWAT model ([Neitsch et al., 2011](#)) which should not be used in cases where high accuracy is needed but which is sufficient for estimation of the energy balance (for which δ is basically used in ECHSE):

$$\delta = \arcsin \left\{ 0.4 \sin \left[\frac{2\pi}{365} (doy - 82) \right] \right\} \quad (10.12)$$

Usage: `sol_decl (doy)`

Where doy (`doy`) is the current *Julian day* or *day of the year*.

10.4.2 Eccentricity correction factor – E_0

The eccentricity correction factor E_0 (dimensionless) accounts for that the Earth's orbit around the Sun is not

a perfect circle but slightly elliptical. ECHSE incorporates a simplified formula following the implementation in the SWAT model (Neitsch et al., 2011):

$$E_0 = \left(\frac{r_0}{r}\right)^2 = 1 + 0.033 \cos\left(\frac{2\pi \text{doy}}{365}\right) \quad (10.13)$$

Usage: `e_corr(doy)`

Where r_0 is the average and r the distance between Earth and Sun for any day of the year, and *doy* (doy) is the current *Julian day* or *day of the year*. For simplification, day 366 at leap years is set to 365 as otherwise the above formula would not give a reasonable value. It should thus not be used in cases where high accuracy is needed.

10.4.3 Daylight time factor – ω_s

The daylight time factor ω_s is the approximate hour angle in [rad] of sunrise and sunset at a specific location at given latitude (φ , lat in [°]) on a specific day of the year (*doy*, doy, dimensionless) following equation 25 of FAO's *Guidelines for computing crop water requirements, Chapter 3: Meteorological data* (<http://www.fao.org/docrep/X0490E/x0490e07.htm#calculation%20procedures>):

$$\omega_s = \arccos[-\tan(\delta(\text{doy}))\tan(\varphi)] \quad (10.14)$$

Usage: `dayTime_fac(doy, lat)`

Where δ is the solar declination in [rad], cf. Sec. 10.4.1. **Note** that units shown are needed for input, internal conversions are applied.

10.4.4 Extraterrestrial radiation – R_{ex}

Extraterrestrial radiation R_{ex} in $[\text{W m}^{-2}]$ is the radiation coming from the Sun and hitting the top of the Earth's atmosphere over a given day of the year (*doy*, doy, dimensionless) at a location of given latitude (φ , lat in [°]).

On a **daily** basis it is calculated by integrating incoming solar radiation from sunrise to sunset. See, e.g., Neitsch et al. (2011) or any textbook for a derivation resulting in the following formula (respect units!):

$$R_{ex, \text{daily}} = \frac{1}{\pi} \cdot R_{SC} \cdot E_0 \quad (10.15)$$

$$[\omega_s \cdot \sin(\delta) \cdot \sin(\varphi) + \cos(\delta) \cdot \cos(\varphi) \cdot \sin(\omega_s)]$$

Usage: `rad_extraterr_daily(doy, lat)`

For R_{SC} see Sec. 10.2 and for E_0 , ω_s , and δ see Sections 10.4.2, 10.4.3, and 10.12, respectively.

To obtain **hourly** values the solar time angles at the beginning and the end of the hour of interest have to be respected. Furthermore, a correction for the local time zone has to be applied. Following equations 28 to 33 of FAO's *Guidelines for computing crop water requirements, Chapter 3: Meteorological data* (<http://www.fao.org/docrep/X0490E/x0490e07.htm#calculation%20procedures>) the subsequent relations are implemented in ECHSE:

Calculation of the solar time angle ω_{mid} in [rad] at the midpoint of the desired hour of the day h (hour, integer number):

$$\omega_{mid} = \frac{\pi}{12}$$

$$\{[(h + 0.5) + 0.06667 \cdot (L_z - L_m) + S_c] - 12\} \quad (10.16)$$

with L_m (L_m) being the longitude of the location of interest in decimal degrees west of Greenwich (e.g. Greenwich: 0°, New York: 75°, Berlin: 346.5°), L_z the longitude of the center of the local time zone which is computed internally from the deviation of the local time zone from universal time (UTC) which has to be given as input (`utc_add`, integer value of $[-12..14]$)¹, and S_c a seasonal correction factor that is computed internally. Using that the solar time angles at begin and end of the hour of interest can be calculated:

$$\omega_{ini} = \omega_{mid} - \frac{\pi}{24},$$

$$\omega_{end} = \omega_{mid} + \frac{\pi}{24} \quad (10.17)$$

¹**Note** that the value might change over the year in case of *daylight saving time* and thus should be given as time series input rather than just being a fixed parameter!

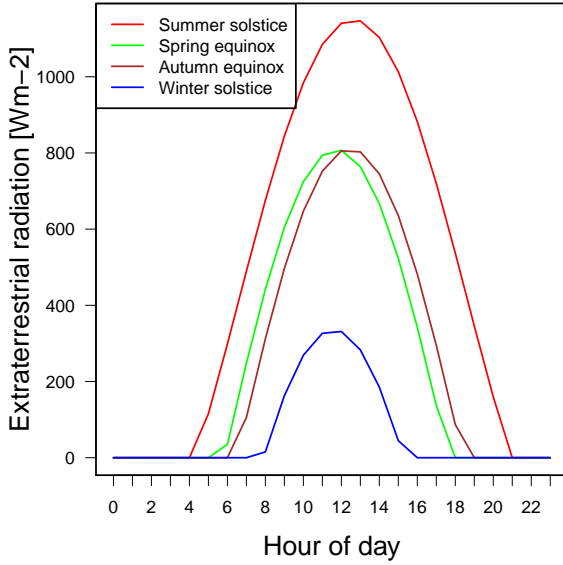


Figure 10.2: Hourly extraterrestrial radiation computed using Eqns. 10.16 to 10.18 over four specific days of year (line colors, see legend) for Berlin taking daylight saving time into account.

where, of course, radiation is zero if $\omega_{mid} < -\omega_s$ or $\omega_{mid} > \omega_s$ (for ω_s see Sec. 10.4.3), i.e. if the Sun is not shining (note from Eqn. 10.16 that the accuracy is \pm half an hour). Eventually, analog to $R_{ex,daily}$, hourly values of R_{ex} can be obtained:

$$R_{ex,hourly} = \frac{12}{\pi} \cdot R_{SC} \cdot E_0 \left[(\omega_{end} - \omega_{ini}) \cdot \sin(\delta) \cdot \sin(\varphi) + \cos(\delta) \cdot \cos(\varphi) \cdot (\sin(\omega_{end}) - \sin(\omega_{ini})) \right] \quad (10.18)$$

Usage:

```
rad_extraterr_hourly(doy, lat, hour,
                    utc_add, L_m)
```

Fig. 10.2 shows example outputs of hourly extraterrestrial radiation computed with Eqns. 10.16 to 10.18 over four specific days of year for Berlin taking *daylight saving time* into account.

Note that units shown are needed for input, internal conversions are applied.

10.5 Energy budget

10.5.1 Incoming short-wave radiation – R_{inS}

Shortwave radiation received by the surface is typically lower than *extraterrestrial radiation* discussed in Sec. 10.4.4 due to processes of absorption, scattering, and reflection in the Earth's atmosphere. It is typically measured at weather stations but can be calculated if no observations are available using the relation of Ångström (see textbooks, e.g. Maidment (1993)):

$$R_{inS} = \left(a_s + b_s \frac{n}{N} \right) R_{ex} \quad (10.19)$$

Usage:

```
calc_glorad(radex, sundur, cloud, lat,
            doy, radex_a, radex_b)
```

R_{inS} is computed in $[W m^{-2}]$, R_{ex} is extraterrestrial radiation ($radex$ in $[W m^{-2}]$, cf. Sec. 10.4.4), $\frac{n}{N}$ is the fraction of measured ($sundur$) to maximum possible sunshine duration, the latter calculated internally from ω_s (cf. Sec. 10.4.3) which needs the current day of year doy and the latitude lat of the location of interest in $[\circ]$ as inputs:

$$N = \omega_s \frac{24}{\pi} \quad (10.20)$$

a_s ($radex_a$) and b_s ($radex_b$) are the Ångström coefficients. The latter define the fraction of R_{ex} that reaches the surface on completely cloudy (a_s) and days of clear sky ($a_s + b_s$), respectively. They can be estimated from measured values (e.g. from a near-by station) or derived from look-up tables (for average climates Maidment (1993) suggests $a_s = 0.25$ and $b_s = 0.50$). Note that measurements of cloudiness ($cloud$) as input to estimate $\frac{n}{N}$ are not yet supported (although the function interface includes it) but planned for the future.

Note that units shown are needed for input, internal conversions are applied. Furthermore this relation only works for **daily time steps** and returns R_{inS} as daily average!

10.5.2 Maximum (clear-sky) incoming short-wave radiation – $R_{inS,cs}$

The maximum possible incoming short-wave radiation in case of clear sky ($R_{inS,cs}$ in $[W m^{-2}]$) is calculated

analogue to R_{inS} (cf. Sec. 10.5.1) assuming full sunshine duration and thus $\frac{n}{N} = 1$ (`ch_gloradmax = 1`):

$$R_{inS,cs} = (a_s + b_s) R_{ex} \quad (10.21)$$

However, Allen et al. (2005) recommend, in case no suitable values of a_s and b_s are available, an empirical relation depending on R_{ex} and elevation above sea level (h , `elev` in [m]) as input which has been incorporated in ECHSE as well (`ch_gloradmax = 2`):

$$R_{inS,cs} = (0.75 + 2 \times 10^{-5}h) R_{ex} \quad (10.22)$$

Usage:

```
calc_glorad_max(ch_gloradmax, radex,
radex_a, radex_b, elev)
```

Note that all inputs have to be given when calling the formula. However, depending on your choice between the two functions, the input not needed can be set to a dummy value, preferably `-9999`.

10.5.3 Net emissivity – ε

Emissivity characterizes the effectiveness of a surface in emitting energy as thermal long-wave radiation. In this case the net emissivity between the Earth's surface and the atmosphere is sought which depends on the amount of water in the air and can thus be empirically related to the water vapor pressure (e in [hPa]; cf. Sec. 10.3.3) (Maidment, 1993):

$$\varepsilon = \varepsilon_a + \varepsilon_b \sqrt{e} \quad (10.23)$$

Usage: `net_emiss(temp, relhum, a, b)`

The parameters ε_a and ε_b are in the range of 0.34 to 0.44 and -0.25 to -0.14 , respectively, whereas for average conditions the values $\varepsilon_a = 0.34$ and $\varepsilon_b = -0.14$ are typically used (Maidment, 1993).

If no measurements of relative humidity (RH , `relhum` in [%]) for estimation of e are available, ε can be as well estimated solely from temperature (TA , `temp` in [°C]) (Maidment, 1993):

$$\varepsilon = -0.02 + 0.261 \exp(-7.77 \times 10^{-4} TA^2) \quad (10.24)$$

Note that units shown are needed for input, internal conversions are applied.

10.5.4 Cloudiness correction factor – f

The cloudiness correction factor (f , dimensionless) is an empirical factor to correct calculations of long-wave radiation at the Earth's surface for cloud cover (cf. Sec. 10.5.5). It can be calculated from the ratio of actual short-wave radiation (R_{inS} , `glorad` in [W m^{-2}]) to maximum short-wave radiation at clear sky ($R_{inS,cs}$, `glorad_max` in [W m^{-2}]) (Maidment, 1993):

$$f = f_a \frac{R_{inS}}{R_{inS,cs}} + f_b \quad (10.25)$$

Usage: `f_cloud(glorad, glorad_max, a, b)`

The long-wave radiation coefficients for clear skies f_a and f_b should be estimated from local radiation measurements. However, Maidment (1993) suggests $f_a = 1.35$ and $f_b = -0.35$ for arid areas, and $f_a = 1.00$ and $f_b = 0.00$ for humid areas.

Note that this relation can be used for daily average values only! However, to avoid this problem the following workaround is suggested for hourly resolution: In your model engine, define $R_{inS,cs}$ and R_{inS} as state variables (`stateScal`). If $R_{inS,cs} > 0$ update the state variables and use the values of $R_{inS,cs}$ and R_{inS} in the usual manner. If $R_{inS,cs} = 0$ it is nighttime and, thus, do not update the state variables but use the old values, i.e. the values of the last hour before sunset for further calculations. In this manner cloudiness of the hour before sunset is extrapolated over night.

10.5.5 Incoming net long-wave radiation –

$$R_{netL}$$

Applying the law of Stefan-Boltzmann the incoming net long-wave radiation at the Earth's surface (R_{netL} in [W m^{-2}]) can be calculated from (Maidment, 1993):

$$R_{netL} = -f\varepsilon\sigma(TA + T_{degK})^4 \quad (10.26)$$

Usage:

```
net_longrad(temp, relhum, glorad,
glorad_max, emis_a, emis_b,
fcorr_a, fcorr_b)
```

R_{netL} is defined positive in direction to the ground, i.e. negative values indicate a net loss, positive values net gain of energy at the Earth's surface. For f (including the radiation coefficients `fcorr_a` and

facorr_b) and ε (including the emissivity parameter emis_a and emis_b) see Sections 10.5.4 and 10.5.3, respectively. For σ and T_{deg-K} see Sec. 10.2. TA (temp) is the air temperature in [°C].

10.5.6 Incoming net radiation – R_{net}

The total incoming net radiation (R_{net} in [W m⁻²]) is the sum of incoming net long-wave radiation (R_{netL} , cf. Sec. 10.5.5) and incoming net short-wave radiation, i.e. the amount of incoming short-wave radiation R_{inS} (cf. Sec. 10.5.1) absorbed by the ground (Maidment, 1993):

$$R_{net} = (1 - \mu)R_{inS} + R_{netL} \quad (10.27)$$

Usage:

```
net_rad(temp, relhum, glorad, glorad_max,
emis_a, emis_b, fcorr_a, fcorr_b)
```

Albedo (μ) is a quantity depending on land cover. It can be derived from local measurements of the radiation balance or from look-up tables. As it might change over the year it is advised to supply it as time series input rather than as a fixed parameter.

10.5.7 Soil heat flux – G_{soil}

Soil heat flux (G_{soil} in [W m⁻²]) is the conduction of heat through the soil. It varies over the day and depends on land-cover conditions. According to textbooks it can be neglected over daily time scales which is generally done in the context of hydrological applications. At sub-daily application, however, it cannot be neglected and is typically defined as a fraction of net radiation R_{net} (net_rad in [W m⁻²]). In equations 45 and 46 of FAO's *Guidelines for computing crop water requirements, Chapter 3: Meteorological data* (<http://www.fao.org/docrep/X0490E/x0490e07.htm#calculation%20procedures>) it is suggested to take 10 % during daylight periods and 50 % during nighttime, Shuttleworth and Wallace (1985) arbitrarily set it to 20 %, and Güntner (2002) identified in a literature study 20 % during daytime and 70 % for nighttime periods as appropriate for (semi-)arid conditions with sparse vegetation cover. These approaches are implemented in ECHSE, taking the fraction of R_{net} over daytime (f_day) and nighttime (f_night), a flag specifying if, at the current time step, it is day

(daynight = 1) or nighttime (daynight = 0), and the current time step length (delta_t in [s]) to differentiate between the two approaches as inputs.

Usage:

```
soil_heatflux(net_rad, f_day, f_night,
daynight, delta_t)
```

For monthly time scales further approaches exist depending on temperature, soil heat conductivity, and effective soil depth (cf. Maidment (1993) or <http://www.fao.org/docrep/X0490E/x0490e07.htm#calculation%20procedures>).

10.6 Turbulence

10.6.1 Displacement height of vegetation – d

10.6.2 Roughness length

For sensible heat flux – z_{om}

For latent heat flux – z_{ov}

Chapter 11

Storage in lakes and reservoirs

11.1 Introduction

This chapter describes approaches to the simulation of water storage in reservoirs. In a wider sense, the term *reservoir* includes natural lakes and the various types of operated reservoirs.

11.2 Storage in uncontrolled lakes

11.2.1 Processes and equations

The fundamental principle for the simulation of lake storage is expressed by the mass balance equation (Eqn. 11.1).

$$\frac{dv}{dt} = q_{in} + p - q_{out} - e \quad (11.1)$$

v	Storage volume	L^3
q_{in}	Inflow rate	L^3/T
q_{out}	Outflow rate	L^3/T
p	Precipitation flux	L^3/T
e	Evaporation flux	L^3/T

For a natural lake with a single outflow, the outflow rate is related to the lake's water level h through a rating curve $Q_{out}(h)$ (Fig. 11.1). Furthermore, the water level h is related to the storage volume v by the storage curve $H(v)$. The latter represents the lake's bathymetry, i. e. the topography of the bottom. Sometimes, the rating curve and the storage curve may be represented by analytical functions, typically using power equations or polynomials, respectively. In practice, however, lookup tables generally allow for greater flexibility as compared to analytical expressions.

The rates of precipitation and evaporation fluxes are obtained by multiplying the corresponding rates (di-

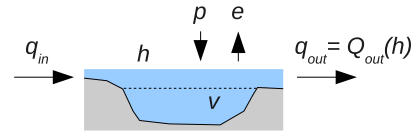


Figure 11.1: Side view of a lake with uncontrolled outflow through an outlet channel. Symbols as in Eqn. 11.1.

mension L/T) with an appropriate value of the lake's surface area (Eqn. 11.2 & 11.3).

$$p = P \cdot a_{max} \quad (11.2)$$

$$e = E \cdot A(H(v)) \quad (11.3)$$

P	Intensity of precipitation	L/T
E	Rate of evaporation	L/T
a_{max}	Maximum extent of the lake's surface area	L^2
$A(h)$	Surface area as a function of water level h	L^2

The reasons for using different values of the surface area in the calculation of precipitation and evaporation fluxes are as follows:

- If a constant surface area would be used in Eqn. 11.3, this would no longer be a continuous function. As long as there was some water in the lake, the evaporation flux would be > 0 . But as soon as the last amount of liquid water has vanished, the flux becomes zero. Such a discontinuity is problematic when solving the differential equation Eqn. 11.1. The choice of a *continuous* function $A(h)$ resolves this problem, as it makes the evaporation flux E decrease gradually, as the storage volume approaches zero.

- In reality, the lake's surface area being exposed to precipitation is variable too, as expressed by $A(h)$. However, in hydrological catchment models, the area of *land surfaces* is typically constant. Therefore, to avoid mass balance errors, the lake's surface area is taken as constant too. The maximum extent of the lake a_{max} is a natural choice. Effectively, rain falling on possibly dry parts of the bottom still contributes to the lake's storage volume.

Using the rating curve $Q_{out}(h)$ and the storage curve $H(v)$ as well as the definitions from Eqn. 11.2 and 11.3, the mass balance (Eqn. 11.1) can be rewritten as Eqn. 11.4.

$$\frac{dv}{dt} = q_{in} + P \cdot a_{max} - Q_{out}(H(v)) - E \cdot A(H(v)) \quad (11.4)$$

11.2.2 Mathematical solution

Strategy

The two functions $Q_{out}(H(v))$ and $A(H(v))$ at the right hand side of Eqn. 11.4 may be arbitrarily complicated. Moreover, the functions are typically available as lookup tables rather than analytical expressions. Therefore, Eqn. 11.4 has to be solved numerically. To obtain accurate and stable (i. e. positive) solutions, an ODE solver with automatic time-step adjustment must be used.

Inflow rates

The currently used implementation allows for a linear variation of the inflow rate within a discrete modeling time step of length Δt . As input, the time-step averaged inflow rate $\overline{q_{in}}$ and the instantaneous rate at the end of the time step $q_{in}(t_0 + \Delta t)$ are used. The missing rate at the begin of the time step $q_{in}(t_0)$ is estimated as described in Sec. 7.2.2 (page 63).

Outflow rates

The numerical solution of Eqn. 11.4 yields the storage volume at the end of a modeling time step and the corresponding outflow rate $q_{out}(t_0 + \Delta t)$ is obtained from the combined rating curve and storage curve $Q_{out}(H(v))$.

An accurate time-step averaged outflow rate $\overline{q_{out}}$ is calculated from a discrete version of the mass balance equation (Eqn. 11.5).

$$\overline{q_{out}} = \frac{v(t_0) - v(t_0 + \Delta t)}{\Delta t} + \overline{q_{in}} + \frac{vp}{\Delta t} - \frac{ve}{\Delta t} \quad (11.5)$$

Here, vp and ve represent the total volumes of precipitation input and evaporation losses within a single time step, respectively. Both vp and ve are treated as state variables which are initialized to zero at the beginning of a time step (t_0). This approach allows for the computation of a proper mass balance even if the rates of precipitation or evaporation are variable over Δt . Currently, this is only the case for evaporation, since the flux is dependent on the storage (see Eqn. 11.3).

11.2.3 Implementation

Table 11.1 relates the identifier names used in the model implementation (names of state variables, parameters, inputs, and outputs) to the symbols used in the process equations (Sec. 11.2.1). Note that this table does not list external input variables used in the calculation of the rate of evaporation (symbol E in Eqn. 11.3). Modeling concepts for evaporation can be found in Chap. 8.

11.3 Notes on input data

In real-world model applications, the required functions $H(v)$, $Q_{out}(h)$, and $A(h)$ are often not known but have to be estimated. Some recommendations are given in the sub-sections below.

11.3.1 Storage curve

Sometimes, information on the lake's bathymetry are available from topographic maps as lines of equal depth. Via the steps of digitizing and vector-to-raster conversion, a digital elevation model (DEM) of the lake's bottom can be obtained using GIS. Alternatively, the DEM can be obtained by interpolation of punctual measurements. The inverse of the storage curve $H(v)$ can be calculated using Eqn. 11.6.

$$V(h) = (\Delta x)^2 \cdot \sum_{i=1}^{nx} \sum_{k=1}^{ny} max(0, h - z(i, k)) \quad (11.6)$$

Table 11.1: Symbols used in the process equations (Sec. 11.2.1) and corresponding identifiers.

Symbol	Identifier	Units	Details
<i>State variables</i>			
v	v	m ³	Storage volume
vp	vp	m ³	Total volume of precipitation in a single time step
ve	ve	m ³	Total evaporated volume in a single time step
<i>Simulated inputs</i>			
$\overline{q_{in}}$	qi_avg	m ³ /s	Inflow rate (time-step average)
$q_{in}(t_0 + \Delta t)$	qi_end	m ³ /s	Inflow rate (value at end of time-step)
<i>Scalar parameters (object-specific)</i>			
a_{max}	area_max	m ²	Maximum surface area
<i>Parameter functions (object-specific)</i>			
$H(v)$	v2h	m	Storage curve (tabulated function)
$A(h)$	h2a	m ²	Area curve to compute evaporation loss (tabulated function)
$Q_{out}(h)$	h2q	m ²	Rating curve at lake outlet (tabulated function)
<i>Outputs</i>			
$\overline{q_{out}}$	qx_avg	m ³ /s	Outflow rate (time-step average)
$q_{out}(t_0 + \Delta t)$	qx_end	m ³ /s	Outflow rate (value at end of time-step)
h	h	m	Water level

$V(h)$	Storage volume corresponding to water level h	L ³
$(\Delta x)^2$	Area of a single raster cell	L ²
nx, ny	Number of cells in x- and y-direction (grid dimensions)	–
$z(i, k)$	Elevation of the bottom at cell with indices i and k	L

11.3.2 Surface area curve

The function $A(h)$ can be obtained from a DEM as well using Eqn. 11.7. By convention, the logical expression $(h > z(i, k))$ equals 1 if true and it is 0 otherwise.

$$A(h) = (\Delta x)^2 \cdot \sum_{i=1}^{nx} \sum_{k=1}^{ny} (h > z(i, k)) \quad (11.7)$$

It is sufficient if $A(h)$ is tabulated for the range of h values which are expected to appear during simulation (including extremes). For lakes which can fall dry, it is important that $A(h)$ is continuous, i. e. the value should *gradually* approach zero for values of h which correspond to minimal storage volumes. In other words, the lake's bottom must not be perfectly flat.

11.3.3 Rating curve (uncontrolled lakes)

For natural lakes, the rating curve $Q_{out}(h)$ can be estimated from the characteristics of the outlet channel using Mannings' equation (see Eqn. 7.8 at page 62). The required information include the cross-section's geometry, the slope of the bottom, and the roughness (Manning's n).

The evaluation of Eqn. 11.6 for discrete values of h yields a lookup table for $V(h)$. The desired function $H(v)$ is then obtained by inverting $V(h)$. Usually, it makes sense to apply some kind of interpolation in order to tabulate $H(v)$ for a reasonable set of arguments v .

For operational model applications, it is important that the table $H(v)$ covers the highest thinkable values of the storage volume v . Otherwise, the model might stop just in the moment where it is needed the most. The choice of a lower limit for v is site-specific. Given that the outflow of the lake never runs dry, it is sufficient if the smallest tabulated value of $H(v)$ corresponds to the lowest point of the channel at the lake's outlet (dashed horizontal line in Fig. 11.1). However, if the water level can fall below this level due to high evaporation (causing the outflow rate to be exactly zero), the table $H(v)$ must also cover those states.

For the special case of a channel whose width W is much greater than the flow depth h_{fl} , the hydraulic radius is approximately equal to h_{fl} . Then, Mannings's equation simplifies to Eqn. 11.8.

$$q(h_{fl}) = \frac{1}{n} \cdot \sqrt{S_f} \cdot h_{fl}^{5/3} \cdot W \quad (11.8)$$

q	Flow rate	m^3/s
S_f	Slope of the energy grade line	–
h_{fl}	Flow depth (x-section average)	m
W	Channel width	m
n	Manning's n (parameter)	Non-physical

List of Figures

1.1	Classes and processes as the basic building blocks of hydrological model engines.	9
4.1	Fluxes of mass and heat to be considered when simulating the snow dynamics.	28
4.2	Relation between energy content and temperature for a sample snow cover.	29
4.3	Synthetic example illustrating the dynamics of the albedo as affected by temperature and precipitation.	32
4.4	Comparison of different empirical formulas for clear sky emissivity.	33
4.5	Dewpoint temperature as a function of temperature and relative humidity.	34
4.6	Saturation vapor pressure over water and ice as a function of temperature.	35
4.7	Observed and simulated snow water equivalent at DWD station 'Fichtelberg'.	38
4.8	Observed and simulated snow water equivalent at DWD station 'Kahler Asten'.	39
5.1	Water fluxes with respect to a soil column with (right) and without snow cover (left).	42
5.2	Influence of the empirical parameter β	42
5.3	Direct runoff computed with Eqn. 5.5 for example values of soil storage and water input.	43
5.4	Effect of the exponent E in a formula $f = s^E$ for s in range $[0,1]$	43
5.5	Discharge hydrograph with manually separated base flow component.	44
5.6	Example of saturated fraction of a soil unit.	54
6.1	Parallel storage model for the case of four runoff components.	57
6.2	Outflow hydrographs from a single linear reservoir for an identical input signal but different storage constants k (hours).	58
6.3	Analysis of the recession following a flow peak.	60
7.1	Sketch of a reach with storage volume v , and the rates of in- and outflow (q_{in} , q_{out}).	61
7.2	Relation between storage volume v and outflow rate q_{out} for a linear reservoir and a river reach.	62
9.1	Relation between the crop factor (for Makkink model) and the leaf-area index (m^2/m^2) for two selected crops.	77
9.2	Ratio of real to potential evapotranspiration et_{act}/et_{pot} as a function of relative soil saturation rs	77
9.3	Typical relation between water content and suction pressure for different soil types. The permanent wilting point is defined as $pF=4.2$ (≈ 1500 kPa). The hatching marks the typical range of the field capacity found in soils. Adapted from Scheffer and Schachtschabel (1998).	77
10.1	Comparison of different approaches for the calculation of saturated water vapor pressure obtained from Dyck and Peschke (1995); Neitsch et al. (2011), and https://en.wikipedia.org/wiki/Clausius-Clapeyron_relation	84
10.2	Hourly extraterrestrial radiation computed using Eqns. 10.16 to 10.18 over four specific days of year (line colors, see legend) for Berlin taking <i>daylight saving time</i> into account.	88

11.1 Side view of a lake with uncontrolled outflow through an outlet channel.	91
---	----

List of Tables

2.1	Classes of the hypsoRR model engine.	13
2.2	Applications of the hypsoRR model engine.	13
3.1	Considered processes in the default sub-basin class.	17
3.2	Data members of the default sub-basin class.	18
3.3	Data members of the default reach class.	21
3.4	Data members of the minireach class.	21
3.5	Data members of the node class with two inflows.	22
3.6	Data members of the lake class.	22
3.7	Data members of the gage class.	23
3.8	Data members of the rain gage class.	24
3.9	Data members of the external inflow class.	24
4.1	Process matrix of the energy balance snow model.	29
4.2	Snow-related physical constants.	29
4.3	Parameters controlling the snow albedo.	32
4.4	Parameters controlling the rate of meltwater outflow.	37
4.5	Calibrated parameters of the energy balance snow model based on daily data from two sites in Germany (Fichtelberg and Kahler Asten).	37
5.1	Symbols used in the process equations (Sec. 5.2.1), corresponding identifiers, and hints for calibration.	45
5.2	Argument list for ECHSE's master function <i>infiltration</i> in the order of occurrence (check the source code for the case of unreported changes!).	47
6.1	Symbols used in the process equations (Sec. 6.2.1) and corresponding identifiers.	59
8.1	Makkink evaporation for different values of temperature and daily-average short-wave radiation.	65
9.1	Argument list for ECHSE's master function <i>et_pot</i> in the order of occurrence (check the source code for the case of unreported changes!).	68
9.2	Arguments for ECHSE's master function <i>et_act</i> in addition to those for <i>et_pot</i> listed in Table 9.1 (check the source code for the case of unreported changes!).	71
9.3	Characteristic values of the soil water content θ and corresponding estimates of model parameters derived from Fig. 9.3.	78
10.1	Constants defined and used in ECHSE.	84
11.1	Symbols used in the process equations (Sec. 11.2.1) and corresponding identifiers.	93

Bibliography

- Allen, R.G., Walter, I.A., Elliott, R., Terry Howell, D.I., Jensen, M., 2005. The ASCE standardized reference evapotranspiration equation. Report prepared by the Task Committee on Standardization of Reference Evapotranspiration. Environmental and Water Resources Institute of the American Society of Civil Engineers (ASCE).
- Bauer, S.W., 1974. A modified horton equation for infiltration during intermittent rainfall. *Hydrological Sciences Bulletin* 19, 219–225. doi:10.1080/02626667409493900.
- Bremicker, M., Homagk, P., Ludwig, K., 2006. Hochwasserfrühwarnung und Hochwasservorhersage in Baden-Württemberg. *Wasserwirtschaft* Jg. 96, Nr. 7-8, 46–50.
- Chow, V.T., Maidment, D.R., Mays, L.W., 1988. *Applied Hydrology*. McGraw-Hill, Inc.
- de Bruin, H.A.R., 1987. From Penman to Makkink, in: Hooghart, J.C. (Ed.), *Evaporation and Weather: Proceedings and information No. 39*, TNO Committee on Hydrological Research, The Hague.
- Domingo, F., Villagarcía, L., Brenner, A., Puigdefábregas, J., 1999. Evapotranspiration model for semi-arid shrub-lands tested against data from SE Spain. *Agricultural and Forest Meteorology* 95, 67–84. doi:10.1016/S0168-1923(99)00031-3.
- Dyck, S., Peschke, G., 1995. *Grundlagen der Hydrologie*. Verlag für Bauwesen.
- Feddes, R.A., 1987. Crop factors in relation to Makkink reference-crop evapotranspiration, in: Hooghart, J.C. (Ed.), *Evaporation and Weather: Proceedings and information No. 39*, TNO Committee on Hydrological Research, The Hague.
- Green, I., 1986. An explicit solution of the modified horton equation. *Journal of Hydrology* 83, 23–27. doi:10.1016/0022-1694(86)90180-0.
- Green, W., Ampt, G., 1911. Studies on soil physics: I. the flow of air and water through soils. *Journal of Agricultural Sciences* 4, 1–24.
- Güntner, A., 2002. Large-scale hydrological modelling in the semi-arid North-East of Brazil. PIK Report 77. Potsdam Institute for Climate Impact Research. Potsdam, Germany.
- Hanan, N., Prince, S., 1997. Stomatal conductance of west-central supersite vegetation in hape-sahel: measurements and empirical models. *Journal of Hydrology* 188–189, 536–562. doi:10.1016/S0022-1694(96)03192-7.
- Hiemstra, P., Sluiter, R., 2011. Interpolation of Makkink evaporation in the Netherlands. Technical Report TR-327. Royal Netherlands Meteorological Institute. De Bilt.
- Hock, R., 2005. Glacier melt: A review of processes and their modelling. *Progress in Physical Geography* 29, 362–391.
- Horton, R.E., 1933. The role of infiltration in the hydrologic cycle. *Transactions, American Geophysical Union* 14, 446–460. doi:10.1029/TR014i001p00446.
- Horton, R.E., 1939. Analysis of runoff-plat experiments with varying infiltration-capacity. *Transactions, American Geophysical Union* 20, 693–711. doi:10.1029/TR020i004p00693.
- Illangasekare, T.H., Walter, R.J., Meier, M.F., Pfeffer, W.T., 1990. Modeling of meltwater infiltration in subfreezing snow. *Water resources research* 26, 1001–1012.
- Jarvis, P.G., 1976. The interpretation of the variations in leaf water potential and stomatal conductance found in canopies in the field. *Philosophical Transactions of the Royal Society of London B: Biological Sciences* 273, 593–610. doi:10.1098/rstb.1976.0035.

- Kirpich, Z.P., 1940. Time of concentration of small agricultural watersheds. *Civil Engineering* 10, 362.
- Knauf, D., 1980. Analyse und Berechnung oberirdischer Abflüsse. Verlag Paul Parey. volume 46 of *Schriftenreihe des DVWK*. chapter Berechnung des Abflusses aus einer Schneedecke. pp. 45–135.
- Kneis, D., 2012a. Eco-Hydrological Simulation Environment (ECHSE) - Documentation of Pre- and Post-Processors. University of Potsdam, Institute of Earth- and Environmental Sciences. URL: http://echse.github.io/downloads/documentation/echse_tools_doc.pdf.
- Kneis, D., 2012b. Eco-Hydrological Simulation Environment (ECHSE) - Documentation of the Generic Components. University of Potsdam, Institute of Earth- and Environmental Sciences. URL: http://echse.github.io/downloads/documentation/echse_core_doc.pdf.
- Kopp, G., Lean, J.L., 2011. A new, lower value of total solar irradiance: Evidence and climate significance. *Geophysical Research Letters* 38, L01706. doi:10.1029/2010GL045777. l01706.
- Kreye, P., Gocht, M., Förster, K., 2010. Development of process descriptions of infiltration and near-surface runoff in water-balance modelling. *Hydrology and Water Resources Management* 54, 268–278.
- Ludwig, K., Bremicker, M. (Eds.), 2006. The water balance model LARSIM - Design, content and application. volume 22 of *Freiburger Schriften zur Hydrologie*. University of Freiburg, Institute of Hydrology.
- Ludwig, K., Moretti, G., Verzano, K., 2010. Effects of different infiltration models on the simulation of extreme events in headwater catchments. *Hydrology and Water Resources Management* 54, 279–292.
- Maidment, D.R. (Ed.), 1993. *Handbook of Hydrology*. McGraw-Hill, Inc.
- Male, D.H., Gray, D.M. (Eds.), 1981. *Handbook of Snow - Principles, Processes, Management and Use*. Pergamon Press. chapter Snowcover Ablation and Runoff. pp. 360–436.
- Mein, R.G., Larson, C.L., 1971. Modeling the Infiltration Component of the Rainfall-Runoff Process. Bulletin 43. Water Resources Research Center, University of Minnesota.
- Mein, R.G., Larson, C.L., 1973. Modeling infiltration during a steady rain. *Water Resources Research* 9, 384–394. URL: <http://dx.doi.org/10.1029/WR009i002p00384>, doi:10.1029/WR009i002p00384.
- Misra, M.K., Misra, B.N., 1981. Seasonal changes in leaf area index and chlorophyll in an indian grassland. *Journal of Ecology* 69, 797–805.
- Mohr, P.J., Taylor, B.N., 2005. CODATA recommended values of the fundamental physical constants: 2002*. *Rev. Mod. Phys.* 77, 1–107. doi:10.1103/RevModPhys.77.1.
- Morris, E.M., Kelly, R.J., 1990. A theoretical determination of the characteristic equation of snow in the pendular regime. *Journal of Glaciology* 36, 179–187.
- Neitsch, S., Arnold, J., Kiniry, J., Williams, J., 2011. Soil and Water Assessment Tool Theoretical Documentation Version 2009. Texas Water Resources Institute Technical Report TR-406. Texas A&M University System. College Station, Texas 77843-2118, USA.
- Peschke, G., 1977. Ein zweistufiges modell der infiltration von regen in geschichtete böden. *Acta hydrophysica* 22, 39–48.
- Peschke, G., 1987. Soil moisture and runoff components from a physically founded approach. *Acta hydrophysica* 31, 191–205.
- Philip, J.R., 1957a. The theory of infiltration: 1. the infiltration equation and its solution. *Soil science* 83, 345–358.
- Philip, J.R., 1957b. The theory of infiltration: 4. sorptivity and algebraic infiltration equations. *Soil science* 84, 257–264.
- Picard, A., Davis, R.S., Gläser, M., Fujii, K., 2008. Revised formula for the density of moist air (cipm-2007). *Metrologia* 45, 149–155. doi:10.1088/0026-1394/45/2/004.
- Rossman, L.A., Huber, W.C., 2016. Storm Water Management Model Reference Manual Volume I – Hydrology (Revised). Technical Report EPA/600/R-15/162A. U.S. Environmental Protection Agency.

- Saugier, B., Katerji, N., 1991. Some plant factors controlling evapotranspiration. *Agricultural and Forest Meteorology* 54, 263–277. doi:[10.1016/0168-1923\(91\)90009-F](https://doi.org/10.1016/0168-1923(91)90009-F).
- Scheffer, F., Schachtschabel, P. (Eds.), 1998. *Lehrbuch der Bodenkunde*. Enke.
- Schulla, J., 1997. Hydrologische Modellierung von Flussgebieten zur Abschätzung der Folgen von Klimaänderungen. Ph.D. thesis. Eidgenössische technische Hochschule Zürich.
- Shuttleworth, W.J., 2007. Putting the "vap" into evaporation. *Hydrology and Earth System Sciences* 11, 210–244. doi:[10.5194/hess-11-210-2007](https://doi.org/10.5194/hess-11-210-2007).
- Shuttleworth, W.J., Gurney, R.J., 1990. The theoretical relationship between foliage temperature and canopy resistance in sparse crops. *Quarterly Journal of the Royal Meteorological Society* 116, 497–519. doi:[10.1002/qj.49711649213](https://doi.org/10.1002/qj.49711649213).
- Shuttleworth, W.J., Wallace, J.S., 1985. Evaporation from sparse crops-an energy combination theory. *Quarterly Journal of the Royal Meteorological Society* 111, 839–855. doi:[10.1002/qj.49711146910](https://doi.org/10.1002/qj.49711146910).
- Stewart, R.D., Rupp, D.E., Najm, M.R.A., Selker, J.S., 2013. Modeling effect of initial soil moisture on sorptivity and infiltration. *Water Resources Research* 49, 7037–7047. doi:[10.1002/wrcr.20508](https://doi.org/10.1002/wrcr.20508).
- Tarboton, D.G., Luce, C.H., 1996. Utah Energy Balance Snow Accumulation and Melt Model (UEB). Technical Report. Utah State University and USDA Forest Service.
- Todini, E., 1996. The ARNO rainfall-runoff model. *Journal of Hydrology* 175, 339–382.
- Winter, T.C., Rosenberry, D.O., Sturrock, A.M., 1995. Evaluation of 11 equations for determining evaporation from a small lake in the north central united states. *Water Resources Research* 31, 983–993.
- Yao, H., 2009. Long-term study of lake evaporation and evaluation of seven estimation methods: Results from dickie lake, south-central ontario, canada. *J. Water Resource and Protection* 2, 59–77.
- Zhao, R.J., Zuang, Y.L., Fang, L.R., Liu, X.R., Zhang, Q.S., 1980. The Xinanjiang model, in: *Hydrological forecasting, Proceedings of the Oxford Symposium*, IAHS Press, Wallingford, UK, pp. 351–356.